

Balansering av motorer for maksimal ytelse

Oda Enger Hoem
Vegard Røsholm

Master i ingeniørvitenskap og IKT
Innlevert: juni 2016
Hovedveileder: Terje Rølvåg, IPM

Norges teknisk-naturvitenskapelige universitet
Institutt for produktutvikling og materialer

Preface

This thesis is part of a Master of Science (MSc) degree at the Norwegian University of Science and Technology (NTNU). The work has been carried out at the Department of Engineering Design and Materials (IPM) under the supervision of Prof. Terje Rølvåg (NTNU).

The motivation behind this thesis has its basis in the development of a tuned HONDA CRF250R. While testing different balancing configurations, our supervisor discovered substantial differences in performance for different balance factors. This thesis is created in order to obtain knowledge and an understanding of how engine balance influence performance.

A comprehensive literary search was conducted in order to find any documented effects on engine performance due to balancing, only to realise that there is no well-documented sources on the topic. When approaching different crankshaft balancing experts we experienced a general reluctance to share any knowledge on the subject. Due to the limited documentation, we had to perform both virtual and physical tests in order to document the performance effects ourselves. The test in Chapter 5 is a test using a simplified rotor without reciprocating piston forces or a varying mass moment of inertia.

As the focus of the thesis changed during the semester, a lot of the initial research proved to be redundant and less relevant for the thesis. Some of this work is, however, provided in the appendices for further reading.

Some of the theory in Chapter 4 is a further development of our project thesis.

Acknowledgements

We would like to express our gratitude to our supervisor Terje Rølvåg for the useful comments, remarks and engagement through the learning process of this master thesis. Furthermore we would like to thank Matteo Bella from MX Real Racing for useful tips in terms of papers and software regarding engine balancing. Also, we would like to thank Jøran Melby for letting us borrow the test rig and helping us adapting and tuning the system for our tests. Last but not least we would like to thank Børge Holen at IPM for manufacturing the simplified crankshaft for the physical test.



Oda Enger Hoem



Vegard Røsholm

Trondheim, June 2016

Abstract

When an engine is equipped with low-weight high-performance racing components, such as the connecting rod, piston, rings and crankpin, the mass moment of inertia changes and the engine needs to be re-balanced. It is performed a significant amount of research relating engine balance to NVH (noise, vibration and harshness), but it is unclear how crankshaft balance influence the engine performance. This thesis concerns how balancing of the crankshaft affects the friction torque in the crankshaft main bearings. Relevant theory is presented, and both a physical test and simulations are conducted. A model for friction torque considering rotating imbalance is presented. The physical test did not give any clear answers, but the simulation verifies the friction torque model.

Sammendrag

Når en motor utstyres med lette racing-komponenter, slik som råder, stempel, ringer og bolter endres treghetsmomentet og motoren må rebalanseres. Det er foretatt en betydelig mengde forskning som omhandler motorbalansering og innvirkningen dette har på vibrasjoner, komfort og støy. Likevel er det uklart hvordan balansering påvirker motorens ytelse. Denne masteroppgaven tar for seg motorbalansering og hvordan dette påvirker friksjonsmomentet i veivlagene. Relevant teori presenteres og simuleringer og en fysisk test utføres og diskuteres. En model for friksjonsmoment som tar hensyn til roterende ubalanse er presentert. Den fysiske testen ga intet entydig svar på hvordan motorbalansering påvirker friksjonsmomentet, men simuleringene verifiserte friksjonsmodellen.

Table of Contents

- Abstract** **iii**
- Sammendrag** **iv**
- Table of Contents** **vi**
- List of Tables** **vii**
- List of Figures** **x**
- Glossary** **xi**
- Abbreviations** **1**
- 1 Introduction** **3**
- 2 Engine dynamics** **7**
 - 2.1 Static and dynamic balancing 7
 - 2.2 Forces in the engine 9
 - 2.2.1 Primary and secondary forces 9
 - 2.3 Varying mass moment of inertia and torque 12
- 3 State of the art in Engine Balancing** **13**
 - 3.1 Different methods of balancing 14
 - 3.1.1 Analytical models – the slider-crank mechanism 14
 - 3.1.2 Semi-empirical models – sensor data during operation 15
 - 3.2 Balancing Machines 17
- 4 Balancing theory** **19**
 - 4.1 Essential theory 19
 - 4.1.1 Static balancing of the slider-crank mechanism 20
 - 4.1.2 Different balance factors 25
 - 4.1.3 Dynamic balancing 29

4.2	Balancing and performance	30
4.2.1	Bearing friction torque	31
4.3	Permissible imbalance	34
5	Performance tests	35
5.1	Performance testing in balancing software	35
5.2	Unbalanced rotor test	39
5.2.1	Test setup	40
5.2.2	Test procedure	42
5.2.3	Results	44
5.2.4	Discussion	45
5.2.5	FEDEM simulation	46
5.2.6	Limitations	50
5.2.7	Conclusion	50
6	CAD-based balancing of the Honda CRF250R	51
6.1	Honda CRF250R specifications	51
6.2	MX Real Racing (MXRR)	51
6.3	Balancing the Honda CRF250R	53
6.3.1	Two balancing cases	53
6.3.2	Formula for calculating the balance factor	54
6.3.3	Finding the counterweight mass, m_{cw} , and its radius, r'	55
6.4	Correction procedure	56
6.5	Modifying the crankshaft geometry	57
6.5.1	Results	57
7	Conclusion	59
	References	61
	Appendices	66
	Appendix A - Friction in journal bearings	66
	Appendix B - Balance correcting methods	69
	Appendix C - Crankshaft stroking and balance	70
	Appendix D - Approaches for automatic balancing	71
	Appendix E - Calculating the dimensions of the simplified crankshaft	76
	Appendix F - Required torque curves from FEDEM simulations	78
	Appendix G - Obligatory Documents	83

List of Tables

- 2.1 Dynamically balanced symmetric and asymmetric rotors. 9
- 4.1 Masses of the slider-crank mechanism. 20
- 5.1 Components in Figure 5.7. 40
- 5.2 The test cases. 42
- 5.3 Results from Test 1. 44
- 5.4 Results from Test 2. 45
- 5.5 Calculated coefficients of friction from the physical test. 46
- 5.6 Comparison of the torques from the physical test and the simulations. . . 49
- 5.7 Differences between the torques in the physical test and the simulations. . 50
- 6.1 Measured mass properties 53
- 6.2 Results after balancing 57
- 7.1 The two test cases. 69
- 7.2 Dimensions of the simplified crankshaft and the moment of inertia of the
original Honda CRF250R crankshaft. 77

List of Figures

- 1.1 The crankshaft design environment in Crankshaft Balance Design Pro Plus. 5
- 1.2 The engine design environment in Crankshaft Balance Design Pro Plus 6
- 1.3 The FEDEM Test Bench with an OEM engine and an MXRR engine. 6

- 2.1 Two examples of static balancing in one correction plane. Crankshaft a) is balanced regarding moments, but not regarding forces. Crankshaft b), on the other hand, is balanced regarding forces, but not regarding moments. 8
- 2.2 Statically force-balanced crankshaft set in motion, creating a rocking couple due to unbalanced moments. 8
- 2.3 The crankshaft is at *Top Dead Centre (TDC)* when the crankpin is at $\approx 0^\circ$ and *Bottom Dead Centre (BDC)* when the crankpin has been moved to $\approx 180^\circ$ 10
- 2.4 The rise of the secondary forces: The distance travelled by the connecting rod is greater from TDC to 90° ATDC than from 90° ATDC to BDC. 10
- 2.5 The piston translates a longer distance from TDC to 90° ATDC than from 90° ATDC to BDC. This is repeated on the way up from BDC to TDC as well. 11
- 2.6 The piston accelerates from TDC to 90° ATDC and from 90° ABDC to TDC, and slows down from 90° ATDC to 90° ABDC, resulting in secondary forces. 11

- 3.1 The first and second modes of a rotor with its corresponding balancing planes. 14
- 3.2 A pivoted-cradle balancing machine [1]. 17
- 3.3 A nodal-point balancing machine [1]. 18

- 4.1 The simplified system with lumped masses at each end of the connecting rod. 20
- 4.2 The masses combined as rotating and reciprocating masses, and the forces they produce. A counterweight is added 180 degrees from the crankpin and dimensions are added to the system. 22

4.3	Attaching m_{rec} to the counterweight balances the reciprocating forces at TDC and BDC, but introduce a transverse force during the rest of the stroke.	25
4.4	In-line and transverse forces with $f_b = 1.0$.	26
4.5	In-line and transverse forces with $f_b = 0.0$.	26
4.6	In-line and transverse forces with $f_b = 0.5$.	27
4.7	The in-line and transverse forces with $f_b = 0.28$.	27
4.8	The resultant forces depending on the balance factor. A $f_b = 0.5$ results in the lowest overall resultant force.	28
4.9	Dynamic balance is maintained as long as the two counterweights of a single-cylinder crankshaft is producing the same rotational forces.	29
4.10	The friction force $F = \mu N$ acts in the opposite direction from the journal rotation, ω , decreasing its speed.	31
4.11	F_{weight} and $F_{imbalance}$.	32
4.12	Graph to visually determine f_m .	33
4.13	The crank pin overlap (CPO) on both sides of the main journal increasing the rigidity of the crankshaft.	34
5.1	Simplified design of the Honda CRF250R crankshaft in the Crankshaft Balance Design Pro Plus interface.	36
5.2	Main bearing friction torque in Nm plotted against the crank angle for 0% balance factor.	36
5.3	Main bearing friction torque in Nm plotted against the crank angle for 28% balance factor.	37
5.4	Main bearing friction torque in Nm plotted against the crank angle for 50% balance factor.	37
5.5	Main bearing friction torque in Nm plotted against the crank angle for 64% balance factor.	38
5.6	Main bearing friction torque in Nm plotted against the crank angle for 100% balance factor.	38
5.7	The test rig with numbered components explained in Table 5.1.	40
5.8	The hexagon transducer-to-crankshaft adapter.	41
5.9	The current output at zero torque is 0.2V while 5V = 5Nm.	41
5.10	0.44 V corresponds to 0.25 Nm.	42
5.11	The flow of Test 1.	43
5.12	The flow of Test 2.	44
5.13	The UCP204 bearing. Image courtesy of The Timken Company	47
5.14	The RBE3 elements representing the bearings, considering the offset of the bearing sleeve.	47

5.15	FEDEM model of the rotor with one sensor, two revolute joints and one applied torque.	48
5.16	Control system for performance testing of the rotor in the FEDEM test bench.	48
5.17	The EL-motor brings the rotor up to a constant speed of e.g. 3000 RPM in 2 seconds and keeps it rotating with a constant speed for 1.5 seconds. . .	49
6.1	The 2015 HONDA CRF250R.	52
6.2	The Honda CRF250R crankshaft with highlighted features.	52
6.3	Simplification of a crankshaft in a balancing machine.	54
6.4	Counterweight + crankweb (highlighted) and their combined centre of gravity.	55
6.5	The balanced crankshafts with the amount of mass removed in terms of mm. Top: balanced to 63.75%. Bottom: balanced to 28%.	58
7.1	The friction force, F , acts in the opposite direction from the journal rotation, ω , reducing its rotational speed.	66
7.2	Dimensions and loading on the journal bearing from the crankshaft due to eccentricity.	68
7.3	Reducing the crankpin diameter increases the stroke.	70
7.4	A counterweight shoulder being modified with the <i>Offset Face</i> command. The correction depth is 3 mm.	72
7.5	Suggested flow of automatic crankshaft balancing program.	73
7.6	A splinified crankshaft counterweight with highlighted control points . . .	75
7.7	The complex Honda CRF250R crankshaft is simplified to a basic rotor. . .	76
7.8	Required torque to keep the rotor in Case 1 at 3000 RPM is 0.1949 Nm. . .	78
7.9	Required torque to keep the rotor in Case 1 at 6000 RPM is 0.3204 Nm. . .	78
7.10	Required torque to keep the rotor in Case 1 at 9000 RPM is 0.3696 Nm. . .	79
7.11	Required torque to keep the rotor in Case 2 at 3000 RPM is 0.1897 Nm. . .	79
7.12	Required torque to keep the rotor in Case 2 at 6000 RPM is 0.3670 Nm. . .	80
7.13	Required torque to keep the rotor in Case 2 at 9000 RPM is 0.3948 Nm. . .	80
7.14	Required torque to keep the rotor in Case 3 at 3000 RPM is 0.1988Nm. . .	81
7.15	Required torque to keep the rotor in Case 3 at 6000 RPM is 0.3555 Nm. . .	81
7.16	Required torque to keep the rotor in Case 3 at 9000 RPM is 0.3861 Nm. . .	82

Glossary

- Balance factor : The percentage of the reciprocating mass added to the counterweight and bob-weight.
- Bob-weight : A physical mass mounted on the crankpin during the balancing procedure to simulate the mass of the connecting rod and piston assembly. Used to determine the mass of the counterweight.
- Counterweight : Mass attached to the crankshaft in order to balance the rotating forces and some of the reciprocating forces.
- Overbalancing : Using a balance factor of more than 50%. resulting in higher transverse forces.
- Piston assembly : Piston, wristpin, clips, rings, oil.
- Stroke : The distance the piston travels from TDC to BDC.
- Underbalancing : Using a balance factor of less than 50%, resulting in higher in-line forces.
- Wristpin : Also called piston pin or gudgeon pin.
- Inertia : Here: short for mass moment of inertia.
- Rotor : Rotating object in a machine e.g. a crankshaft.

Nomenclature

m_{rec}	=	Reciprocating mass
	=	Mass of piston assembly, connecting rod small-end and small-end bearing.
m_{rot}	=	Rotating mass
	=	Mass of crankshaft, crankpin, connecting rod big-end and big-end bearing.
f_b	=	Balance factor
	=	The percentage of the reciprocating mass added to the counterweight.
m_{cw}	=	Counterweight mass
	=	$m_{rot} + f_b \cdot m_{rec}$
TDC	=	Top Dead Centre
	=	Position of the crankshaft when the piston is at the top position in the cylinder.
BDC	=	Bottom Dead Centre
	=	Position of the crankshaft when the piston is at the bottom position in the cylinder.
U	=	Unbalance due to an eccentric mass away from the rotational axis.
	=	$m_u \cdot e$
U_{per}	=	Permissible unbalance after the balancing procedure.
NVH	=	Noise, Vibration and Harshness.
θ	=	Crank angle.
	=	ωt
CG	=	Centre of gravity.
OEM	=	Original Equipment Manufacturer.
MMOI	=	Mass Moment of Inertia.

d = Bearing bore diameter.

μ = Constant bearing coefficient of friction.

F_m = Mean equivalent dynamic bearing load.

Chapter 1

Introduction

This thesis studies how engine balancing affects the performance of a single cylinder engine. Balancing is the act of redistributing the mass of a rotor, such that the rotor mass centre line coincides with the axis of rotor rotation [2]. Multiple research papers evaluate engine balance in terms of noise, vibrations and harshness (NVH), but very few document how engine balance affect engine performance specifically. During the research of this project, it was experienced that the engine-balancing community is roughly divided into those who possess knowledge but are reluctant to share it, and those who are not able to accurately justify their choices. This seems to be the general consensus:

Jack Kane in Race Engine Technology Magazine [3] states *"There was a general reluctance among the crankshaft experts with whom I spoke to discuss the expected or observed effects of these strategies"* when discussing different balancing strategies. Understanding the relevant software without proper documentation is also difficult, as Muszynska [2] points out: *"The balancing software of most vendors work as a "black box", which limits the understanding of the physical phenomena occurring in an unbalanced engine"*.

The considered key performance indicators (KPIs) are:

1. maximum crankshaft acceleration (Throttle response)
2. maximum operating speed (RPM)
3. maximum engine torque

Properties that may relate engine balance to these KPIs are friction loss in the crankshaft journal bearings and the influence on cylinder pressure build-up. As the latter require a profound knowledge of thermodynamics, this thesis focuses on how the crankshaft balance affects frictional losses, KPI #3. Also, the Appendices introduce a

discussion on how performing *crankshaft stroking* in the balancing process increases the engine displacement.

Chapter 2 explains the different types of balancing; static and dynamic, as well as the forces that arise in a reciprocating engine; primary and secondary. The complexity of the forces and moment to be balanced due to the varying inertia is introduced.

Chapter 3 presents several methods of performing the balancing procedure, as well as previous work by other researchers within this field. The balancing machine, which is still widely used and recommended, is described.

Chapter 4 investigates the slider-crank mechanism which is often used as a simplification of the single-cylinder reciprocating engine. An expression for the crankshaft bearing forces is derived, and how these forces are affected by using different balance factors is shown. A model for the bearing friction torque is derived as a means of predicting the loss of torque. The international standard for permissible residual imbalance is explained.

Chapter 5 presents both the physical testing and simulations of an unbalanced rotor. Performance testing in the software *Crankshaft Balance Design Pro Plus* is conducted where the friction torque in the main bearings is compared for crankshafts designed with different balance factors. The physical test is performed for both balanced and unbalanced cases to investigate the effects on friction torque due to imbalance. The friction data from this test is used in simulations to validate the derived friction model in Chapter 4.

Chapter 6 describes a general CAD-based procedure to predict the optimal correcting mass and its radius for crankshafts without having to use a balancing machine. The Honda CRF250R crankshaft is balanced using this procedure to 28% balance factor and 64% balance factor.

The software used in the different stages of this project are briefly presented below.

Crankshaft Balance Design Pro Plus

Crankshaft Balance Design Pro Plus [4] is utilised in the design and balancing of crankshafts in single-cylinder engines. The crankshaft design is given by the user as input parameters before it is analysed by the software (see Figure 1.1). The software will then produce information about the engine, such as the inertia and balance factor. The program can

suggest design changes to achieve a particular balance factor by inserting counterweights or by drilling holes in the crankshaft. The user supplies the program with engine characteristics (see Figure 1.2), and the software will perform calculations and produce graphs of bearing forces, engine torque, and acceleration.

The software was originally acquired to analyse how various balancing methods and balance factors affect the engine torque curves. That was, however, not possible as the torque curve is to be given as an input parameter, not produced as an output parameter. The software has instead been used mainly to validate the derived equations in Section 6.3.2 - *Formula for calculating the balance factor*, and to learn about how different balancing techniques (adding or removing a mass in various ways) affect the inertia, etc. in Appendix B.

Note that the software does not allow for a detailed crankshaft design. It is, unfortunately, developed for two-stroke engines only.

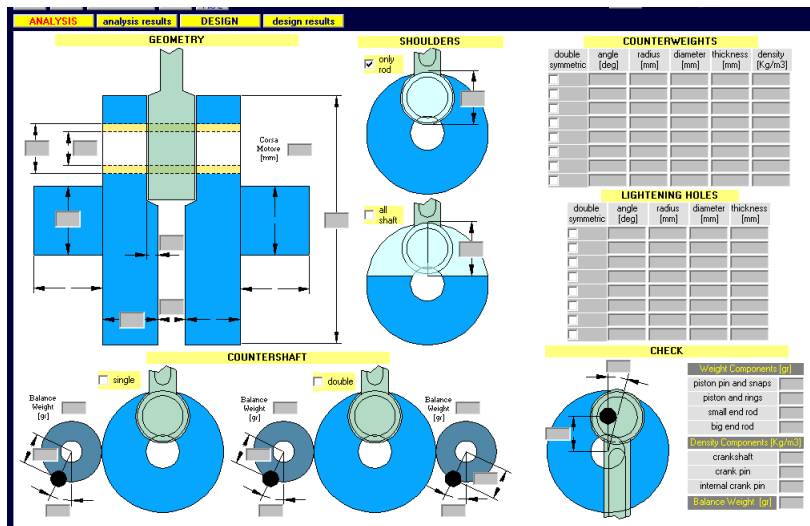


Figure 1.1: The crankshaft design environment in Crankshaft Balance Design Pro Plus.

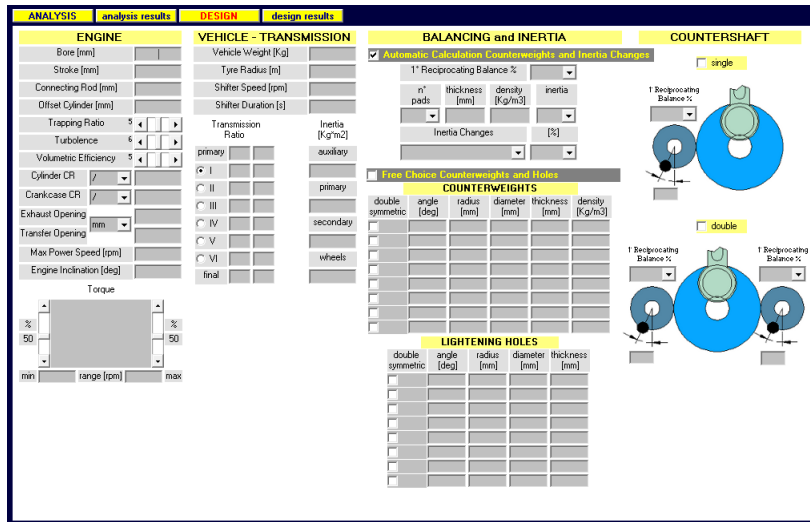


Figure 1.2: The engine design environment in Crankshaft Balance Design Pro Plus

FEDEM Test Bench (FTB)

The FEDEM Test Bench (FTB) is developed by Terje Rølvåg and Matteo Bella to simulate forces, stresses, and displacements in engine components under high-speed conditions [5]. Simulations in the FTB result in accelerations-, bearing force- and output torque curves, which is used to evaluate the balanced crankshafts in Chapter 6 - *CAD-based balancing of the Honda CRF250R*.

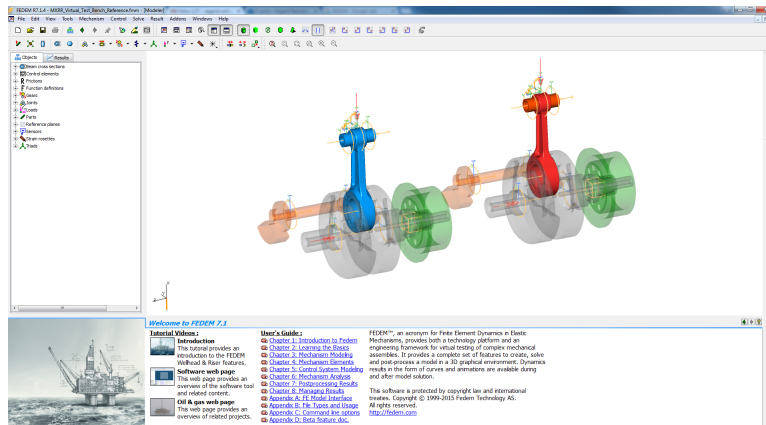


Figure 1.3: The FEDEM Test Bench with an OEM engine and an MXRR engine.

Siemens NX

Siemens NX [6] is used to obtain the mass properties of different engine components and to create 3D-models of the balanced crankshafts in Chapter 6. NX is also used when evaluating approaches for automatic engine balancing in Appendix D and to model and mesh the simplified crankshaft for FEDEM simulation in Chapter 5.

Chapter 2

Engine dynamics

The motion of, and the complex forces acting in a single-cylinder reciprocating engine are complicated to predict and makes analytical balancing difficult. The following sections discuss the essential theory of balancing and the rise of the different forces and moments in such an engine. At the end of the chapter a short presentation of the modelling of the inertia and engine torque is presented, where accuracy considering performance predictions is emphasised.

2.1 Static and dynamic balancing

When balancing a crankshaft where the mass cannot be assumed to be in a single rotating plane, one must ensure that it is both statically and dynamically balanced. A crankshaft is statically balanced when every mass is coupled with a mass that results in the same force on the opposite side of the rotational axis [1].

In Figure 2.1a, the crankshaft is statically balanced regarding the moments, but not regarding the forces. In Figure 2.1b, the forces are balanced, but not the moments. The unbalanced moments create a *rocking couple* as seen in Figure 2.2 [7].

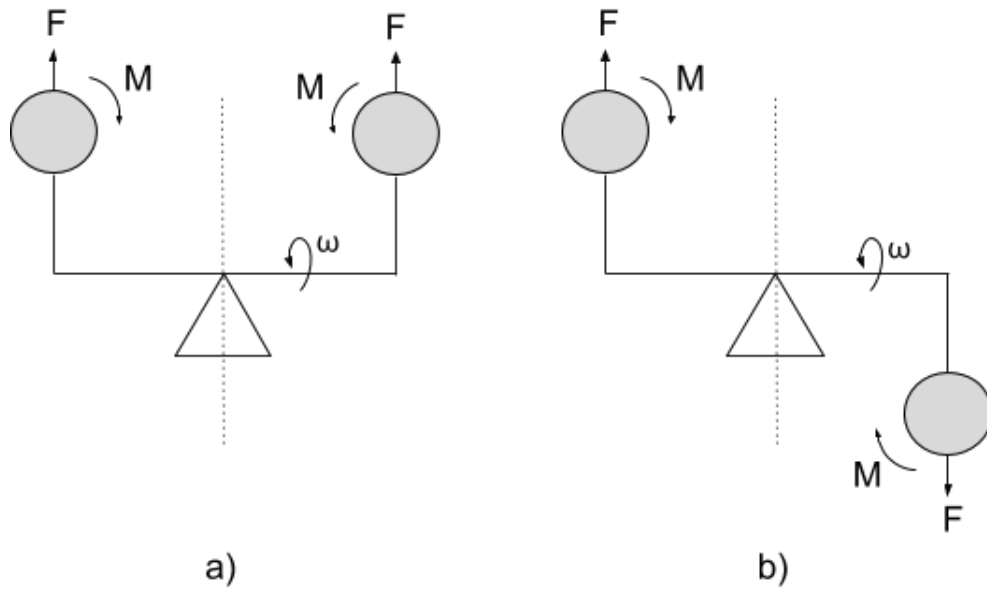


Figure 2.1: Two examples of static balancing in one correction plane. Crankshaft a) is balanced regarding moments, but not regarding forces. Crankshaft b), on the other hand, is balanced regarding forces, but not regarding moments.

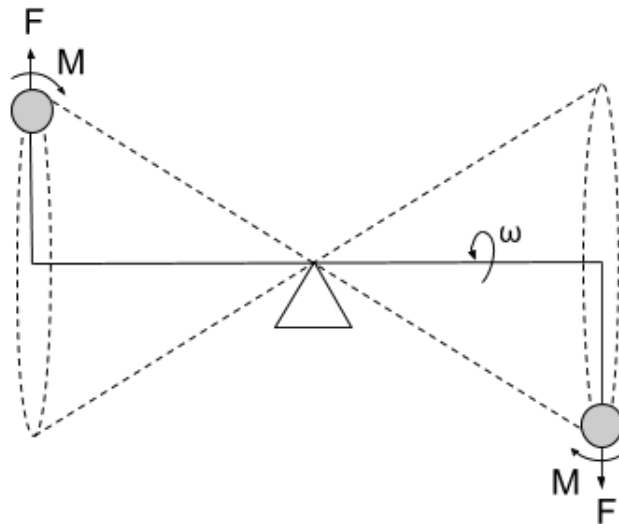
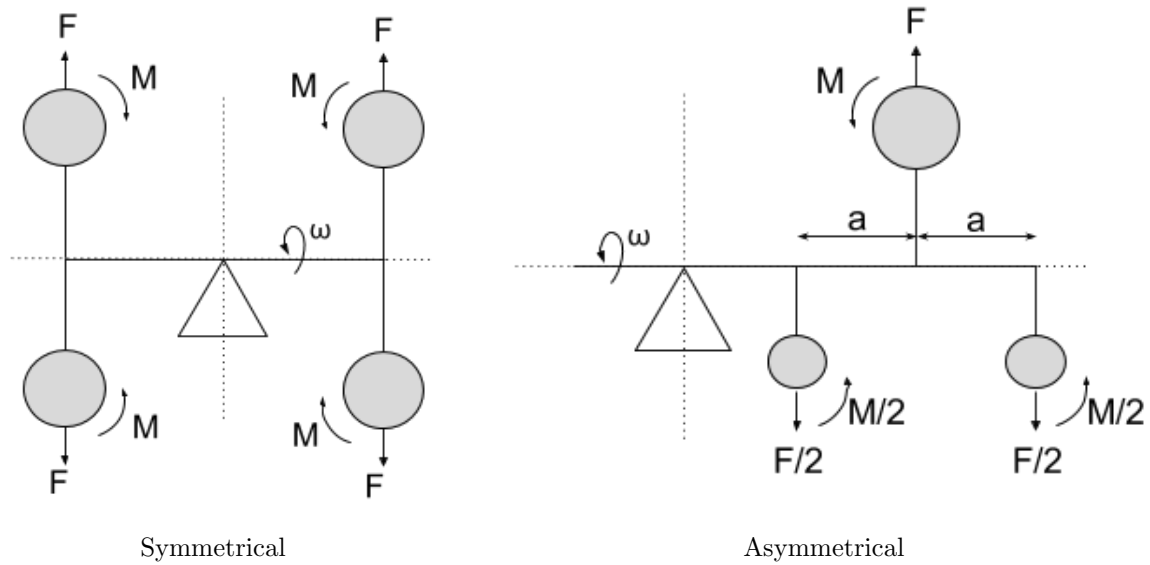


Figure 2.2: Statically force-balanced crankshaft set in motion, creating a rocking couple due to unbalanced moments.

The rocking couple in Figure 2.2 is balanced by adding another couple of the same magnitude on the opposite side of the rotational axis [1], as shown in the examples in Table 2.1.

Table 2.1: Dynamically balanced symmetric and asymmetric rotors.



A rotor is dynamically balanced when both the sum of forces and the sum of moments about the centre of gravity are zero. A dynamically balanced rotor is therefore always statically balanced, but the opposite is not necessarily true.

2.2 Forces in the engine

The crankshaft is subjected to forces from the rotating and the reciprocating masses of the engine as well as combustion forces [7]. The orientation of the reciprocating forces changes with the translation of the piston inside the cylinder. The rotating masses cause forces that rotate with the crankshaft.

2.2.1 Primary and secondary forces

As the piston moves, the connecting rod transfers the reciprocating motion into rotational motion of the crankshaft. The maximum combustion pressure occurs just after *top-dead-centre* (*TDC*) (see Figure 2.3), resulting in the rotation of the crankshaft.

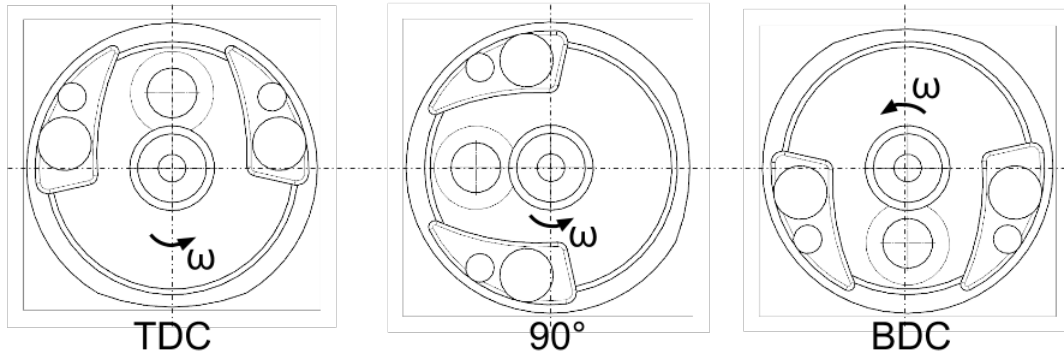


Figure 2.3: The crankshaft is at *Top Dead Centre (TDC)* when the crankpin is at $\approx 0^\circ$ and *Bottom Dead Centre (BDC)* when the crankpin has been moved to $\approx 180^\circ$.

Primary forces are the forces which frequency is equal to that of the crankshaft [8].

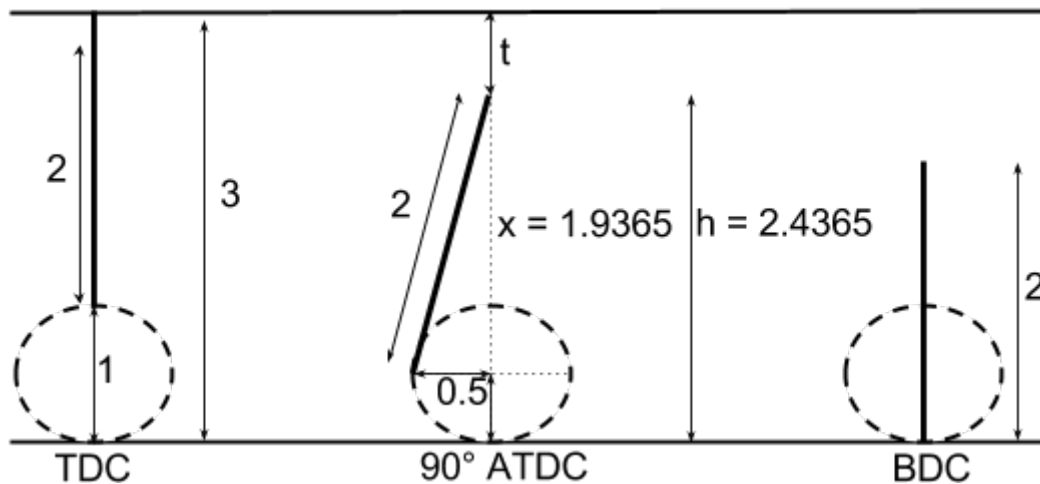


Figure 2.4: The rise of the secondary forces: The distance travelled by the connecting rod is greater from TDC to 90° ATDC than from 90° ATDC to BDC.

In Figure 2.4 the stroke is of 1 unit length and the connecting rod is equal to 2 units, resulting in a total height of 3 units. Intuitively, one would think that when the crankshaft has rotated to 90° after TDC (ATDC), the piston would have travelled half the stroke, but simple geometric calculations prove otherwise. Using Pythagoras, the value of x is calculated, and by using the dimensions in Figure 2.4, the piston translation, t , from TDC to 90° ATDC is calculated to:

$$t = 3 \text{ units} - h = 3 \text{ units} - 2.4365 \text{ units} = 0.5635 \text{ units}$$

It is easy to see that the piston has travelled more than half its stroke when the crankshaft has rotated from TDC to 90° ATDC:

$$\frac{1}{2} \cdot S = 0.5 \text{ units} < t = 0.5635 \text{ units}$$

This is also shown graphically in Figure 2.5:

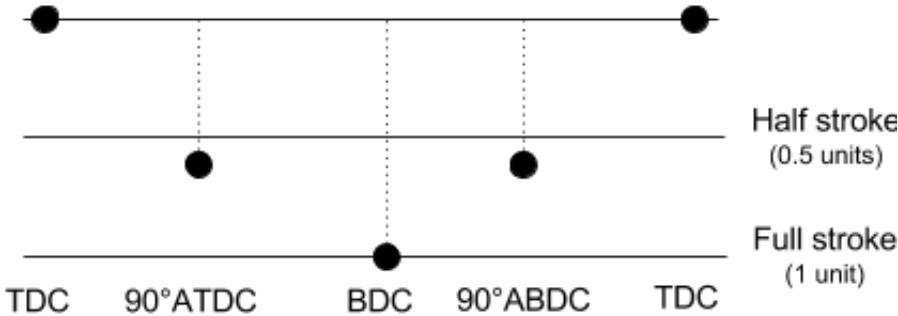


Figure 2.5: The piston translates a longer distance from TDC to 90° ATDC than from 90° ATDC to BDC. This is repeated on the way up from BDC to TDC as well.

As the piston travels a longer distance in the first and fourth quadrant of the rotating circle, the crankshaft is accelerated, and this acceleration means that the piston is moving faster at the top than at the bottom of the rotational circle (see Figure 2.6). The change of acceleration twice in one crankshaft rotation gives rise to secondary forces, i.e. forces with a frequency equal to twice the crankshaft rotation.

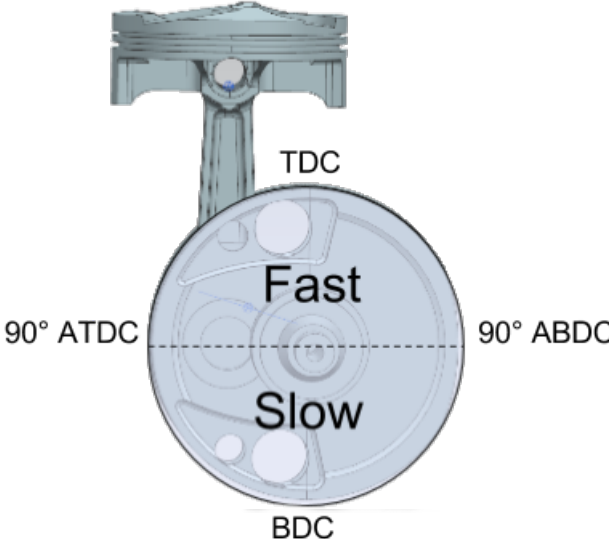


Figure 2.6: The piston accelerates from TDC to 90° ATDC and from 90° ABDC to TDC, and slows down from 90° ATDC to 90° ABDC, resulting in secondary forces.

2.3 Varying mass moment of inertia and torque

As the position of the reciprocating mass of the engine and the connecting rod changes during the crank revolution, the inertia of the crankshaft assembly varies with each crank angle. Many published analytical models for calculating engine characteristics use the average inertia as a simplification, ignoring its cyclical behaviour [9].

Combustion in the cylinder exerts a force on the crankpin and creates a torque around the crankshaft. The magnitude of the torque affects the engine acceleration due to the relation: $T = I \cdot \dot{\omega}$. The engine torque comprises of three torques that change with the crank angle θ :

$T_{inertia}(\theta)$: torque due to varying mass moment of inertia of the connecting rod and piston masses.

$T_{gas}(\theta)$: torque due to gas forces in the cylinder.

$T_{friction}(\theta)$: torque due to friction in bearings.

$$T = T_{inertia}(\theta) + T_{gas}(\theta) - T_{friction}(\theta)$$

A common simplification of the reciprocating engine is the slider-crank mechanism which is discussed in Chapter 4. This model can be used when calculating forces and bending moments quite accurately, but may be too inaccurate in torque calculations [10].

Chapter 3

State of the art in Engine Balancing

The act of balancing is a means of evening out unwanted vibrations and forces in the engine caused by an unbalanced mass. The primary unbalance is usually balanced by adding or subtracting mass to the crankshaft, while secondary unbalance is generally handled by balancing shafts, which will not be addressed in this thesis. The state of the art of calculating the correcting masses for high-speed rotors is either by using the analytical Modal Analysis Method or the empirical Influence Coefficient Method [2].

Modal Analysis Method

When an engine is required to operate at high speeds, it often needs to pass through *critical speeds* before it reaches its *operational speed*. At critical speeds, where the torsional vibrations are severe, resonance may occur [10]. Therefore, the engine needs to be balanced so that vibrations during operating speed does not result in resonance. In general, a rigid rotor can be balanced in two planes, while a flexible rotor is balanced in N planes, where N is the number of modes needed to be balanced [11].

Jeffcot and Föppl were some of the first to develop vibration theory for rotor dynamics [12]. Their simplified model of a rotor was extended for modal analysis by Bishop [13], which consists of balancing the different modes of the rotor one after the other. Figure 3.1 shows the two first modes of a rotor with the corresponding balancing planes where mass is either added or removed to obtain balance. It is important that a correctional mass in the current balancing plane does not interfere with the previously balanced modes [2].

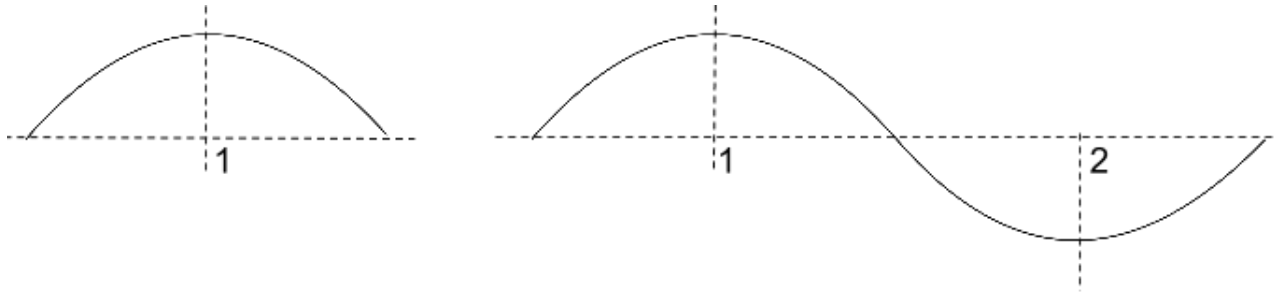


Figure 3.1: The first and second modes of a rotor with its corresponding balancing planes.

Influence Coefficient Method

In this method, the corrective mass is determined empirically by using a balancing machine (see Section 3.2). Mass is added to or removed from predetermined balance planes in a progressive manner until the optimal vibration tolerance is achieved [2]. Thus, the unbalance occurring somewhere in the engine is translated to corresponding unbalance at the correction planes, where it can be balanced. The Influence Coefficient method often requires a higher number of engine runs compared to the Modal Analysis method, as the latter retrieves more information from initial analysis [2].

3.1 Different methods of balancing

Analytical models of reciprocating engines have traditionally included a simplification of the engine to a slider-crank mechanism with two concentrated masses. The concentrated masses allows for assuming one purely rotating mass and one purely reciprocating mass of the engine when calculating forces on the system, as will be explained in Chapter 4.1. As sensors and computer power evolved, sensor data has been added to the analytical models during engine operation to help predict more accurate correction weight for balancing. In the following sections, several research papers and educational books concerning balancing of a reciprocating engine will be presented.

3.1.1 Analytical models – the slider-crank mechanism

The reciprocating engine is usually modelled as a slider-crank mechanism where the forces that act on the connecting rod, and ultimately on the crank throw, are comprised of the piston pressure, inertia forces, and friction forces. The piston pressure and inertia forces have a cyclic behaviour, but the friction force is often omitted or made constant as it is difficult to predict at each crank angle [14].

Patterson [14] calculates the torque on the crankshaft from the product of the net force and the effective lever arm using the slider-crank mechanism approach. However, the friction forces are not included in the net force. Balancing of the first harmonic (primary force) is performed by adding a counterweight on the crankshaft at the opposite side of the unbalance. This is done to change the direction of the lateral forces.

Borowski *et al.* [15] suggest balancing by the use of a pendulum. Both their nonlinear computer analysis and a physical test showed a 90% decrease of torsional vibrations in a four-cylinder in-line engine. A problem for four-cylinder engines is high block translational vibrations at high speeds. Unfortunately, the tests showed marginal improvements in reduction of block shaking forces. The research focuses mainly on performance regarding NVH (noise, vibration and harshness).

Norton [16] is a well-known, often-cited professor who has written several books on machine dynamics. He simplifies the reciprocating engine to a slider-crank mechanism as well but does not include the rotating masses in the engine torque equation. In practice, this means that one can attach an infinitely large rotating mass at the counterweight or crankpin without experiencing any difference in total torque. This seems unreasonable, and begs the question whether these equations can be considered valid.

3.1.2 Semi-empirical models – sensor data during operation

Analytical models can be extended with empirical data measured while the engine is operating. The data usually concerns the temperature, pressure, and viscosity of the oil film in the bearings and piston assembly, cylinder pressure throughout the stroke, or measured engine torque or bearing forces. Balancing is performed in a trial-and-error manner in a Balancing Machine but data can be analysed on the computer simultaneously to find the optimal correction weight faster.

O’Leary and Gatecliff [17] present a software that calculates the cyclic bearing forces and the dynamic unbalance of a single-cylinder engine based on the inertia, the geometry and the location of all the moving parts of the engine, as well as the cylinder pressure history. The output is polar plots where circles represent different $m_u \cdot e$ pairs. Balancing is done by trial and error using different correctional masses at various locations to fit the unbalanced forces within the smallest possible circle in the polar plot.

Levecque *et al.* [18] present a numerical method to calculate the single-cylinder reciprocating compressor's counterweight masses and locations in a trial-and-error manner. The forces used in this method are based on the reaction forces in the bearings, as the result of an analysis of a finite element model of the compressor. Only the synchronous part of the reciprocating forces are considered in the balancing procedure, as it is assumed that this corresponds to the load supported by the bearings.

Yang *et al.* [19] created a CAD model of the connecting rod to establish its precise centre of mass. Thus, the rotating part and the reciprocating part of the connecting rod are completely separated at this point, and their respective masses can be calculated. A multi-body dynamics model is made of the crankshaft, piston, flywheel, balance shafts and a flexible connecting rod. The masses of the piston, piston pin, crankshaft and flywheel densities are set to zero, and there is no gas pressure acting on the piston during analysis. This is because the test is to show the effect on the main bearing loads due to inertial forces caused by the connecting rod's motion only. The optimal counterweight mass is found by trial-and-error as the mass that results in the lowest measured bearing load.

As can be seen from the above-mentioned research papers and books, as well as additional research, there is a substantial amount of literature about engine balancing. They mainly focus on reducing vibrations to reduce noise and discomfort for the rider, and present inaccurate analytical models or are highly dependent on sensor data. There is, however, little documentation of how engine balancing specifically affects the engine performance regarding engine speed, throttle response or engine torque. Due to simplifications in analytical models, authors still encourage the use of a balancing machine.

3.2 Balancing Machines

A balancing machine is used to measure the unbalanced force couple in rotors. Mass is added or removed from the correction planes to create a new couple in the opposite direction, i.e. balance the forces created by the imbalance [20]. Both the magnitude and the angular location of the correctional masses need to be measured in each correction plane. The mass of the piston assembly and the connecting rod is added to the crankshaft as a *bob-weight* [5], and the crankshaft is rotated by an electrical motor.

Pivoted-cradle

In a pivoted-cradle balancing machine, such as the one in Figure 3.2, the vibration amplitudes are measured by transducers in half bearings or rollers. The cradle can be rocked about either of the two pivot points which coincide with the correction planes. By locking one pivot at a time, the unbalance measured for one correction plane is entirely independent of the unbalance in the other correction plane [1]. The mass and angle of an unbalance in the crankshaft that is measured at the bearings can be translated to the correction planes where they are balanced.

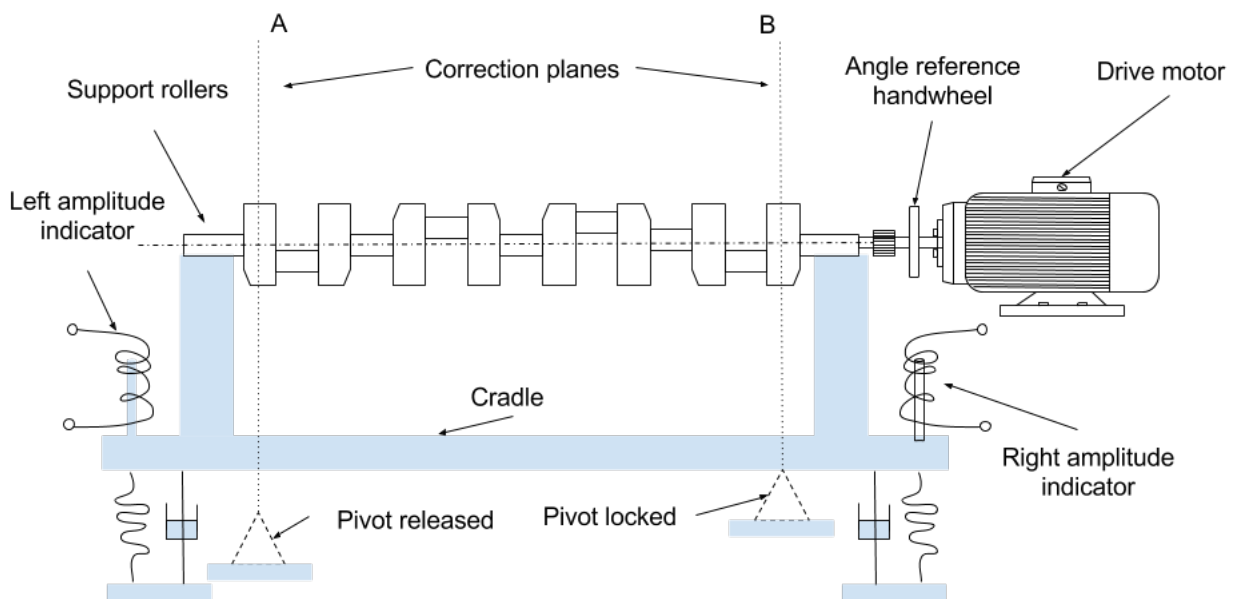


Figure 3.2: A pivoted-cradle balancing machine [1].

Nodal-point

The other common type of balancing machines is the nodal point balancing machine. A nodal point is a point on the rotor where the vibration is zero or at its minimum [1]. The unbalance in correction plane B in Figure 3.3 causes the entire assembly to oscillate around the nodal point O. The nodal point, is located by sliding a dial indicator along the nodal bar. The unbalance in correction plane A can be measured at the nodal point and is independent from the unbalance in correction plane B. After adding or removing a correctional weight in plane A, the next nodal point can be found and the balancing procedure is repeated until satisfactory unbalance tolerances are obtained.

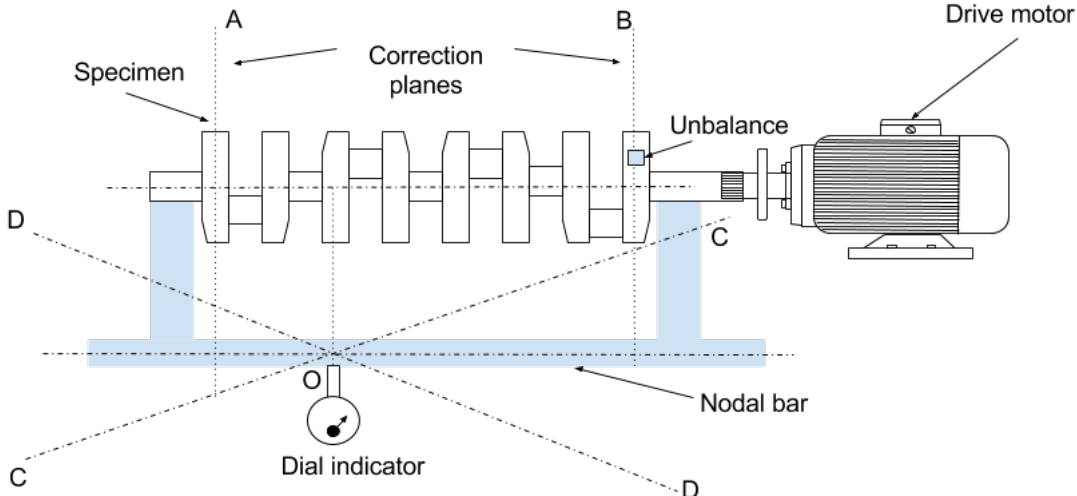


Figure 3.3: A nodal-point balancing machine [1].

Chapter 4

Balancing theory

This chapter presents the essential theory in engine balancing, including a mathematical model of the forces arising during engine operation for a single cylinder engine. Research regarding performance effects due to balancing is discussed. The maximum allowed residual unbalance for a Honda CRF250R is determined at the end of the chapter using the international ISO1940 standard.

4.1 Essential theory

The single-cylinder reciprocating engine is subjected to rotational forces from the crankshaft and reciprocating forces from the piston assembly. The complex motion of the connecting rod is one of the challenges when working with this system: The big-end, which is attached to the crankpin, is subjected to a purely rotating motion. The small-end, attached to the wristpin is restricted to the reciprocating motion of the piston. The rest of the connecting rod will move in a motion that is neither purely rotational nor purely reciprocal [14]. Unless properly balanced, these forces may negatively affect the engine performance, as well as causing vibrations that may be harmful to the vehicle and the rider.

This section considers the unbalanced forces, and how attaching counterweights to the crankshaft can help balance the system.

4.1.1 Static balancing of the slider-crank mechanism

The challenges that occur when working with the complex motion of the connecting rod are avoided by considering the single-cylinder engine as a slider-crank mechanism. The connecting rod is divided into two concentrated masses located at the crankpin and wristpin, making the connecting rod itself mass-less. The connecting rod simplification is illustrated in Figure 4.1.

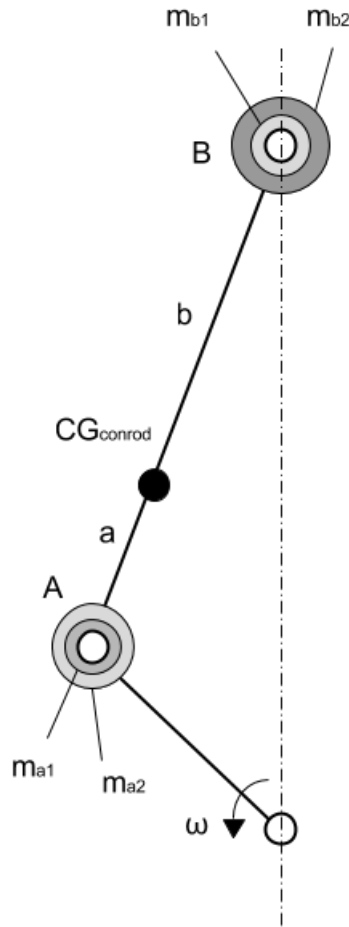


Figure 4.1: The simplified system with lumped masses at each end of the connecting rod.

The decomposed system now consists of a set of different masses:

Table 4.1: Masses of the slider-crank mechanism.

m_{a1}	The mass of the connecting rod big-end, located at the crankpin
m_{b1}	The mass of the connecting rod small-end, located at the wristpin
m_{a2}	The mass of the crankpin
m_{b2}	The mass of the piston assembly (piston, wristpin, clips, rings and oil)

The crankweb is considered massless for the time being but has to be accounted for when balancing an actual crankshaft in Chapter 6.

The decomposed, simplified connecting rod must fulfil three conditions to be valid:

1. The combined mass of the connecting rod big-end, m_{a1} , and the connecting rod small-end, m_{b1} , must be equal to the mass of the entire connecting rod, m_{conrod} :

$$m_{a1} + m_{b1} = m_{conrod}$$

2. The centre of gravity of the connecting rod is unaffected:

$$m_{a1} \cdot a = m_{b1} \cdot b \quad , \text{ where } a \text{ and } b \text{ are the distances from } m_{a1} \text{ to } CG_{conrod} \text{ and } m_{b1} \text{ to } CG_{conrod}, \text{ respectively.}$$

3. The moment of inertia is unaffected:

$$m_{a1} \cdot a^2 + m_{b1} \cdot b^2 = I_{conrod}$$

As there are only two unknown parameters (m_{a1} and m_{b1}) in these three equations, it is only possible to satisfy two out of the three conditions. According to Prof. Amitabha Ghosh [21], it should be sufficient to satisfy only equation 1 and 2.

The different masses listed in Table 4.1 can be combined as two distinct masses, m_{rot} and m_{rec} , depending on whether they are subjected to a rotating- or reciprocating motion.

The rotating mass consists of the crankpin and the big-end of the connecting rod:

$$m_{rot} = m_{a1} + m_{a2} \tag{4.1}$$

The reciprocating mass consists of the piston assembly and the small-end of the connecting rod:

$$m_{rec} = m_{b1} + m_{b2} \tag{4.2}$$

These masses produce unbalanced forces when the engine is operating, shown as F_{rot} and F_{rec} in Figure 4.2.

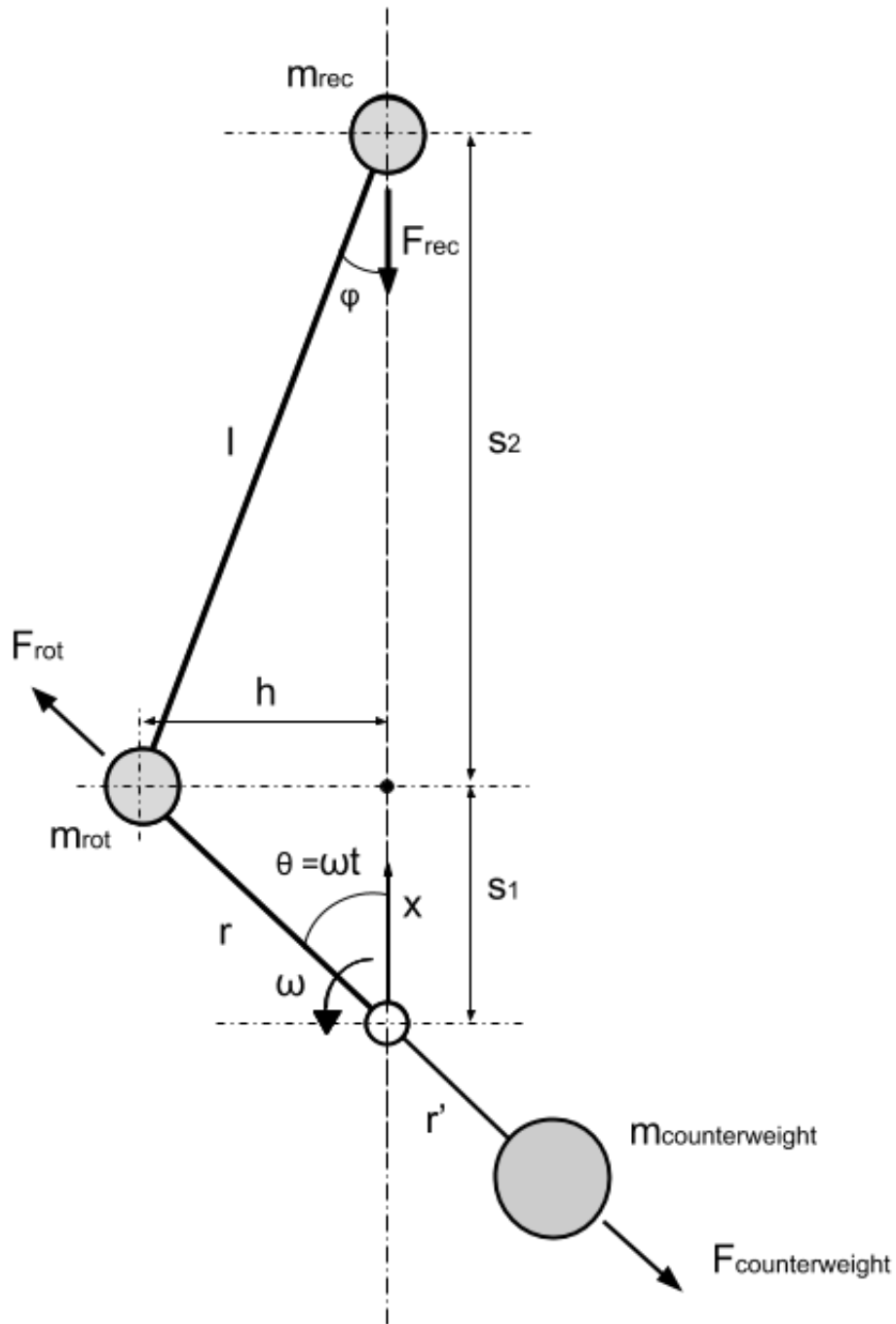


Figure 4.2: The masses combined as rotating and reciprocating masses, and the forces they produce. A counterweight is added 180 degrees from the crankpin and dimensions are added to the system.

The force from the rotating mass, m_{rot} , is easily balanced by attaching a rotating counterweight on the crankshaft 180° opposite to m_{rot} . The reciprocating force, on the other hand, is more difficult to balance. The reciprocating force is transmitted from the piston along the connecting rod, through the crankshaft and onto the main journal where it causes what may be severe vibrations. To reduce these vibrations, the effect of the unbalanced forces acting on the crankpin need to be investigated. The reciprocating force is the only one that needs to be considered, as the counterweight balance the rotating force.

The reciprocating force is expressed as $F_{rec} = -\ddot{x} \cdot m_{rec}$, where \ddot{x} represents the acceleration of the piston. An expression for \ddot{x} is needed to calculate the reciprocating force, F_{rec} . The relations and dimensions used are found in Figure 4.2.

The piston displacement, x , can be expressed as : $x = s_1 + s_2 = r \cdot \cos \theta + l \cdot \cos \phi$
and the leverage at each crank angle : $h = r \cdot \sin \theta = l \cdot \sin \phi$

Further, $\sin \phi = \lambda \sin \theta$ and $x = r \cdot \cos \theta + l(1 - \lambda^2 \sin^2 \theta)^{1/2}$, where $\lambda = \frac{r}{l}$

$$\frac{x}{r} = \cos \theta + \frac{1}{\lambda}(1 - \lambda^2 \sin^2 \theta)^{1/2} \quad , \quad \lambda^2 \sin^2 \theta < 1$$

Expanded into a rapidly converging series by the binomial theorem [22]:

$$\frac{x}{r} = \cos \theta + \frac{1}{\lambda} - \frac{\lambda}{2} \sin^2 \theta - \frac{\lambda^3}{8} \sin^4 \theta - \dots$$

$$\begin{aligned} \frac{x}{r} &= \left(\frac{1}{\lambda} - \frac{\lambda}{4} - \frac{3\lambda^3}{64} - \frac{5\lambda^5}{256} - \dots \right) \cos \theta \\ &+ \left(\frac{\lambda}{4} + \frac{\lambda^3}{16} + \frac{15\lambda^5}{512} + \dots \right) \cos 2\theta \\ &- \left(\frac{\lambda^3}{64} + \frac{3\lambda^5}{256} + \dots \right) \cos 4\theta \\ &+ \left(\frac{\lambda^5}{512} + \dots \right) \cos 6\theta \end{aligned}$$

Resulting in:

$$\frac{-\ddot{x}}{r} = \omega^2 (\cos \omega t + A_2 \cos 2\omega t - A_4 \cos 4\omega t + A_6 \cos 6\omega t + \dots), \quad \theta = \omega t$$

where: $A_2 = \lambda + \frac{\lambda^3}{4} + \frac{15\lambda^5}{128} \dots$, $A_4 = \frac{\lambda^3}{4} + \frac{3\lambda^5}{16} + \dots$, $A_6 = \frac{9\lambda^5}{28} + \dots$

Considering the practical situation, it is possible to simplify the infinite series by

requiring that $\lambda = \frac{l}{r} < 1$. Hence, λ^2 and higher orders are sufficiently small to be omitted. By this assumption, the acceleration of the piston can be expressed as:

$$\ddot{x} = -\omega^2 \cdot r \cdot \cos \omega t - \lambda \cdot \omega^2 \cdot r \cdot \cos 2\omega t \quad (4.3)$$

The reciprocating force is then expressed as:

$$F_{rec} = m_{rec} \cdot \omega^2 \cdot r \cdot \cos \omega t + \frac{\lambda \cdot m_{rec}}{4} \cdot (2\omega)^2 \cdot r \cdot \cos 2\omega t \quad (4.4)$$

Where $(m_{rec} \cdot \omega^2 \cdot r \cdot \cos \omega t)$ and $(\frac{\lambda \cdot m_{rec}}{4} \cdot (2\omega)^2 \cdot r \cdot \cos 2\omega t)$ represents the primary and secondary force, respectively.

Balancing the secondary force requires the use of balance shafts, and will not be considered here. The primary reciprocating force to be balanced is then written as:

$$F_{rec} = m_{rec} \cdot \omega^2 \cdot r \cdot \cos \omega t \quad (4.5)$$

The reciprocating force acting along the cylinder axis (in-line) can be balanced by adding m_{rec} to the counterweight. The first order reciprocating force will then be completely balanced when the piston is at TDC and BTC. However, adding m_{rec} to the counterweight will also create a force equal to F_{rec} acting transversely to the cylinder axis, with its peak at mid-stroke. Instead of eliminating the unbalanced force, it is shifted 90 degrees, illustrated in Figure 4.3.

The reciprocating force can be reduced along the cylinder axis by adding a percentage of the reciprocating mass to the counterweight. This percentage is called the *balance factor* and is denoted by f_b . A low balance factor will give higher in-line forces while a high balance factor will give higher transverse forces. The mass of the counterweight, m_{cw} , will then be:

$$m_{cw} = m_{rot} + f_b \cdot m_{rec} \quad (4.6)$$

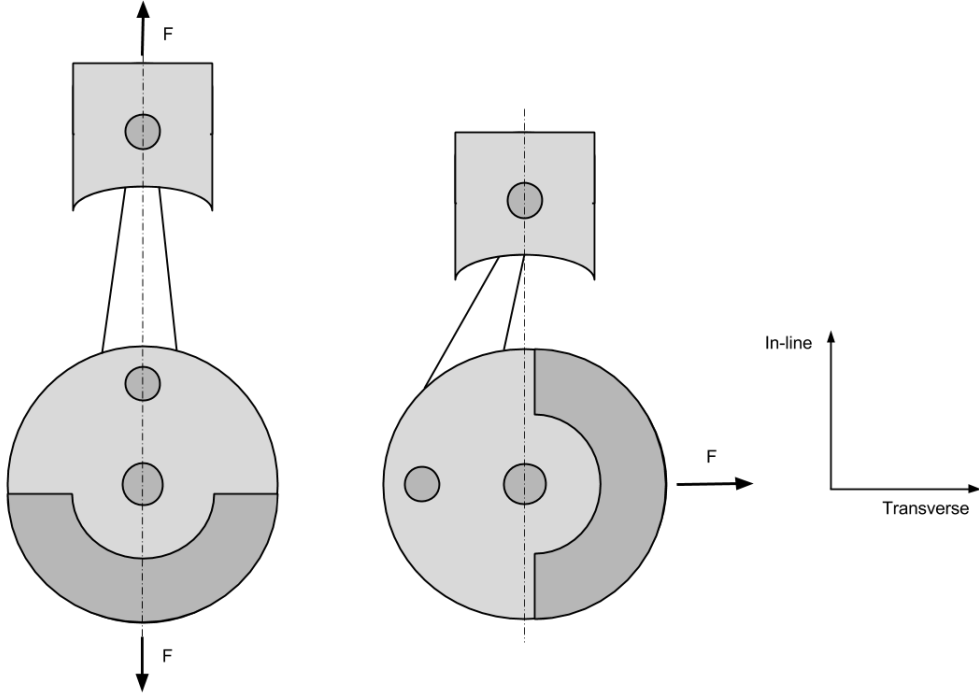


Figure 4.3: Attaching m_{rec} to the counterweight balances the reciprocating forces at TDC and BDC, but introduce a transverse force during the rest of the stroke.

4.1.2 Different balance factors

The following section (Chapter 4.1.2) is based on our project thesis [23]. A simple MATLAB script is created to analyse the effect of different balance factors. The in-line and transverse forces are plotted with the crank angle. In the script, the in-line and transverse forces are expressed as

$$F_i = m_{rec}r\omega^2 \cdot \cos\theta - m_{rec}r\omega^2 \cdot f_b \cdot \cos\theta \quad (4.7)$$

$$F_t = 0.0 - m_{rec}r\omega^2 \cdot f_b \cdot \sin\theta \quad (4.8)$$

respectively, where $m_{rec}r\omega^2 = 1$ for simplicity when interpreting the results.

Equations 4.7 and 4.8 require that the distance from the main journal to the counterweight (r') equals the distance from the main journal to the crankpin (r). $m_{rec}r\omega^2 \cdot \cos\theta$ in Equation 4.7 represents the force from the reciprocating mass along the cylinder axis. This force does not exist in the transverse direction and is therefore set to 0.0 in Equation 4.8.

As shown in Figure 4.4, a balance factor $f_b = 1.0$ will balance the in-line force entirely, but introduce a transverse force normal to the axis of the cylinder. The reciprocating

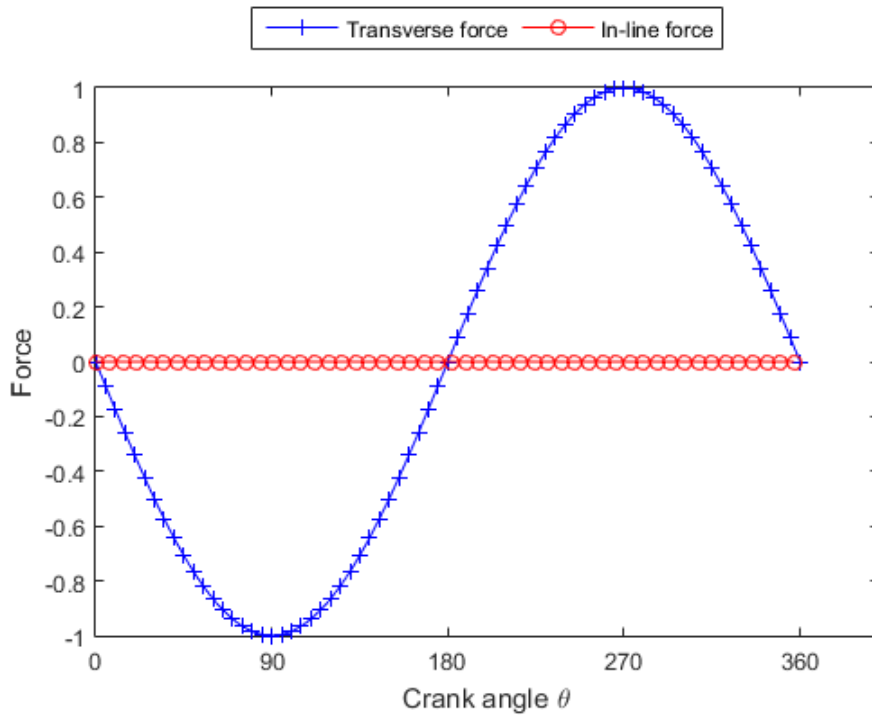


Figure 4.4: In-line and transverse forces with $f_b = 1.0$.

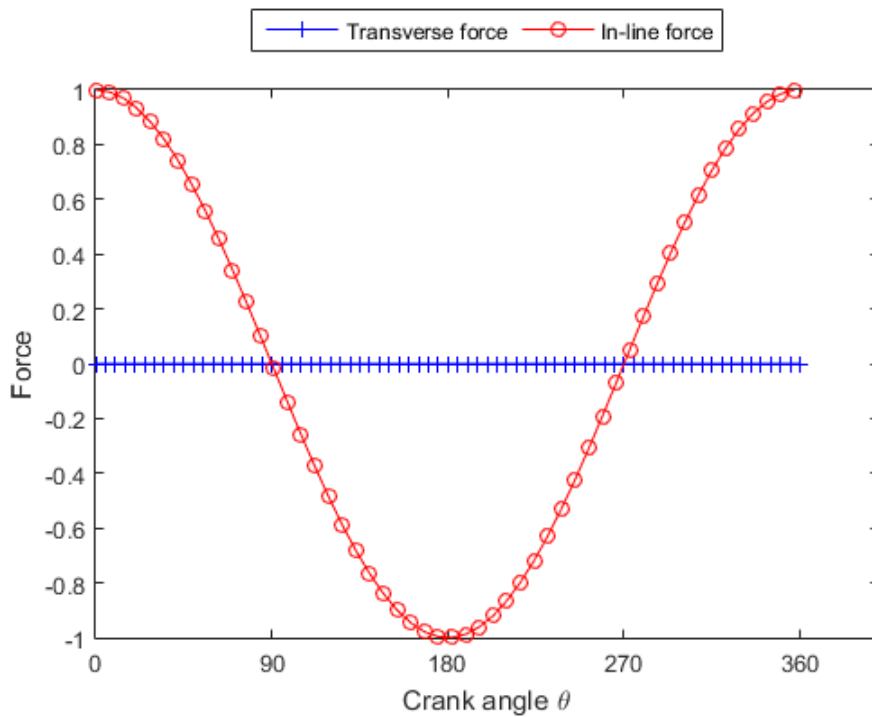


Figure 4.5: In-line and transverse forces with $f_b = 0.0$.

force is only balanced when the cylinder is at TDC (0° and 360°) and BDC (180°), while the transverse rotating force is acting during the rest of the stroke.

Conversely, a balance factor $f_b = 0.0$ will result in an in-line force only (Figure 4.5).

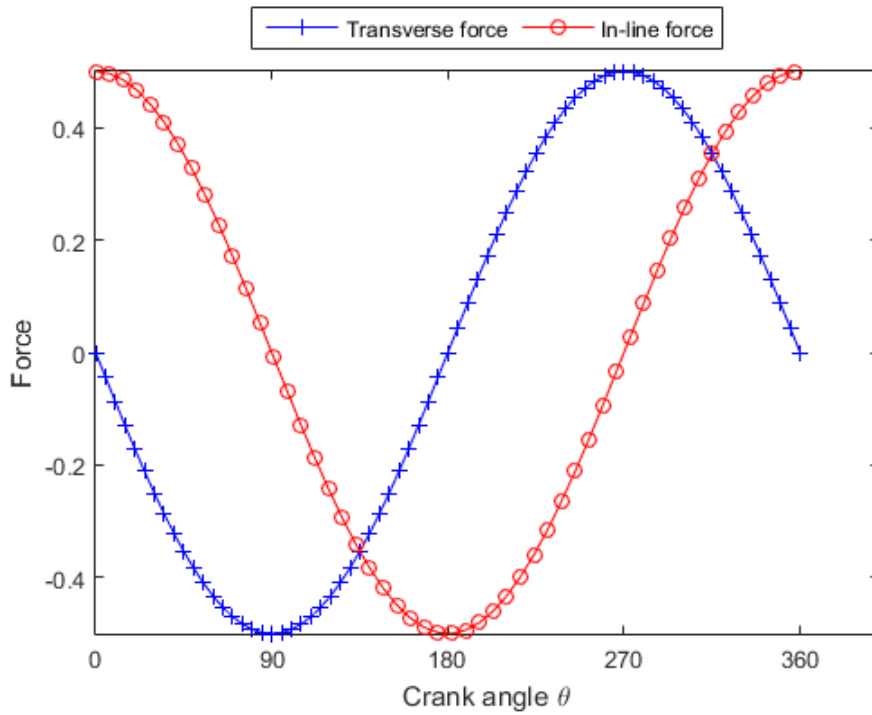


Figure 4.6: In-line and transverse forces with $f_b = 0.5$.

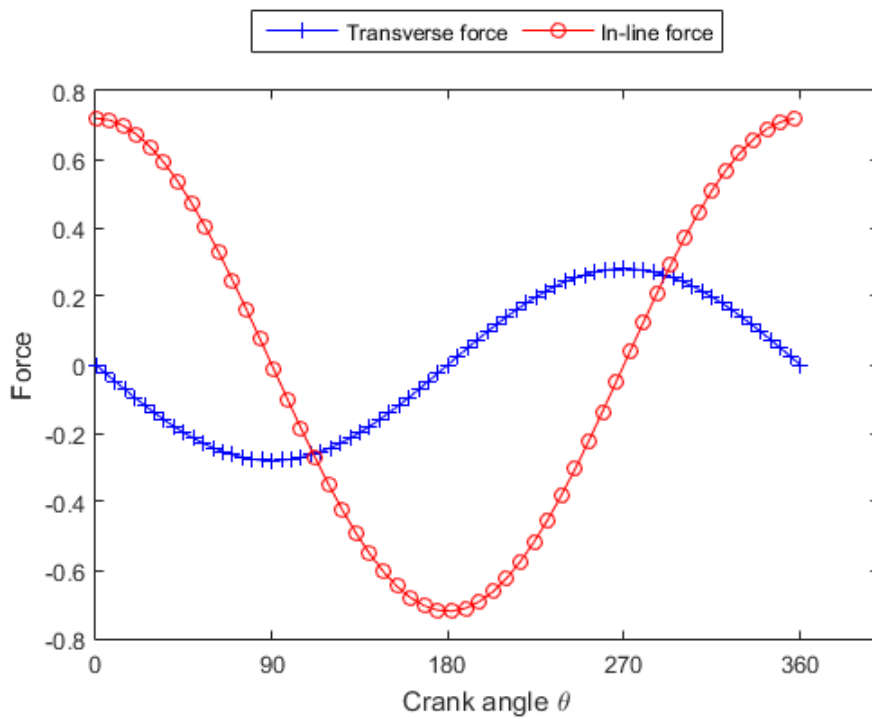


Figure 4.7: The in-line and transverse forces with $f_b = 0.28$.

A balance factor of 50% is often used as it results in the lowest resultant force (see Figure 4.8): half the reciprocating force is pointing radially outward from the crank axis. However, it is important to notice that this does not automatically mean that a 50% balance factor is ideal in all situations. The correct balance factor is determined by several factors, such as engine layout, how the engine is mounted in the frame, the stiffness of the frame in various directions and the vibration characteristics of the entire motorcycle. It often needs to be determined through experiments [24]. 28% balance factor is tested in the scripts, as this balanced factor has indicated good results for the Honda CRF250R [5]. Patterson [14] states that overbalancing (using more than 50% balance factor) may be favourable for a motorcycle as it is more comfortable for the rider having vibrations in the horizontal plane.

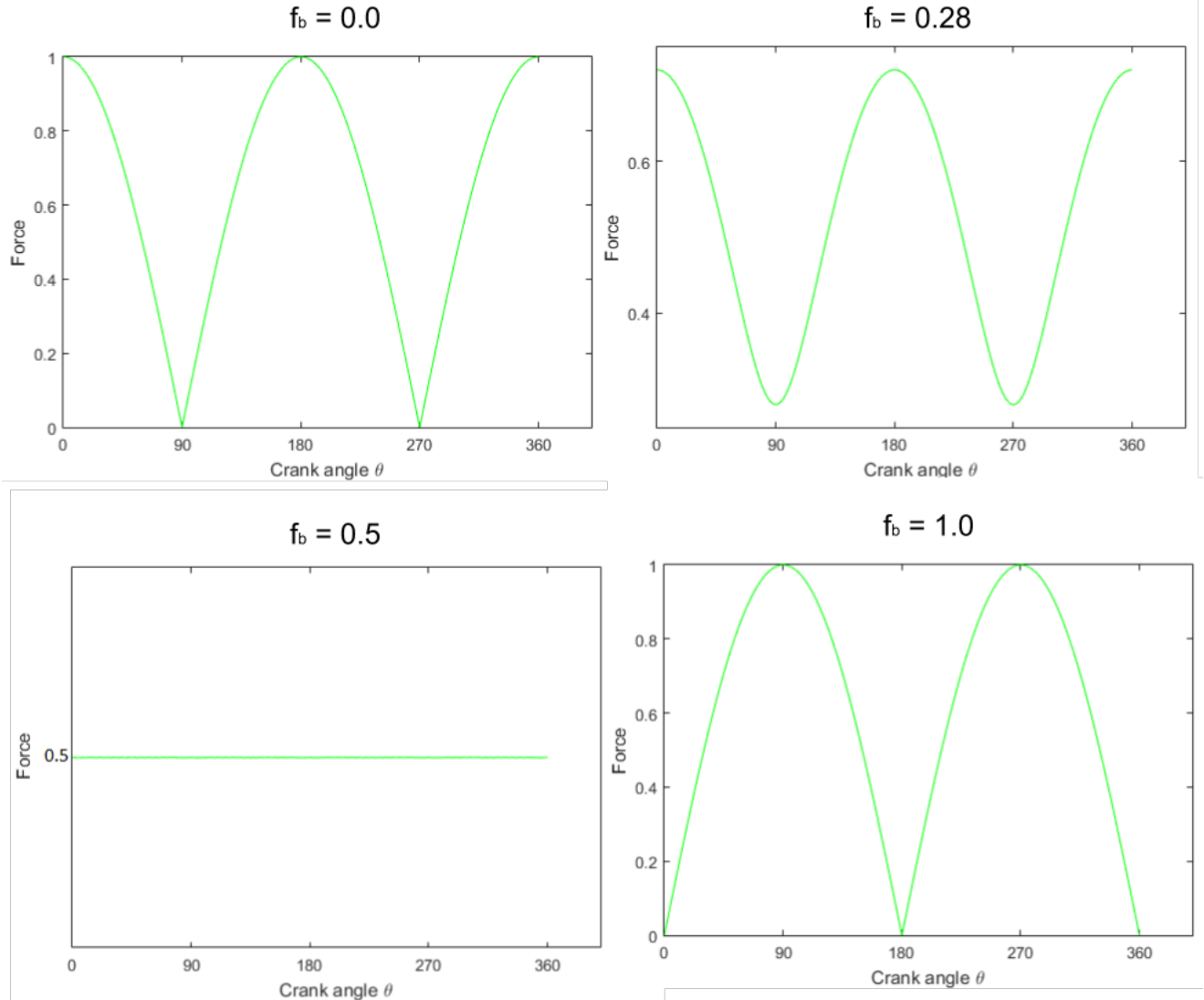


Figure 4.8: The resultant forces depending on the balance factor. A $f_b = 0.5$ results in the lowest overall resultant force.

One of the challenges related to calculation of imbalance, and the use of bob-weight when balancing the crankshaft, is the accuracy required when weighing each engine component. It includes determining the rotating and reciprocating amounts of the connecting rod. This simplification is a source of inaccuracy itself, as the connecting rod, in reality, is neither purely rotating nor purely reciprocating.

4.1.3 Dynamic balancing

The previous section considers static balancing. This thesis is about single-cylinder crankshafts, which eases the dynamic balancing: The dynamic balance is maintained by correcting each counterweight with an equal mass. This is not necessarily the case for multi-cylinder engines.

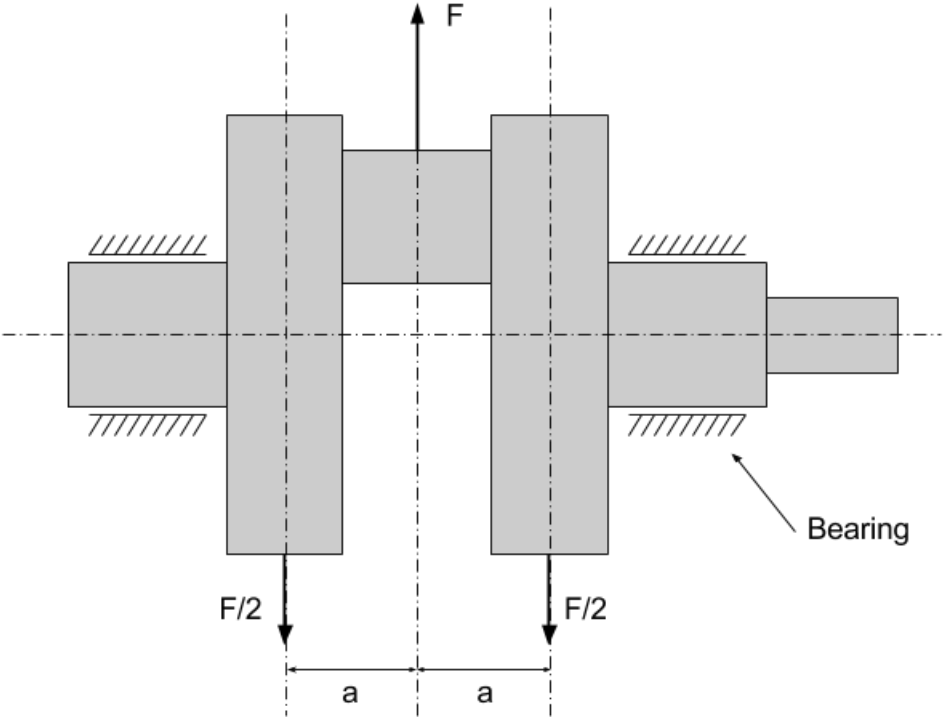


Figure 4.9: Dynamic balance is maintained as long as the two counterweights of a single-cylinder crankshaft is producing the same rotational forces.

4.2 Balancing and performance

Performance effects associated with balancing are rarely addressed directly in papers and research. Usually, it is just briefly mentioned that vibrations may affect performance negatively due to "lost energy", or that proper balancing allows for higher operating speed of the engine [20], without further explanation. There are, however, some papers that address the topic of increased power consumption due to imbalance in **purely rotating** machines:

- Gaberson and Cappillino [25] measured a negligible loss of energy of less than 0.5% due to unbalance at 25% of the engine power. The test was conducted by adding weights in terms of bolts and washers to balance and unbalance a *balance wheel*.
- Elkhatib [26] concluded that there is a strong correlation between the vibration levels occurring in the bearings and the engine power consumption. His test was not, however, limited to vibrations due to imbalance alone.
- Taneja [27] measured the frequency of vibrations in a centrifugal pump subjected to imbalance, resulting in 5% loss of power.
- Bulsara *et al.* [28] conclude that vibrations need to be reduced to save engine power, as their test showed an increase in power consumption in the engine as they increased the imbalance.

The above-mentioned papers regarding the performance effects due to imbalance does not provide an analytical model to make predictions, and depend on empirical tests using data from different sensors and measuring equipment. They do not include any reciprocating forces either. Therefore, sources of power loss due to an unbalanced reciprocating engine need to be investigated. According to Heywood [29], the crankshaft bearings are responsible for approximately 10% of the total friction in an engine. The loads on the crankshaft journal consist mainly of the inertial loads of the piston/connecting rod mechanism and the cylinder gas load. Thus, an unbalanced engine may affect the friction torque in the bearings.

4.2.1 Bearing friction torque

In this section expressions for calculating bearing friction torque are derived, first for a balanced rotor, and then for an unbalanced rotor. Lastly, necessary considerations for calculating crankshaft bearing friction torque is discussed.

Friction torque in balanced rotors

The crankshaft is mounted in two journal bearings and subjected to a load W , which in this case is the weight of the rotor. As the crankshaft journal rotates, it climbs along the bearing wall until it reaches a point, at an angle ϕ , where it starts to slip [30]. At this angle, the force $\mu \cdot N$ and the tangential component F of the load W will balance each other (see Figure 7.1).

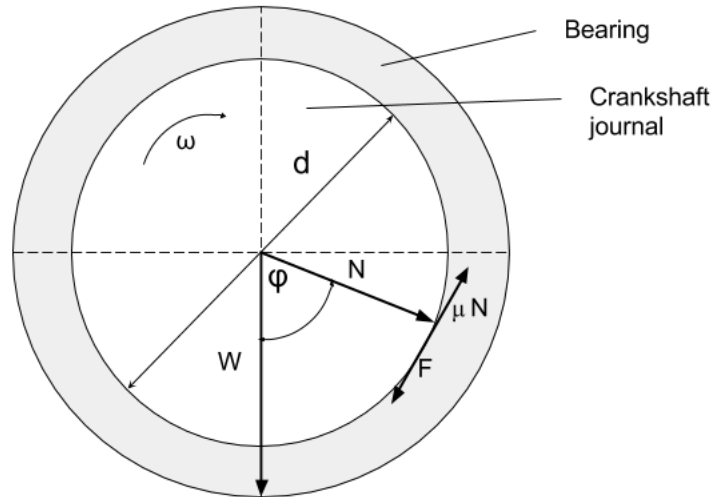


Figure 4.10: The friction force $F = \mu N$ acts in the opposite direction from the journal rotation, ω , decreasing its speed.

$$\begin{aligned} F &= W \cdot \sin\phi = N \cdot \mu \\ N &= W \cdot \cos\phi \\ \Rightarrow \mu &= \frac{F}{N} = \tan\phi \end{aligned}$$

The friction force depends on the crankshaft load W and the attitude angle ϕ . If the attitude angle is small the simplification $\mu = \tan\phi \approx \sin\phi$ can be made, and the friction force and friction torque are expressed as:

$$F = W \cdot \sin\phi \approx W \cdot \mu \quad (4.9)$$

$$T = W \cdot \mu \cdot 0.5d \quad (4.10)$$

The friction torque should be as low as possible to ensure a large crankshaft torque:

$$T_{loss, friction} = T_{applied} - T_{friction} \quad (4.11)$$

Friction torque in unbalanced rotors

In the case of the unbalanced rotor, the unbalanced force must be accounted for. The equation for friction torque is modified to [31]:

$$T = F_m \cdot \mu \cdot 0.5d \quad (4.12)$$

where F_m is the *mean equivalent dynamic bearing load* [32], and can be expressed by:

$$F_m = f_m \cdot (F_{weight} + F_{imbalance}) \quad (4.13)$$

where F_{weight} is the load from the weight of the rotor, constant in both magnitude and direction. $F_{imbalance}$ is the constant rotating load from the unbalanced mass. These loads are illustrated in Figure 4.11. The factor f_m can be found from the graph in Figure 4.12 or be calculated from:

$$f_m = \left(\frac{F_{weight}}{F_{weight} + F_{imbalance}} \right)^2 - \left(\frac{F_{weight}}{F_{weight}} + F_{imbalance} \right) + 1 \quad (4.14)$$

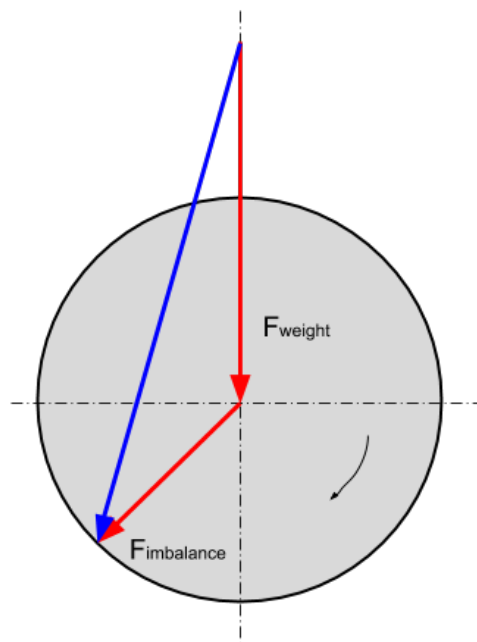


Figure 4.11: F_{weight} and $F_{imbalance}$.

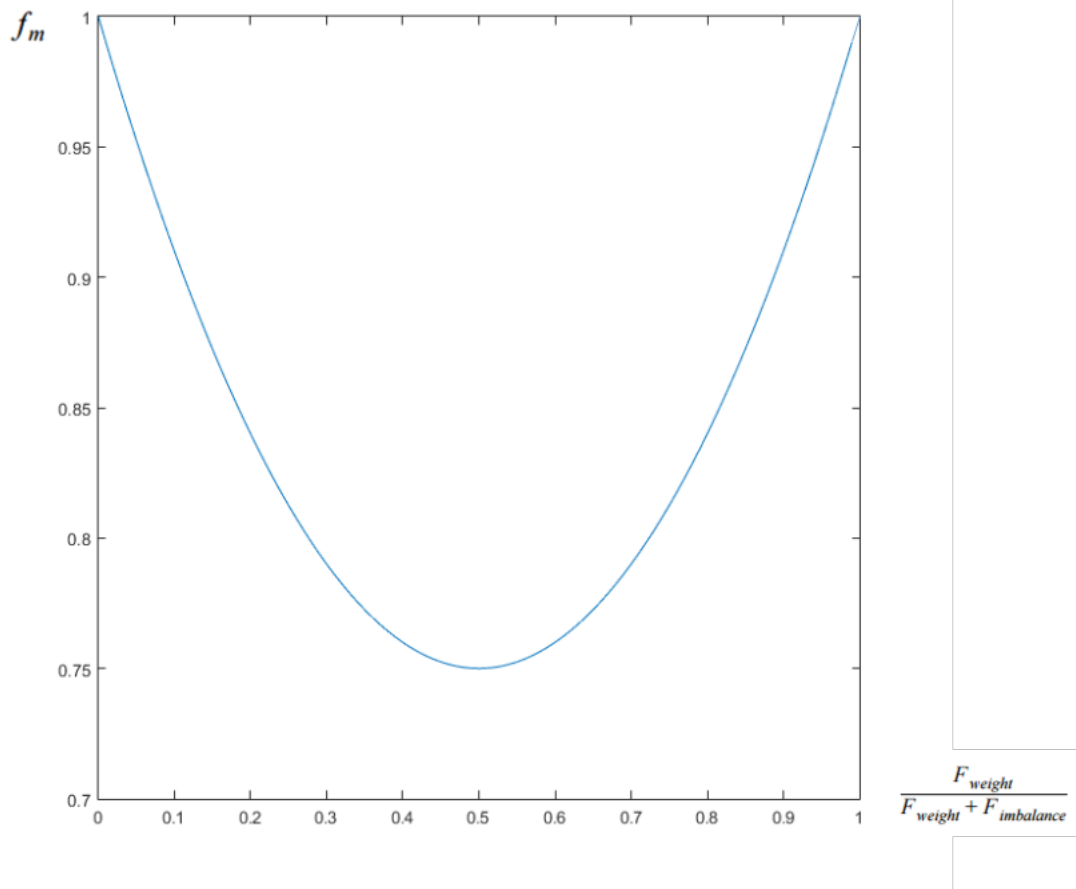


Figure 4.12: Graph to visually determine f_m .

Friction torque in crankshaft bearings

The friction torque model from the previous section needs to be further extended to include reciprocating forces from the inertia of the reciprocating components F_{rec} , derived in Chapter 3, and the gas forces from the combustion F_g .

The total number of loads needed to be included in a final friction model are:

1. The weight of the crankshaft
2. The rotating unbalanced force, which in the case of a crankshaft is the amount of the reciprocating mass added to the counterweight: $f_b \cdot m_{rec}$.
3. The inertia loads from the reciprocating mass and the gas forces from combustion.

A more elaborate friction model, incorporating the possible eccentricity between the journal centre axis and the bearing centre axis due to a pulsating crankshaft load is presented in Appendix A. The appendix also includes a section about damping in the bearings, which may reduce engine vibrations.

4.3 Permissible imbalance

As a single-cylinder engine cannot be completely balanced, there will always be some residual imbalance left after a balancing procedure [33]. The ISO1940 standard is used to ensure that a rigid rotor is balanced within a certain amount of residual imbalance, based on its intended usage. The standard presents an equation for calculating the permissible unbalance based on a quality grade, G :

$$U_{per} = \frac{1000 \cdot G \cdot m_{rotor}}{\omega}, [g \cdot mm] \quad (4.15)$$

The quality grade value (G) of a rotor intended for racing is 6.3 mm/s [34]. For a crankshaft of 2.7 kg¹ at 15200 rpm², the permissible imbalance becomes:

$$U_{per} = \frac{1000 \cdot G \cdot m_{rotor}}{\omega} = \frac{1000 \cdot 6.3 \text{ mm/s} \cdot 2.7 \text{ g}}{\frac{2\pi \cdot 15200 \text{ rpm}}{60 \text{ s}}} \approx 10.69 \text{ g} \cdot \text{mm}$$

The single-cylinder engine is assumed rigid. Thus, the ISO1940 standard can be used. The crankpin overlap (CPO) increases the rigidity of the crankshaft and is a measurement of how much the crank pin overlaps with the main journal [3] (see Figure 4.13).

$$CPO = \frac{\text{mainjournal diameter} + \text{crankpin diameter} - \text{stroke}}{2}$$

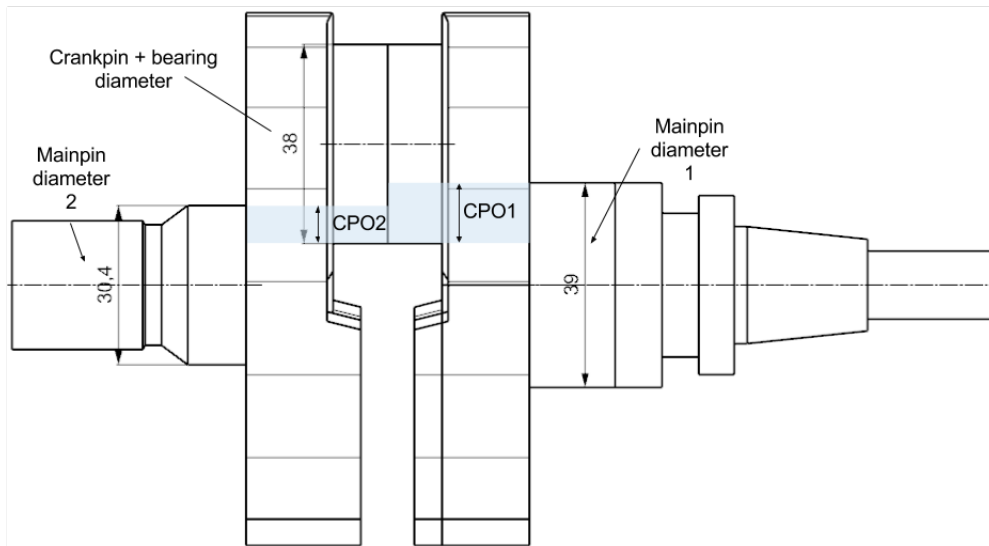


Figure 4.13: The crank pin overlap (CPO) on both sides of the main journal increasing the rigidity of the crankshaft.

¹Approximate mass of Honda CRF250R crankshaft.

²The peak velocity for the Honda CRF250R equipped with MXRR performance parts [5].

Chapter 5

Performance tests

This chapter introduces both a physical test and simulations aiming to reveal the torque loss due to increased friction torque in the bearings of an unbalanced rotor. First, a simulation performed in Crankshaft Balance Design Pro Plus is presented, showing the bearing friction torque during combustion. A physical test using a rotor as a simplified Honda CRF250R crankshaft is conducted and the friction torque from rotating unbalance is investigated. Finally, the same rotor is modelled in NX and tested in FEDEM to verify the friction model.

5.1 Performance testing in balancing software

A simplified crankshaft is created in Crankshaft Balance Design Pro Plus, having the same design characteristics as the Honda CRF250R crankshaft. The software does not allow for any great detailing of the design. Thus, it proved impossible to replicate the original crankshaft accurately. The rest of the engine characteristics, such as bore, stroke, compression ratio, etc. are entered into the program. The test engine is driven from 5000 to 14500 RPM, with maximum power at 9000 RPM. Additional masses are added to the counterweight to obtain different balance factors. Figure 5.1 shows the dimensions of the rotor.

The different balance factors that are tested are 0%, 28%, 50%, 64% and 100%. For each case, the Main Bearing Friction Torque curve are retrieved for comparison, and can be found in Figures 5.2 - 5.6.

The software only allows simulations of two-stroke engines; thus, the results are not accurate for the Honda CRF250R. The overall tendency, however, is considered to be valid as the maximum friction torque occurs during the power stroke.

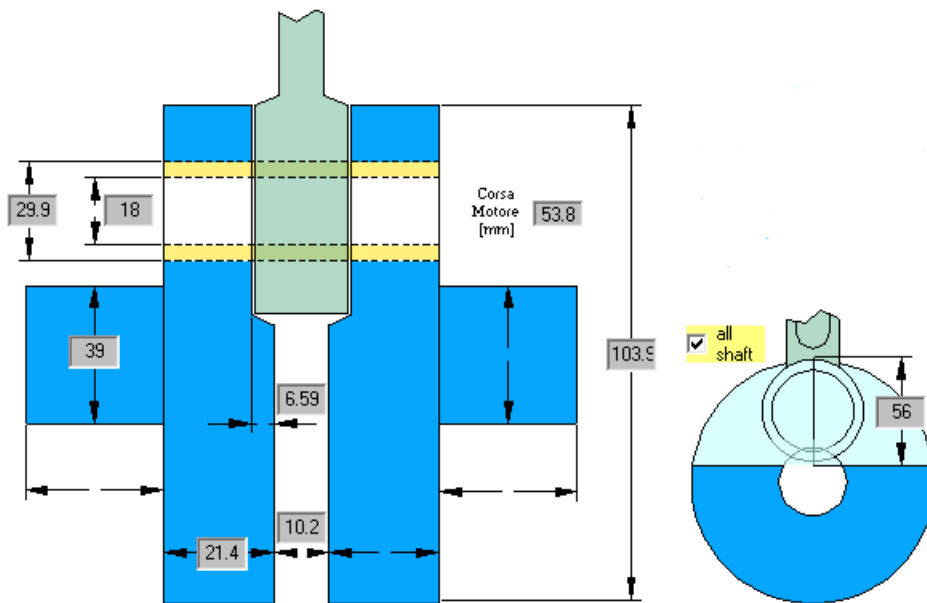


Figure 5.1: Simplified design of the Honda CRF250R crankshaft in the Crankshaft Balance Design Pro Plus interface.

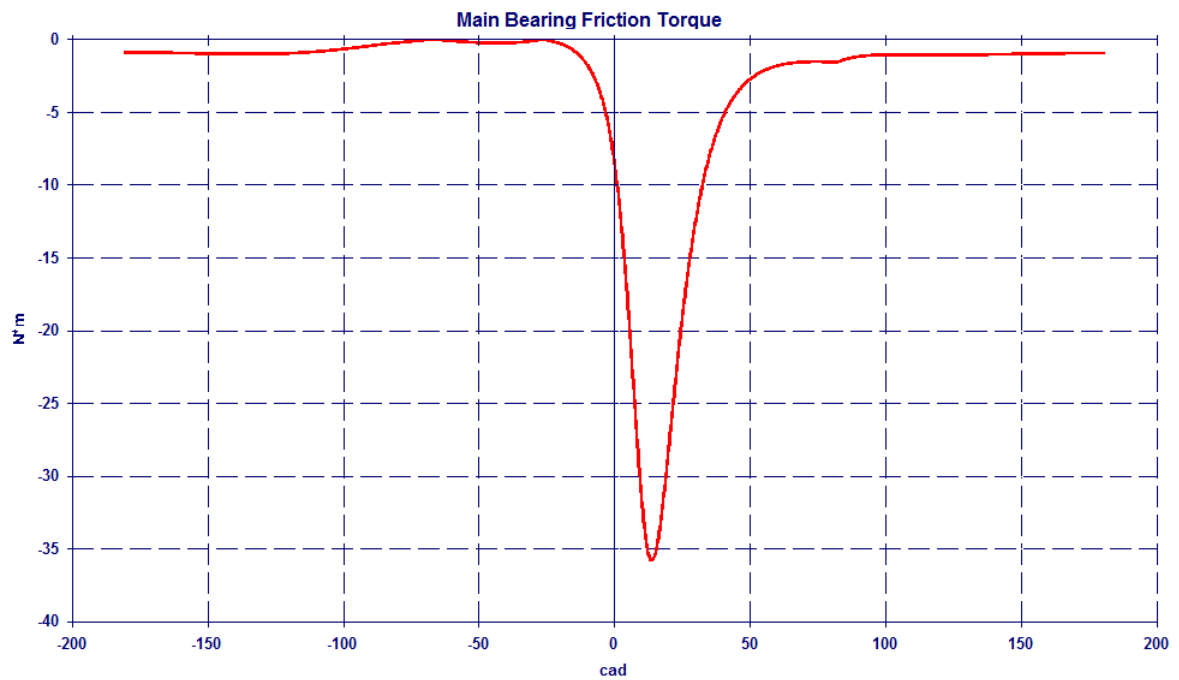


Figure 5.2: Main bearing friction torque in Nm plotted against the crank angle for 0% balance factor.

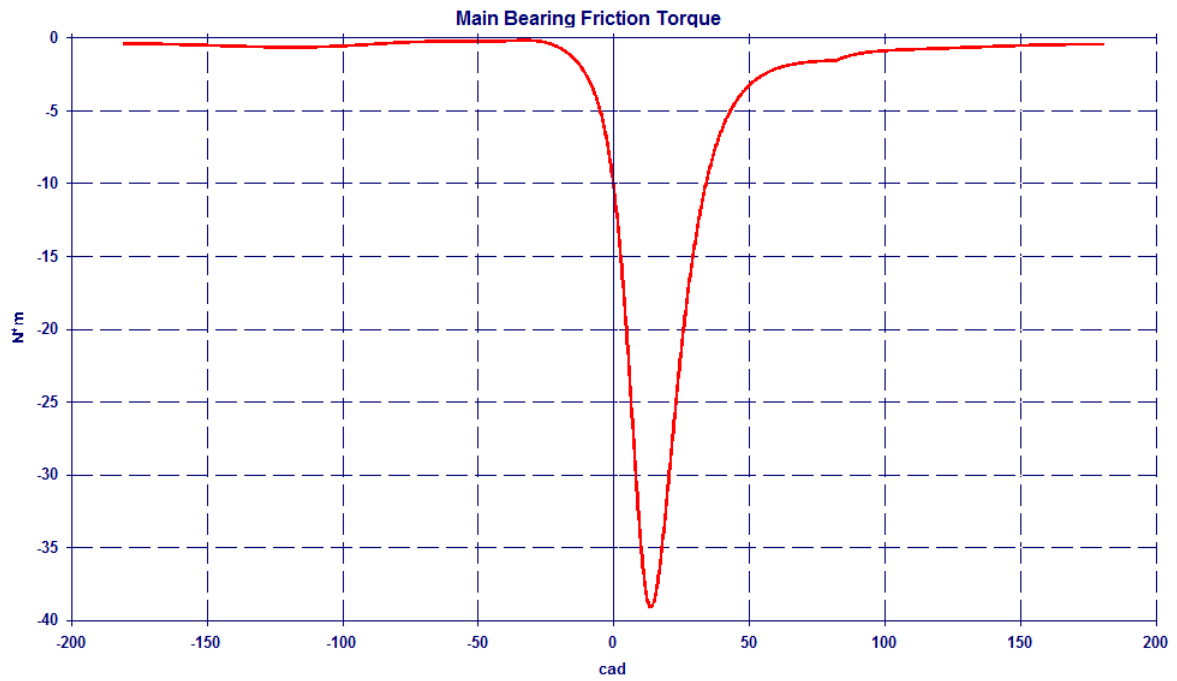


Figure 5.3: Main bearing friction torque in Nm plotted against the crank angle for 28% balance factor.

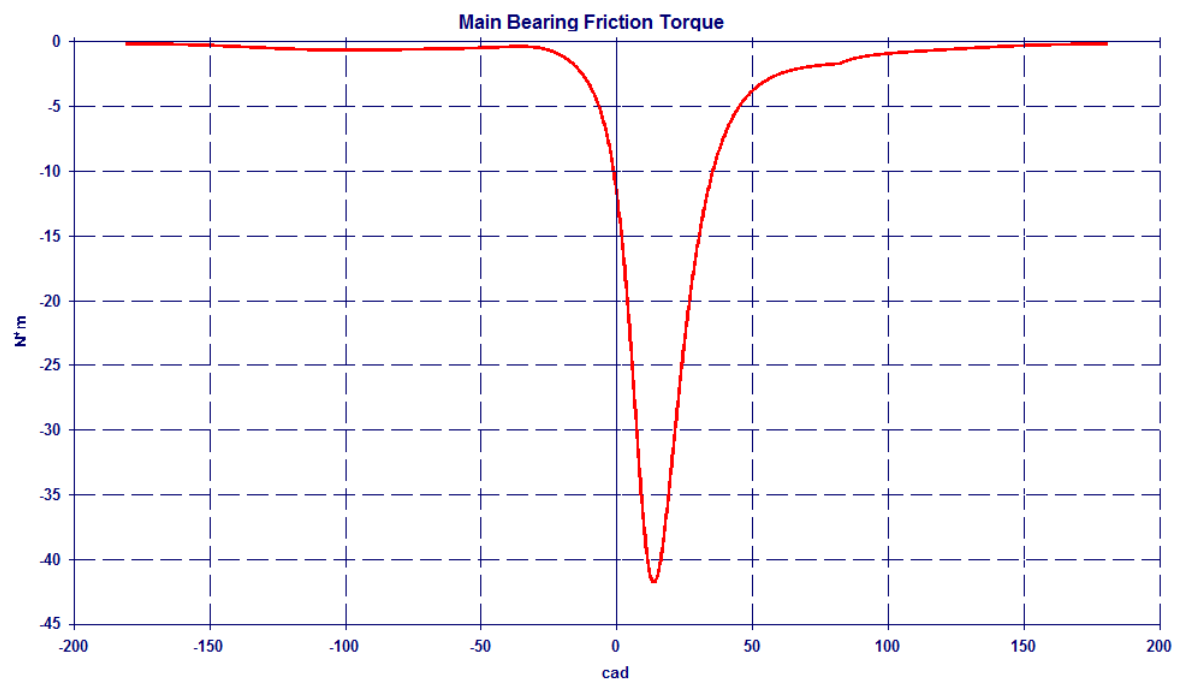


Figure 5.4: Main bearing friction torque in Nm plotted against the crank angle for 50% balance factor.

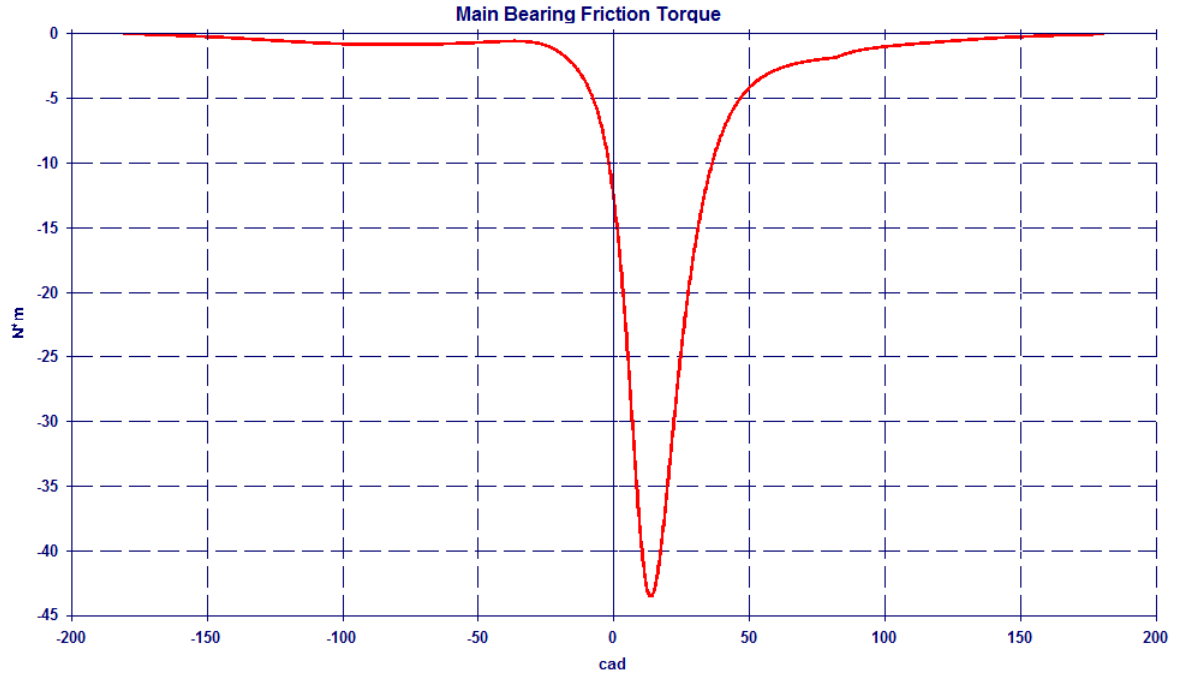


Figure 5.5: Main bearing friction torque in Nm plotted against the crank angle for 64% balance factor.

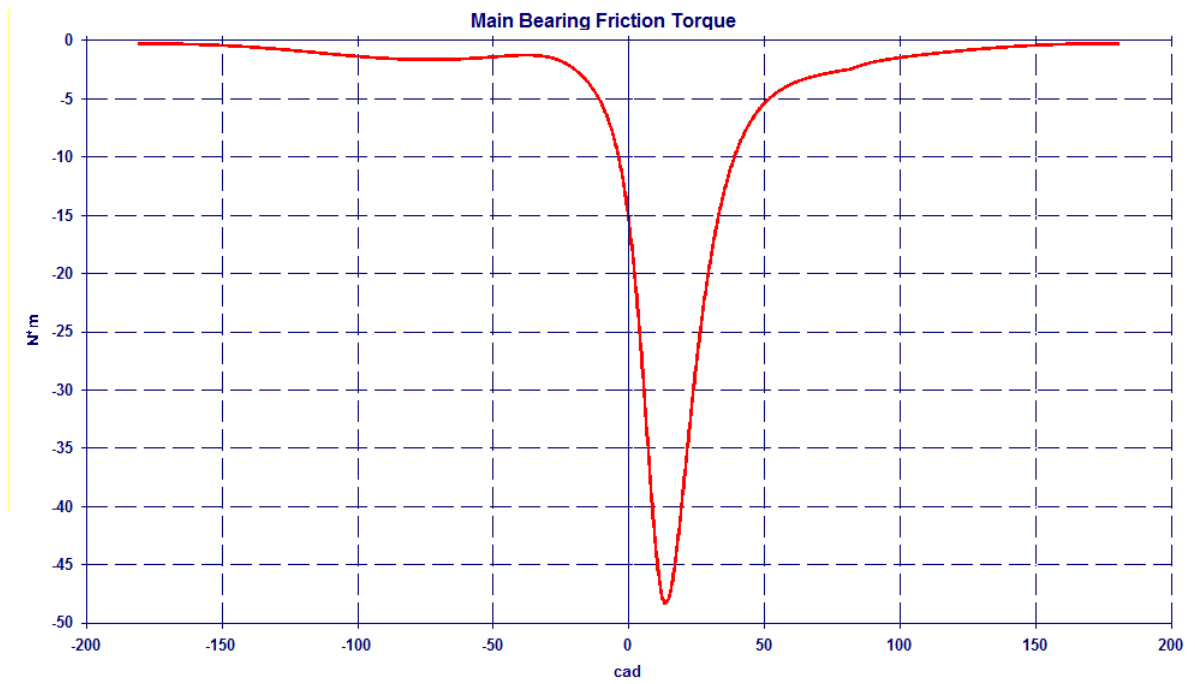


Figure 5.6: Main bearing friction torque in Nm plotted against the crank angle for 100% balance factor.

Comparing the values from Figures 5.2-5.6 with Figure 4.8 in Chapter 4.1.2, the relationship between the resultant forces and the crankshaft bearing friction torque is apparent. Figure 4.8 shows that a balance factor of 0 % gives the highest bearing friction torque at 90° and 270° , while 100 % results in the lowest. This can also be observed in Figures 5.2-5.6 . The bearing friction torque increases immediately after the spark is initiated, in this case at some angle BTDC, and continues to increase as the air/fuel mixture is burning. The friction torque increases until it is at its highest where the combustion pressure is at its maximum. In this case, that happens around 17° ATDC. Note that these angles may not be the same for the actual Honda CRF250R. The curves for a 4-stroke engine would be different, regardless of the ignition timing, as there are only one combustion stroke every two revolutions, unlike in a 2-stroke engine where there is a combustion stroke for every revolution. Note also that the maximum friction torque at maximum combustion pressure is about 33% higher for the 100% balance factor compared to the 0% balance factor, although the difference in inertia is just 5%. A friction model including the reciprocating forces and gas forces in the bearing load would be necessary to further investigate these results. The heavily increased friction torque at maximum combustion pressure could indicate that the balance influence the compression build-up.

5.2 Unbalanced rotor test

A physical test of a rotor is conducted aiming to document the loss of torque in the crankshaft main bearings due to imbalance. Loss of torque is presumed to be a result of increased frictional torque as the imbalance increases. As mentioned in Section 4.2 there have been conducted tests on friction loss in unbalanced rotors before, but with varying results. This test is performed using a rotor that is designed to represent the Honda CRF250R crankshaft. Unbalance is introduced by drilling holes in the rotor. The mass moment of inertia from the original crankshaft is preserved in the simplified version, and its dimensions are derived in Appendix E. Simulations are performed in FEDEM in order to verify the friction model from Chapter 4.2.1.

5.2.1 Test setup

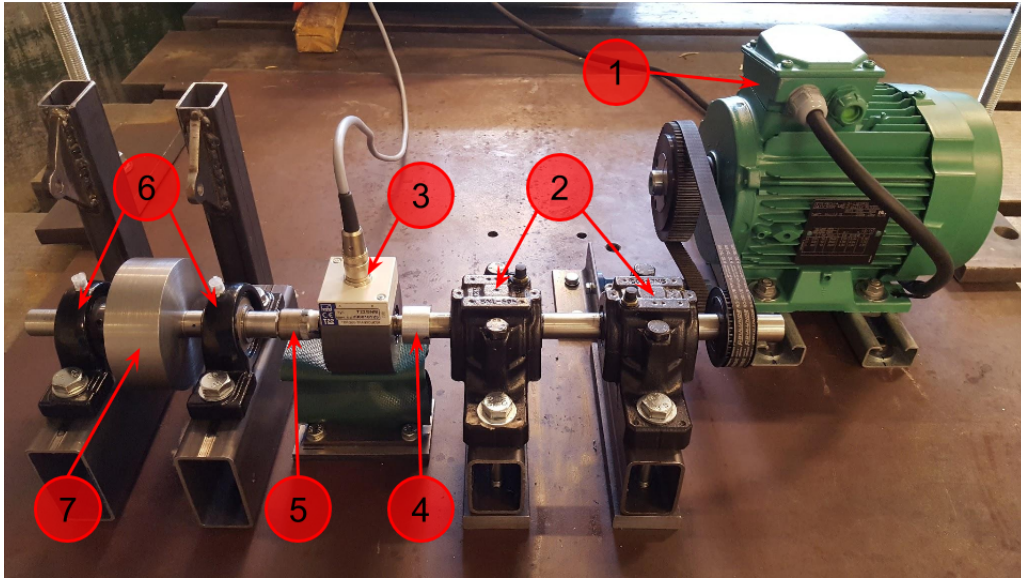


Figure 5.7: The test rig with numbered components explained in Table 5.1.

Table 5.1: Components in Figure 5.7.

No. on picture	Component
1	Induction motor
2	Shaft bearings
3	Torque transducer
4	Adaptor
5	Hexagon adaptor
6	Rotor bearings
7	Rotor

The rotor is driven by a Leroy-Somer LSES induction motor providing 1.5 kW [35] (1). The motor spins a 20mm steel shaft by belt drive at a 2:1 gear ratio. Two FAG 1205 K TVH C3 self-aligning ball bearings with H205 sleeves [36] in SNL 505 block housings [37] (2) support the shaft. The shaft is attached to an HBM T22 torque transducer [38] (3) by a custom adapter (4) that are shrunk onto the shaft and the transducer. Another custom adapter (5) is shrunk onto the other end of the transducer with a hexagon shaped cup at the other end. The rotor's journal end is machined into a hexagon that fits into the hexagon adaptor and is allowed to move freely in the axial direction while having no other degrees of freedom. This is important as there has to be some clearance in the adapter for the rotor to move, to cope with the potential axial thermal expansion of the crankshaft during operations. Figure 5.8 shows a conceptual draft of the hexagon

adaptor. Two Timken UCP204 ball bearings in pillow block units [39] (6) support the simplified crankshaft (7).

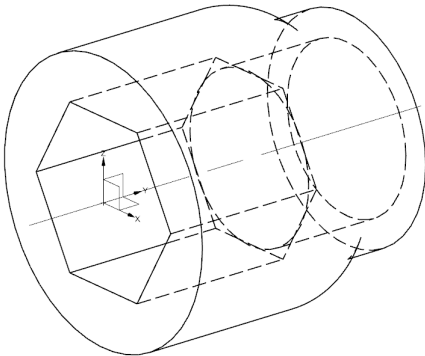


Figure 5.8: The hexagon transducer-to-crankshaft adaptor.

The torque transducer measures the torque required to rotate the simplified crankshaft at a certain velocity. As the air resistance is neglected, the friction torque is the only resistance that needs to be overcome to obtain a constant rotational velocity. The output torque of the transducer is presented as volts from a Voltmeter. Volt is converted to Newton-meter by the following relations: The voltage output at zero torque ($= 0 \text{ Nm}$) is $\pm 0.2 \text{ V}$, while $5 \text{ V} = 5 \text{ Nm} \pm 0.5\%$, according to the HBM T22 Mounting Instructions [40]. The graph shown in Figures 5.9 and 5.10 show the linear curves of both units, thus the magnitude in Newton-meter can be found for a certain measurement in V. The linearity deviation is stated to be $\pm 0.3\%$. These tolerances may result in slightly erroneous torque converting.

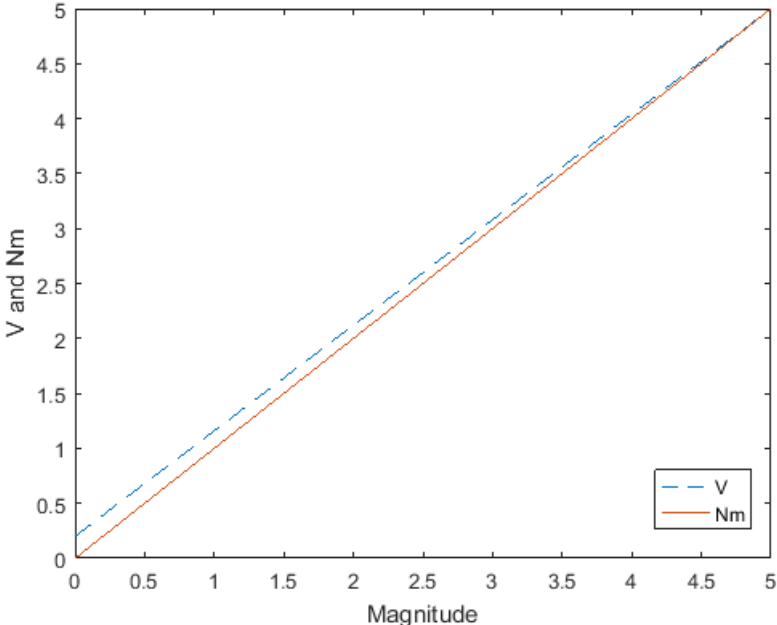


Figure 5.9: The current output at zero torque is 0.2V while $5\text{V} = 5\text{Nm}$.

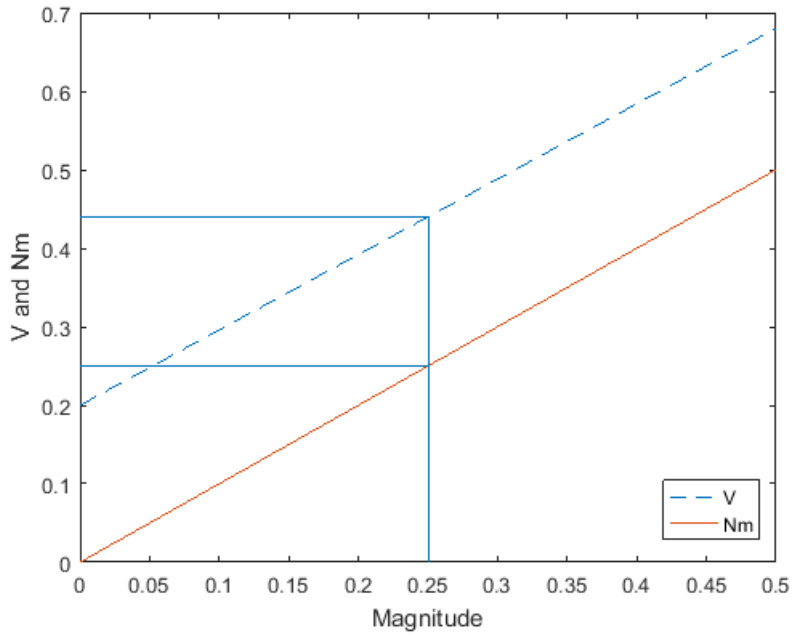


Figure 5.10: 0.44 V corresponds to 0.25 Nm.

5.2.2 Test procedure

Four different balancing cases were studied in two tests and are presented in Table 5.2.

Table 5.2: The test cases.

			Unbalanced Forces [N], $F = m_u r \omega^2$		
Case	d [mm]	m_u [g]	$\omega = 3000RPM$	$\omega = 6000RPM$	$\omega = 9000RPM$
1 (balanced)	-	-	-	-	-
2	8	14.6	42.2	168.88	379.97
3	16	58.4	168.88	675.51	1519.89
4	19.5	86.74	250.85	1003.39	2257.57

r: The radius where mass is removed ($r = 29.6\text{mm}$ for all cases)
d: The diameter of the hole drilled to remove mass
 m_u : The removed mass creating unbalance

The temperature in the rotor bearings is one of the main factors of inaccuracy influencing the results. The viscosity of the oil film in the bearings increases as the temperature increases, resulting in lower rotational resistance and friction torque. Two tests were conducted with different approaches for handling the bearing temperatures. Test 1 was carried out for Case 1, 2 and 3 in three runs for each case. The procedure for Test 1 is described in Figure 5.11. Test 2 was carried out for Case 3 and 4 with one run for each case. The procedure for Test 2 is described in Figure 5.12.

In Test 1, the rotor is accelerated up to 6000 RPM before letting the bearing temperature stabilise for 30 seconds. The friction torque is recorded before the rotor is accelerated up to 9000 RPM where the temperature is stabilised for 15 seconds. The new value for the friction torque is recorded. The procedure is repeated for 3000 RPM and 0 RPM.

Test 2 starts at 0 RPM before preceding to 3000 RPM, 6000 RPM and then 9000 RPM. At each interval, the temperature is stabilised until the friction torque is stable for at least 30 seconds, unlike in Test 1, where the temperature was allowed to stabilise for maximum 15 seconds. This ensures more stable temperatures for each RPM level than in Test 1. Values are recorded for 0 RPM in both Test 1 and 2 to verify the voltage-output for zero torque.

The procedure in Test 1 handles the temperature challenge by aiming to get data recordings at approximately equal bearing temperature for each test case. The temperature will however not be precisely the same, as the bearing loads are different for each case. Test 2 does not focus on stable temperatures and does not require the bearing temperature to be equal for the different cases.

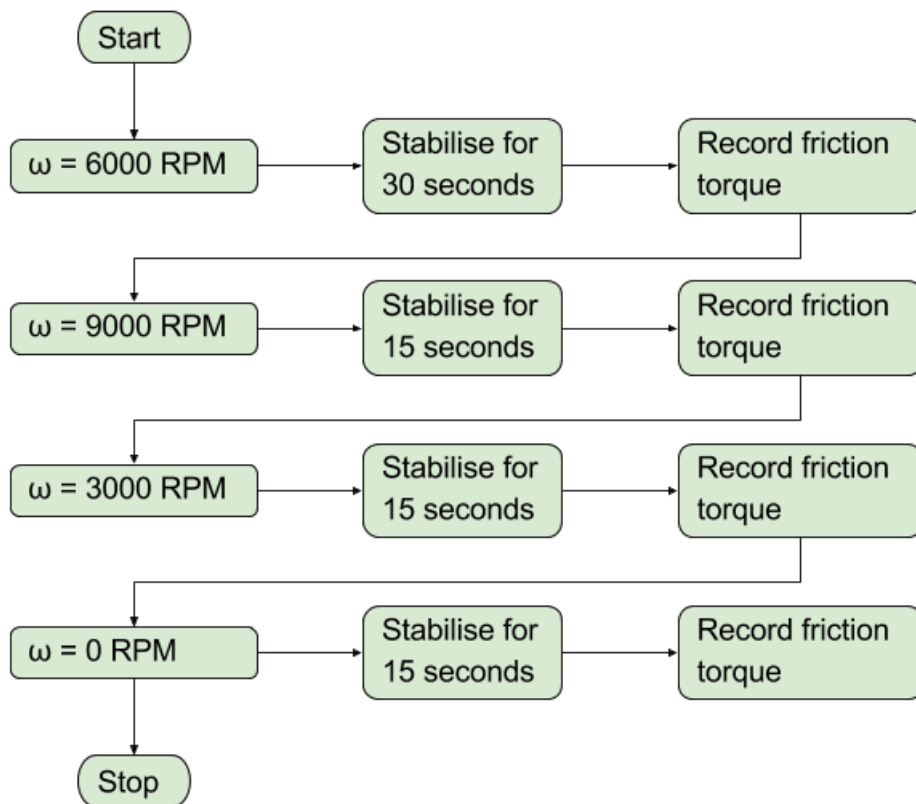


Figure 5.11: The flow of Test 1.

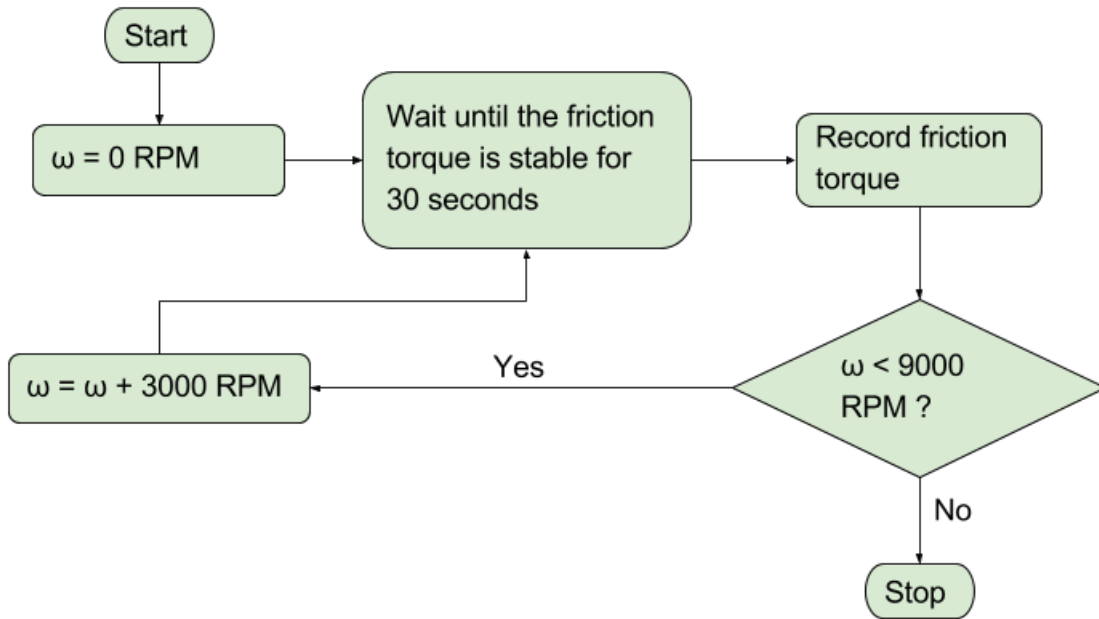


Figure 5.12: The flow of Test 2.

5.2.3 Results

The results from Test 1 is presented in Table 5.3, recorded in volts.

Table 5.3: Results from Test 1.

	Case 1	Case 2	Case 3
Run 1			
0 RPM	0.15	0.16	0.17
3000 RPM	0.40	0.40	0.36
6000 RPM	0.49	0.57	0.49
9000 RPM	0.56	0.58	0.52
Run 2			
0 RPM	0.15	0.17	0.15
3000 RPM	0.38	0.40	0.39
6000 RPM	0.52	0.55	0.53
9000 RPM	0.55	0.58	0.57
Run 3			
0 RPM	0.12	0.14	0.15
3000 RPM	0.38	0.40	0.40
6000 RPM	0.51	0.55	0.56
9000 RPM	0.55	0.58	0.58

The results from Test 2 is presented in Table 5.4, recorded in volts.

Table 5.4: Results from Test 2.

	Case 3	Case 4
Run 1		
0 RPM	0.16	0.16
3000 RPM	0.46	0.46
6000 RPM	0.47	0.45
9000 RPM	0.44	0.44

5.2.4 Discussion

The results from Test 1 show consistent data for each case in each run. This indicates that the temperature is quite consistent with each run, every time the friction torque is recorded. One exception is Run 1 for Case 3, which differs from the two other runs for that case. This inconsistent result is suspected to be a result of mistiming of the initial temperature stabilisation; too much time was spent before recording the data on 6000 RPM. Due to this compromised result, Case 3, Run 1 is omitted from the results.

Further, Test 1 indicates a slight increase in friction torque from the balanced Case 1 to the unbalanced Case 2. However, a small decrease in friction torque is observed between the unbalanced Case 2 and Case 3. This can be a result of either mistiming the stabilisation period or due to a generally increased temperature level, meaning that the bearings have not yet cooled down between each run, resulting in higher start temperature and viscosity.

The underestimation of the varying viscosity in the bearings created the foundation for Test 2. This test shows no differences in friction torque at different RPMs in each case, even though the load on the bearing increases. Although the temperature stabilises at a certain RPM, it will yet increase when the RPM is raised to a new level. It seems that the increased viscosity at this RPM-dependent temperature equalises the effect of the increased bearing loads. Test two did not show any friction loss for the two cases even though the imbalance was increased by 737.7N at 9000 RPM.

Another interesting observation during the tests was the increased magnitude of vibrations in the test rig. Case 1 and 2 ran relatively smoothly at 9000 RPM, and would have been able to withstand higher RPMs. Case 3, and especially Case 4 produced substantial

vibrations at 9000 RPM, and the tests gave clear indications that maximum rotational velocity is influenced by the balance.

Coefficient of friction

The friction torque is given by Equation 4.12, and the coefficient of friction can be expressed as:

$$\Rightarrow \mu = \frac{T_{friction}}{F_m \cdot 0.5 \cdot d} \quad (5.1)$$

Using Equation 5.1 and the friction torques in Table 5.3 (converted to Nm), the coefficients of friction in Test 1 are calculated for each case at the constant velocities, and are listed in Table 5.5. Note that the recorded volt output for zero torque were around 0.16V as opposed the 0.2V used in the model described previously. The converted values (listed in Table 5.6) can therefore not be considered as entirely correct.

Table 5.5: Calculated coefficients of friction from the physical test.

Calculated coefficient of friction			
Case	3000 RPM	6000 RPM	9000 RPM
1	0.7773	1.2771	1.4718
2	0.4044	0.2138	0.1027
3	0.1170	0.0526	0.0254

5.2.5 FEDEM simulation

The simplified crankshaft is modelled in NX and meshed with 4 mm CTETRA10 elements. RBE3 elements are used to model the bearings. The Timken UCP240 bearing sleeve is not located in the middle of the bearing house, shown in Figure 5.13. Figure 5.14 shows how the RBE3 elements model the bearings in the FEM model. Two RBE3 elements are also placed at the end of each journal.

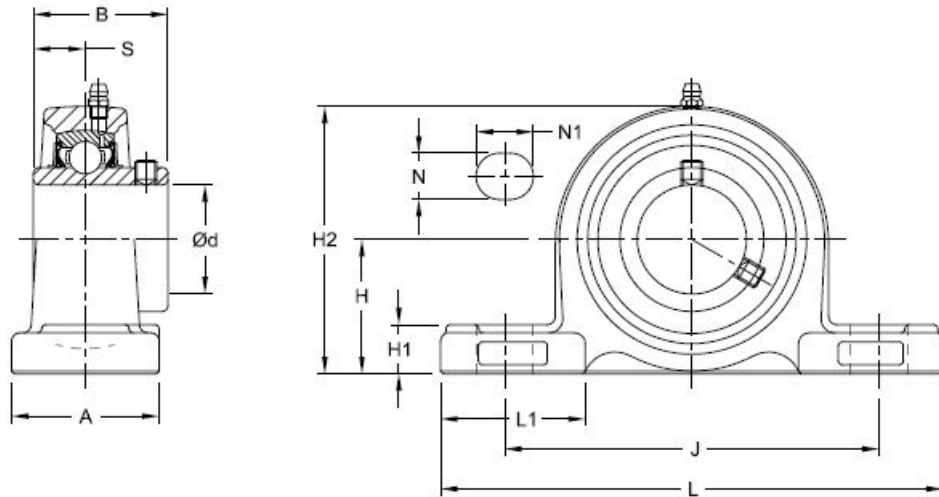


Figure 5.13: The UCP204 bearing. Image courtesy of The Timken Company
<http://cad.timken.com/item/pes-housed-unit-bearings-ball-bearing-housed-units/ucp-pillow-block-units/ucp204-12>)

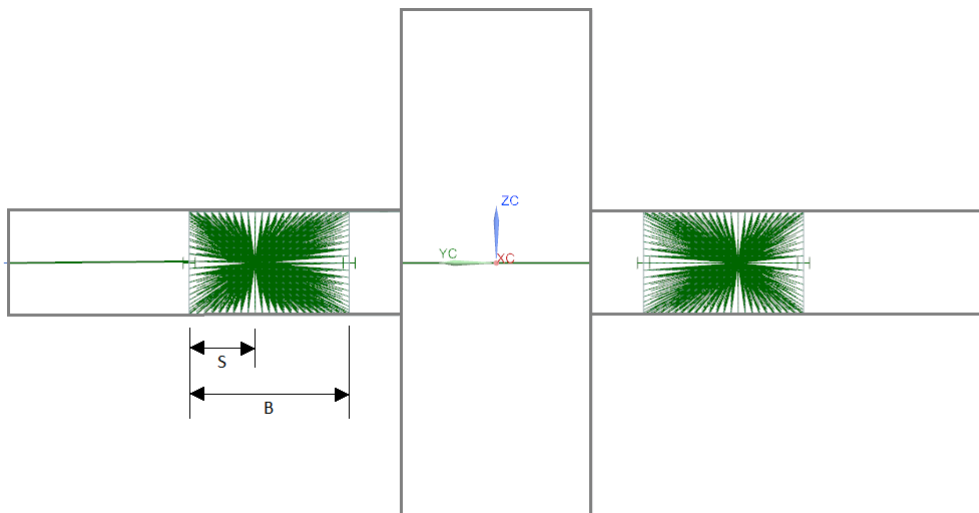


Figure 5.14: The RBE3 elements representing the bearings, considering the offset of the bearing sleeve.

The finished FEM model is imported to FEDEM. Two joints are attached to the RBE3 bearing elements, constraining their degrees of freedom, to simulate the journal bearings.

A sensor is attached to one of the bearings to measure the rotor velocity and torque. The electrical motor driving the rotor is simulated by an applied torque in one of the RBE3 elements at the journal end opposite from the sensor. A control system, which can be seen in Figure 5.16, is created to ensure that the rotor is accelerated up to, and rotates at a specific constant speed regardless of the amount of imbalance. The sensor measures the rotor velocity which is compared to the reference speed. The PI controller signals the electrical motor to increase or decrease its input torque depending on how much torque is required to rotate.

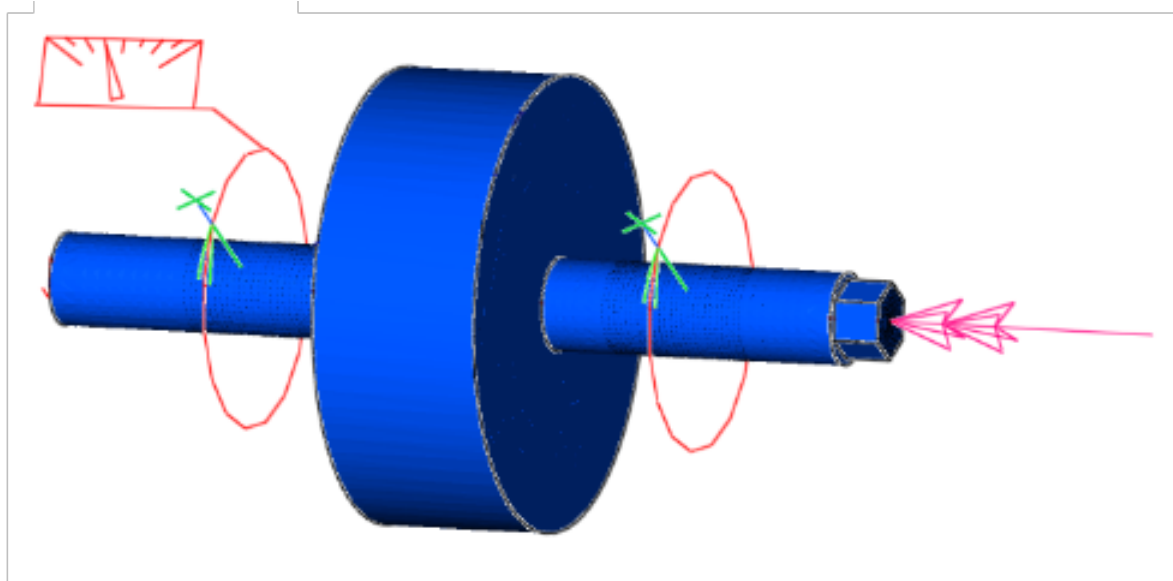


Figure 5.15: FEDEM model of the rotor with one sensor, two revolute joints and one applied torque.

The EL-motor uses 2 seconds to bring the rotor up to the reference speed, and then the rotor rotates at a constant speed for 1.5 seconds before the simulation is finished (Figure 5.17). The required torque is defined as the mean value during the last 1.5 seconds of the simulation.

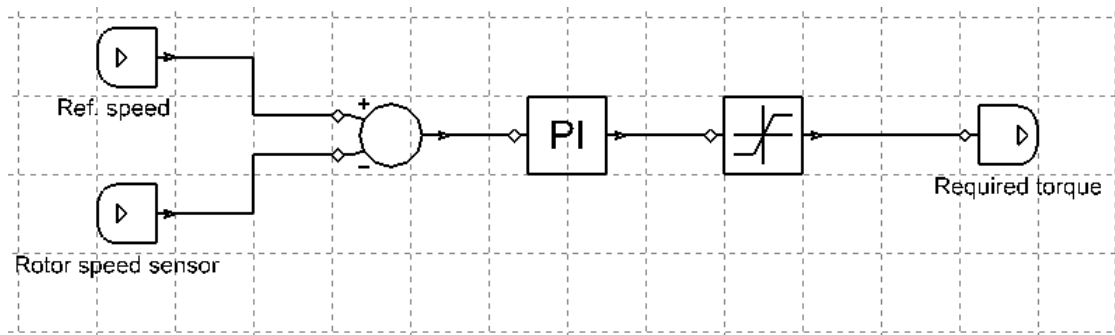


Figure 5.16: Control system for performance testing of the rotor in the FEDEM test bench.

The simulation in FEDEM is conducted in a similar way as the physical test: each rotor is rotated at 3000 RPMs, 6000 RPMs and 9000 RPMs. The coefficient of friction is calculated based on the measured friction torque in the physical test (Test 1), and are listed in Table 5.5. The friction is applied in the rotational joints of the virtual model as *Coulomb friction*.

The whole torque curve in each case at all three constant speeds can be found in Appendix F, while the required torque to keep the rotor at constant speed is listed in Table 5.6.

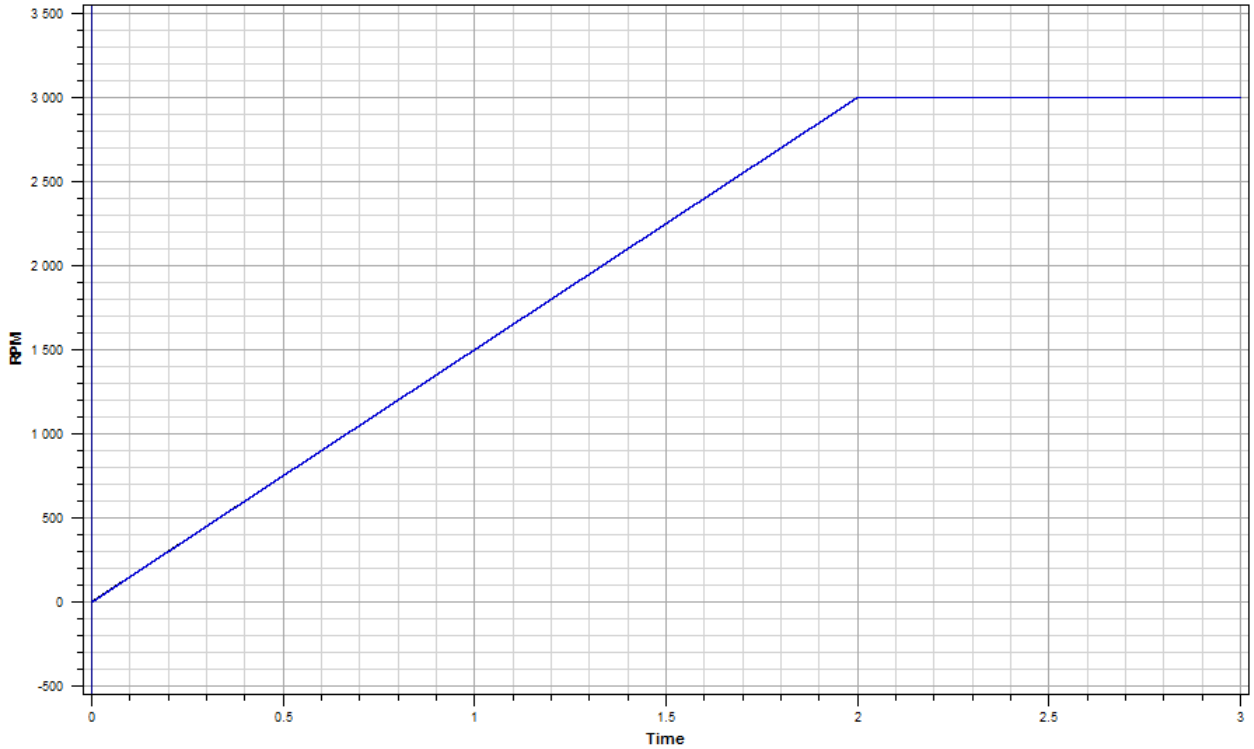


Figure 5.17: The EL-motor brings the rotor up to a constant speed of e.g. 3000 RPM in 2 seconds and keeps it rotating with a constant speed for 1.5 seconds.

Table 5.6: Comparison of the torques from the physical test and the simulations.

Measured torques from the physical test (top) and FEDEM simulations (bottom)

Case	3000 RPM	6000 RPM	9000 RPM
1	0.1944 Nm	0.3194 Nm	0.3681 Nm
2	0.2083 Nm	0.3715 Nm	0.3715 Nm
3	0.2031 Nm	0.3594 Nm	0.3906 Nm
1	0.1949 Nm	0.3204 Nm	0.3696 Nm
2	0.1897 Nm	0.3670 Nm	0.3948 Nm
3	0.1988 Nm	0.3555 Nm	0.3861 Nm

By comparing the data in Table 5.6 it is clear that the results from the physical test and the simulations in FEDEM corresponds well. There are only two exceptions, highlighted in Table 5.7, for the unbalanced rotor in Case 2 at 3000 RPM and 9000 RPM. These irregularities may be a result of inaccurate data recordings in the physical test.

Table 5.7: Differences between the torques in the physical test and the simulations.

Difference between torques in physical and virtual tests

Case	3000 RPM	6000 RPM	9000 RPM
1	0.26%	0.31%	0.41%
2	9.81%	1.23%	6.27%
3	2.16%	1.09%	1.17%

5.2.6 Limitations

The rotor in the test rotates by the use of an electrical motor and does not account for the reciprocating forces produced from the piston combustion and the moment of inertia of the reciprocating masses. A fired test where the crankshaft is driven by combustion would be too comprehensive for this project.

5.2.7 Conclusion

The underestimated magnitude of the viscous effects in the rotor bearing lubrication has resulted in partly compromised results. Means to control the bearing temperatures would have provided more reliable test results. A new test is recommended with thermometers mounted at the bearings to monitor the bearing temperatures so that the torque can be measured at a predefined bearing temperature. Test 1 and 2 have slightly contradictory results; Test 1 indicates that the friction torque may be influenced by the imbalance. This tendency is not found in Test 2. The rotor is tested in FEDEM with different coefficients of friction based on the physical test, to investigate the friction torque further. It concludes that the friction model is valid.

Chapter 6

CAD-based balancing of the Honda CRF250R

Honda is a renowned company for making motorcycles for motocross racing; in 2015, racing teams using Honda bikes finished second and third in MXGP [41]. This chapter focuses on the Honda CRF250R motorcycle and how the crankshaft can be re-balanced in NX after new high-performance, low-weight parts have been installed.

6.1 Honda CRF250R specifications

The Honda CRF250R features a 249cc, four-stroke single-cylinder, direct injection engine with a 76.8 mm bore and a 53.8 mm stroke. The bike has a curb weight of approximately 105 kg [42]. Figure 6.2 shows the CRF250R crankshaft highlighting important features used throughout this chapter.

6.2 MX Real Racing (MXRR)

MX Real Racing (MXRR) is an Italy-based company that provides racing components for motocross bikes [43]. To compete at the highest level in racing, the CRF250R is equipped with high-performance engine components delivered by MXRR. The engine is to be balanced with new high-performance, low-weight connecting rod, and wrist pin.



Figure 6.1: The 2015 HONDA CRF250R.
Image courtesy of Honda Powersports:
<http://powersports.honda.com/2015/crf250r/accessories.aspx>

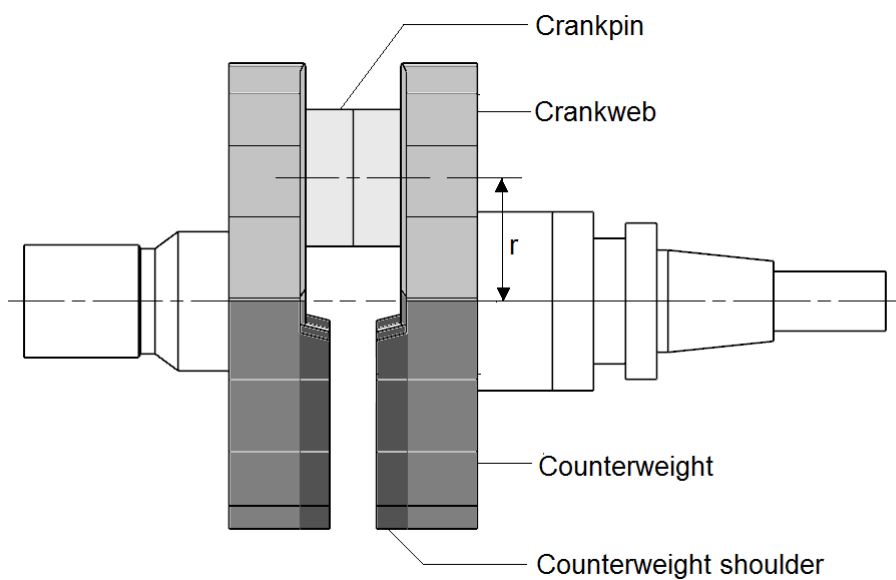


Figure 6.2: The Honda CRF250R crankshaft with highlighted features.

6.3 Balancing the Honda CRF250R

When a Honda CRF250R engine is equipped with MXRR high-performance components, both the reciprocating and the rotating masses change. Re-balancing the crankshaft is then essential to ensure an acceptable level of vibration and high performance.

6.3.1 Two balancing cases

Two CRF250R crankshafts are balanced, each to a different balance factor.

Case 1: Factory balance factor.

We can assume that the choice of the original balance factor is well justified and evaluated by Honda engineers, and that they consider it as the best balance factor for this particular engine.

Case 2: 28% balance factor.

Previous studies in the FEDEM Test Bench has indicated good results for 28% balance factor for the Honda CRF250R engine [5].

The masses of the various components have been obtained from models in NX and FEDEM. The rotating and reciprocating masses are calculated for both OEM parts and MXRR parts, where m_{rot} consists of the crankpin, connecting rod big-end and big-end bearing. m_{rec} consists of the wrist pin, connecting rod small-end, small-end bearing, piston and clips, rings and oil. The measured values are listed in Table 6.1. The values for *small-end bearing* and *clips, rings and oil*, are just estimates, as these values could not be found in NX or FEDEM.

Table 6.1: Measured mass properties

	OEM	MXRR
Connecting rod big-end [g]	129.04	95.04
Connecting rod small-end [g]	46.62	34.00
Big-end bearing [g]	39.00	39.00
Small-end bearing [g]	~12.50	~12.50
Piston [g]	158.00	158.00
Clips, rings and oil [g]	~30.00	~30.00
Crankpin [g]	114.65	114.65
Wrist pin [g]	35.00	27.00

Honda CRF250R OEM parts:	Honda CRF250R MXRR parts:
$m_{rot} = 282.96g$	$m_{rot} = 248.69g$
$m_{rec} = 282.12g$	$m_{rec} = 261.50g$

6.3.2 Formula for calculating the balance factor

The first objective in Case 1, is to determine the original balance factor. When a crankshaft is physically balanced, it is placed in a balancing machine, as described in Section 3.2, with bob-weights attached to the crankpin. The balancing machine rotates the crankshaft at a speed ω , and the reaction forces on the main journal bearings are retrieved. A simplified balancing machine and the considered masses are illustrated in Figure 6.3.

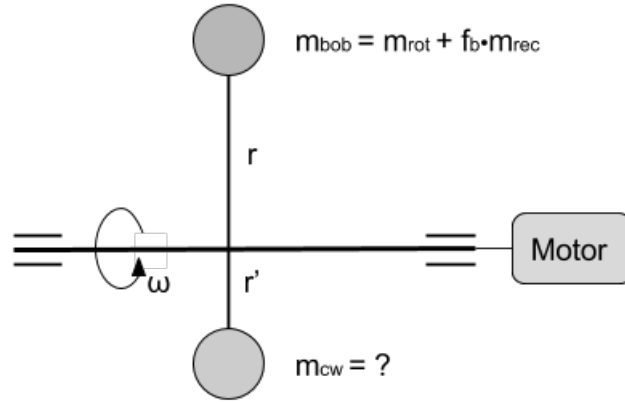


Figure 6.3: Simplification of a crankshaft in a balancing machine.

r : Distance from the crankshaft centre to the crankpin centre (half the stroke).

r' : Distance from the crankshaft centre to the counterweight centre.

The unknown mass of the counterweight (m_{cw}), is calculated by considering the sum of forces. An expression of the balance factor can then be determined.

$$\sum F = m_{cw} \cdot r' \cdot \omega^2 - m_{bob} \cdot r \cdot \omega^2 = 0$$

$$m_{cw} \cdot r' = (m_{rec} + f_b \cdot m_{rec}) \cdot r \quad (6.1)$$

$$f_b = \frac{m_{cw} \cdot \frac{r'}{r} - m_{rot}}{m_{rec}} \quad (6.2)$$

The crankshafts in this chapter are statically balanced in a virtual model without

having to rotate the crankshaft, as opposed to the physical balancing in a balancing machine.

6.3.3 Finding the counterweight mass, m_{cw} , and its radius, r'

As mentioned in Chapter 4.1.1, the mass of the crankweb needs to be accounted for to determine m_{cw} and r' for a real crankshaft. When calculating the correctional mass, the counterweight mass is defined as the combined mass of the crankweb and the counterweights. r' is defined as the distance from the crankshaft centre axis to the centre of this combined mass. This is illustrated in Figure 6.4.

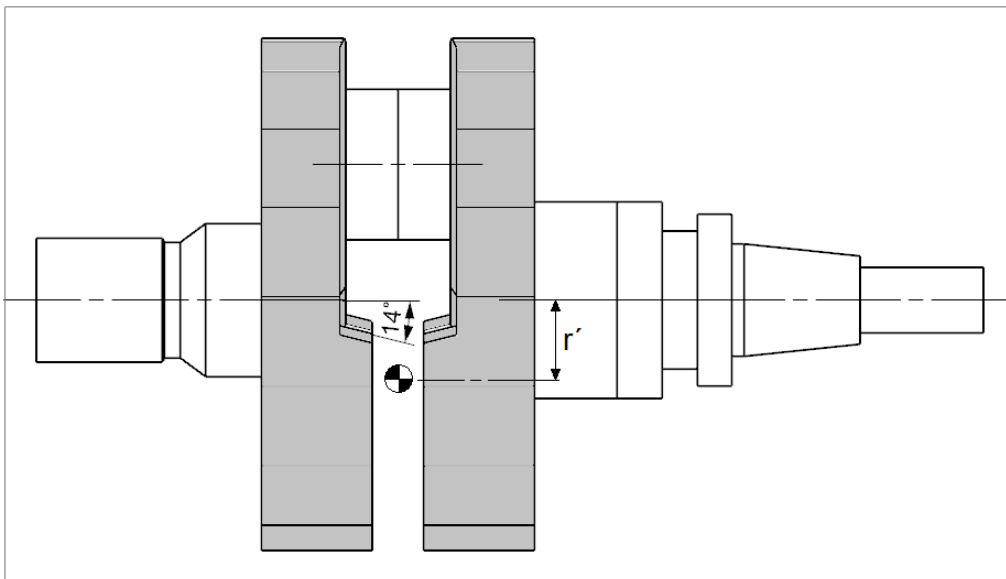


Figure 6.4: Counterweight + crankweb (highlighted) and their combined centre of gravity.

Several crankshaft designs have been analysed in NX and Crankshaft Balance Design Pro Plus with accurate results for the balance factor, supporting the validity of the approach and the derived formula. m_{cw} and r' have been measured in NX, and the balance factor has been calculated from Equation 6.2:

$$m_{cw} = 2020.40 \text{ g}$$

$$r' = 6.16 \text{ mm}$$

$$r = \text{stroke}/2 = 26.9 \text{ mm}$$

$$f_b = 0.6375$$

The crankshaft in Case 1 will, therefore, be balanced to a balance factor of 63.75%.

6.4 Correction procedure

A general algorithm for finding the unbalance and determining the appropriate correctional mass has been developed to balance the crankshaft for MXRR parts:

Step 1: Find the product of the counterweight mass m_{cw} and the distance r' to the counterweight CG for both the new and the old components using equation (6.1):

$$m_{cw} \cdot r' = (m_{rot} + f_b \cdot m_{rec}) \cdot r$$

Step 2: Calculate the unbalance by determining the difference between the original and the new components:

$$m_u \cdot r_u = (m_{cw} \cdot r')_{old} - (m_{cw} \cdot r')_{new} \quad (6.3)$$

Step 3: Choose a distance r_{corr} from the crankshaft centre axis to the centre of gravity for the correctional mass to be placed. The location depends on the crankshaft geometry and preferred method of correction.

Step 4: Calculate the correctional mass by dividing the unbalance by the radius of the correction:

$$m_{corr} = \frac{m_u \cdot r_u}{r_{corr}} \quad (6.4)$$

Step 5: Appropriately compensate for m_{corr} by adding or removing mass from the crankshaft at r_{corr} .

Step 6: Measure the new, corrected counterweight mass and its radius $m_{cw,balanced}$ and $r'_{balanced}$ from the modified geometry.

Step 7: Find the remaining unbalanced mass after correction:

$$m_{u,corr} = (m_{cw} \cdot r')_{balanced} - (m_{cw} \cdot r')_{original} \quad (6.5)$$

Step 8: Determine if the new unbalance is within the given tolerance e.g. by using the ISO1940 standard [34]. Repeat the process with updated properties if the imbalance exceeds the allowed limit.

6.5 Modifying the crankshaft geometry

Replacing OEM components with lighter, high-performance parts enable mass to be removed from the counterweight to regain the balance. Alternatively, mass could be added to the crankweb or crankpin, but it is not preferred in this case as it would result in increasing the total mass and inertia of the crankshaft. Mass can be removed in several ways, either by drilling holes into the counterweight or by grinding mass off of the surface of the shoulder.

Two correction methods are tested in Crankshaft Balance Design Pro Plus to reveal any effects they may have on the main bearing friction torque. Details about the test can be found in Appendix B. The test concludes that the correction method does not significantly influence the main bearing torque. Grinding mass off of the shoulder is preferred as no detailed geometry is introduced. Thus, no additional detailed meshing is required to prepare the crankshaft for the FEDEM test bench. An equal amount of material has to be removed from each of the two counterweights to maintain the dynamic balance.

6.5.1 Results

The maximum allowed unbalance for a Honda CRF250R crankshaft spinning at 15200 RPM (maximum speed with MXRR parts [5]) is $U_{per} = 10.69 \text{ g} \cdot \text{mm}$ according to the ISO1940 standard [34]. The calculation is performed in Section 4.3. The results for the two crankshafts after balancing are presented in the table below, and both have less residual unbalance than $10.69 \text{ g} \cdot \text{mm}$.

Table 6.2: Results after balancing

Balance factor [%]	Imbalance after balancing $\text{g} \cdot \text{mm}$	Material removed [mm]	Number of corrections
28	7.39	2.807	2
63.75	8.01	0.948	1

The remaining imbalance after the balancing procedure is equal to a mass of $\approx 0.3 \text{ g}$ located $\approx 24 \text{ mm}$ from the crankshaft centre ($0.3 \text{ g} \cdot 24 \text{ mm} \approx 7.39 \text{ g} \cdot \text{mm}$). The imbalance is a result of a 14° angle on the top of counterweight shoulder (see Figure 6.4), altering the surface area and CG of the shoulder as the material is removed.

As this error increases with the amount of material being removed, two iterations had to be performed to achieve an acceptable level of imbalance for the case of a 28% balance factor. Figure 6.5 shows the mass to be removed from the crankshaft in terms of millimetres in each of the two cases (Top: Balanced to 64%, Bottom: Balanced to 28%).

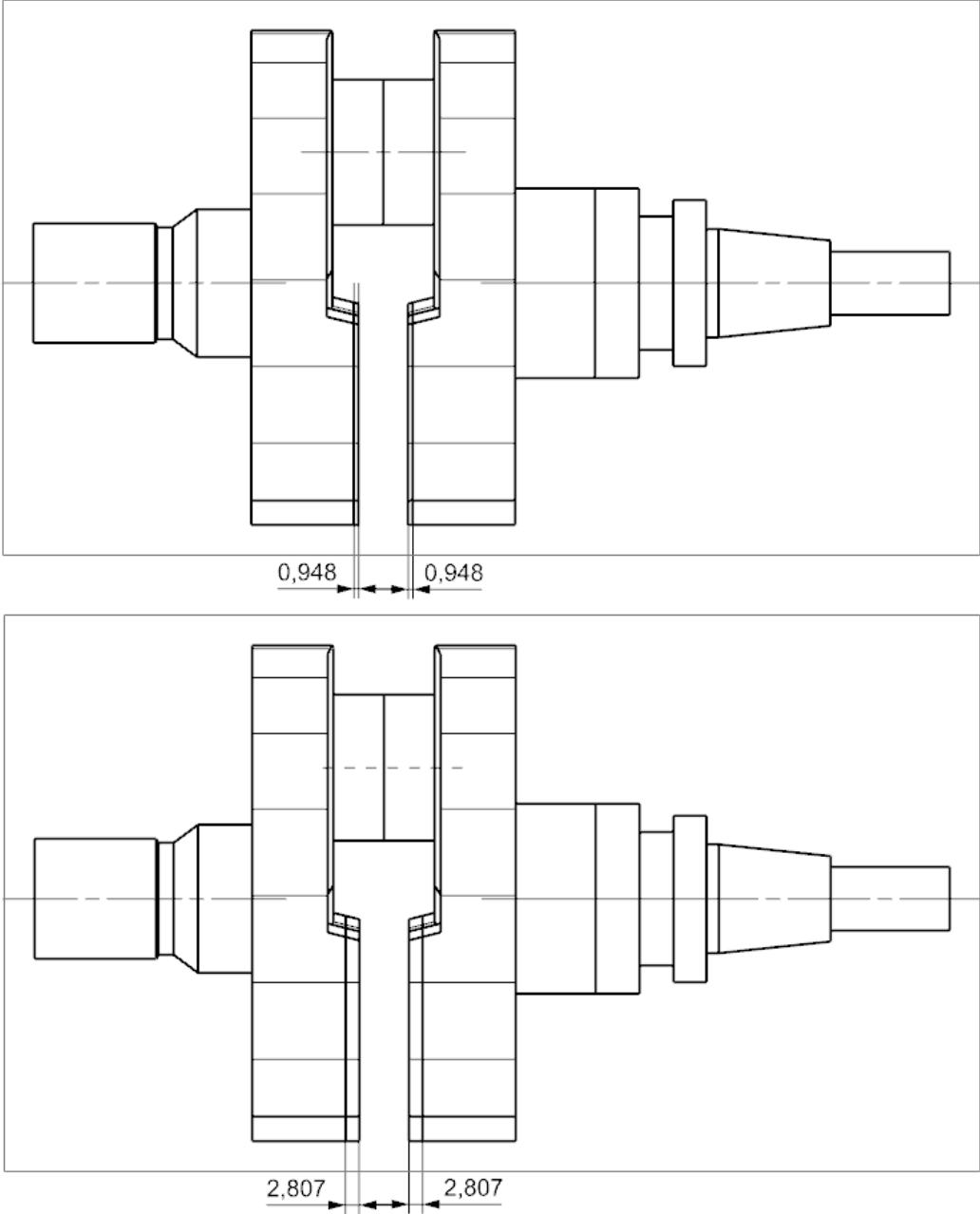


Figure 6.5: The balanced crankshafts with the amount of mass removed in terms of mm. Top: balanced to 63.75%. Bottom: balanced to 28%.

Appendix 7 describes an approach for automatic crankshaft balancing.

Chapter 7

Conclusion

The literature search revealed a lack of documentation relating engine balance to performance. Based on this observation, both virtual and physical tests were performed to investigate the effects of engine balance on crankshaft bearing friction.

In Chapter 4.2.1, a friction model for unbalanced rotors are derived. The formula is verified by comparing the results from the physical test with the simulations in FE-DEM. However, as the physical test failed to fully account for the varying viscosity of the crankshaft bearings, the test could not precisely predict the effect of the rotating imbalance on the friction torque. In the case of an actual crankshaft, the rotating bearing load $F_{imbalance}$ in the friction model for unbalanced rotors (Equation 4.13) should consist of the mass corresponding to the portion of the reciprocating mass added to the counterweight:

$$F_{imbalance} = f_b \cdot m_{rec}$$

In order to properly consider friction torque in crankshaft bearings, an extended friction model that includes the forces from the reciprocating components and combustion would need to be derived. The test results indicate that balancing has very little effect on bearing friction, but the differences in friction torque with the use of different balance factors in Section 5.1 indicate that engine balancing may affect the cylinder pressure build-up.

Future work should include a new physical test where the bearing temperatures can be monitored so that data can be recorded at certain temperatures. A new friction model that includes the forces from the reciprocating components of the engine should also be created, and testing and monitoring of how balancing the crankshaft affects the pressure build-up in the cylinder should be investigated.

Bibliography

- [1] Uicker, J., Pennock, G. and Shigley, J. *Theory of Machines and Mechanisms*, pages 635–638. Oxford University Press, New York, US, 3rd edition, 2003.
- [2] Muszynska, A. *Rotordynamics*, pages 711–733. CRC Press Taylor & Francis Group, Florida, US, 2005.
- [3] Kane, J. Contemporary Crankshaft Design. *Race Engine Technology Magazine*, 33, 2015.
- [4] NT Project. Crankshaft Balance Design Pro Plus. http://www.ntproject.com/software_cbd_eng.htm.
- [5] Rølvåg, T. and Bella, M. Dynamic test bench for motocross engines. *Submitted to: International Journal of Automotive and Mechanical Engineering*, 2015.
- [6] Siemens PLM Software. NX 10.0. https://www.plm.automation.siemens.com/en_us/.
- [7] Engineering Explained. Engine balancing - explained. <https://www.youtube.com/watch?v=aonbw0xooGA>, 2014. [Online; accessed 8-May-2016].
- [8] Engineering Explained. Primary engine balance - explained. <https://www.youtube.com/watch?v=9Bdc9CuB0zc>, 2014. [Online; accessed 8-May-2016].
- [9] Guzzomi, A., Hesterman, D. and Stone, B. Variable inertia effects of an engine including piston friction and crank or gudgeon pin offset. In *Proceedings of the Institution of Mechanical Engineers: Part D: Journal of Automobile Engineering*, 222(D3), pages 397–414, 2008.
- [10] Taylor, C. *The Internal-Combustion Engine in Theory and Practice*, volume 2, pages 240–280. The M.I.T. Press, Massachusetts, US, revised edition, 1985.
- [11] Tiwari, R. Chapter 13 - dynamic balancing of rotors. http://www.iitg.ernet.in/scifac/qip/public_html/cd_cell/chapters/rtiwari_rotor_bearing_system/rt_chapter13_part1.pdf, 2010. [Online; accessed 05-May-2016].

- [12] Surovec, R., Bocko, J. and Sarlosi, J. Lateral rotor vibration analysis model. *American Journal of Mechanical Engineering*, 2(7):282–285, 2014.
- [13] Bishop, R. and Gladwell, G. The vibration and balancing of an unbalanced flexible rotor. *Journal of Mechanical Engineering Science*, 1(1):p. 66–77, 1959.
- [14] Patterson, D. Energy torque and balance characteristics. *SAE Technical Paper*, 1982. 821575.
- [15] Borowski, V., Denman, H., Cronin, D., Shawn, S., Hanisko, ., Brooks, L., Mikulec, D., Crum, W. and Anderson M. Reducing vibration of reciprocating engines with crankshaft pendulum vibration absorbers. In *International Off-Highway & Powerplant Congress and Exposition, Milwaukee, Wisconsin, US, September 9–12, 1991*.
- [16] Norton, R. *Design of Machinery*, pages 630–699. McGraw-Hill, New York, US, 5th edition, 2012.
- [17] O’Leary, J. and Gatecliff, G. Computer aided balance of single-cylinder slider-crankic engines. In *Small Engine Technology Conference, Milwaukee, Wisconsin, US, September 11–13, 1989*.
- [18] Leveqcue, N., Mahfoud, J., Violette, D., Ferraris, G. and Dufour, R. Vibration reduction of a single cylinder reciprocating compressor based on multi-stage balancing. *Mechanism and Machine Theory*, 46(1):p.1–9, 2010.
- [19] Yang, C., Hao, Z. and Zheng, G. Balance Mechanism Design of Single Cylinder Engine Based on Continuous Mass Distribution of Connecting Rod. *Transactions of Tianjin University*, 15(4):p.255–259, 2009.
- [20] Norfield, D. *Practical balancing of rotating machinery*, pages 99–181. Elsevier Ltd., Oxford, UK, 1st edition, 2006.
- [21] Ghosh, A. Dynamics of machines chap 4 lecture 1 single cylinder engine balancing. <https://www.youtube.com/watch?v=NY-GNTfQCXs>, 2014. [Online; accessed 13-May-2016].
- [22] Wolfram Mathworld. Binomial theorem. <http://mathworld.wolfram.com/BinomialTheorem.html>, 2016. [Online; accessed 13-June-2016].
- [23] Hoem, O. and Røsholm, V. Virtual crankshaft balancing machine, 2015. Project thesis.
- [24] Foale, T. *Motorcycle Handling and Chassis Design*, pages 11–1 – 11–3. Tony Foale., Alicante, Spain, 1st edition, 2002.

- [25] Gaberson, H. and Cappillino, R. Energy losses caused by machinery misalignment and unbalance. <https://www.sem.org/Proceedings/ConferencePapers-Paper.cfm?ConfPapersPaperID=38337>, 1999. [Online; accessed 21-April-2016].
- [26] Elkhatab, A. Energy consumption and machinery vibrations. In *International Congress on Sound & Vibrations, Cairns, Australia, July 9-12*, pages 1-6, 2007.
- [27] Taneja, S. Effect of unbalance on performance of centrifugal pump. *International Journal of Scientific & Technology Research*, 2(8):p.55-60, 2013.
- [28] Bulsara, M. , Hingu, A. and Vaghasiya, P. Energy loss due to unbalance in rotor-shaft system. *Journal of Engineering, Design and Technology*, 14(2), 2016.
- [29] Heywood, J. *Internal Combustion Engine Fundamentals*, pages 725-736. McGraw-Hill, New York, US, 1988.
- [30] Eshback, O., Tapley, B. and Poston, T. *Eshback's Handbook of Engineering Fundamentals*, pages 353-354. John Wiley & Sons, New York, US, 1990.
- [31] SKF. Estimating frictional moment. <http://www.skf.com/au/products/bearings-units-housings/ball-bearings/principles/friction/estimating-frictional-moment/index.html>, 2016. [Online; accessed 17-June-2016].
- [32] SKF. Equivalent dynamic bearing load. <http://www.skf.com/sg/products/bearings-units-housings/bearing-units/roller-bearing-units/roller-bearing-units-general/equivalent-dynamic-bearing-load/index.html>, 2016. [Online; accessed 16-June-2016].
- [33] Hillier, V. *Fundamentals of motor vehicle technology*, page 64. Stanley Thornes Ltd., UK, 4th edition, 1991.
- [34] International standard ISO 1940. Mechanical vibration - balance quality requirements for rotors in a constant (rigid) state - part 1: Specification and verification of balance tolerances. http://www.dcma.mil/NPP/files/ISO_1940-1.pdf, 2016. [Online; accessed 02-May-2016].
- [35] Emerson Industrial Automation. Lses. <http://www.emersonindustrial.com/en-EN/leroy-somer-motors-drives/Products/asynchronous-motors/3-phase-motors-for-standard-applications/Pages/LSES.aspx>, 2016. [Online; accessed 13-June-2016].

- [36] Medias Schaeffler. Self-aligning ball bearings 1205-k-tvh-c3 + h025. http://medias.schaeffler.com/medias/en!hp.ec.br.pr/12..-K%20%2\%20H*1205-K-TVH-C3%20%2B%20H, 2016. [Online; accessed 13-June-2016].
- [37] SKF. Split plummer block housings, snl and se series for bearings on adapter sleeve, with standard seals. <http://www.skf.com/group/products/bearings-units-housings/bearing-housings/split-plummer-block-housings-snl-2-3-5-6-series/snl-se-series-adapter-sleeve-with-standard-seals/index.html?designation=SNL%20505%20%2B%201205%20K%20%2B%20H%20205>, 2016. [Online; accessed 13-June-2016].
- [38] Hottinger Baldwin Messtechnik (HBM). T22 cost effective torque transducer for standard industrial applications. <https://www.hbm.com/en/2384/t22-torque-transducer-for-simple-torque-applications>, 2016. [Online; accessed 13-June-2016].
- [39] The Timken Company. Timken part number ucp204-12, ucp - pillow block units. <http://cad.timken.com/item/pes-housed-unit-bearings-ball-bearing-housed-units/ucp-pillow-block-units/ucp204-12>, 2016. [Online; accessed 13-June-2016].
- [40] Hottinger Baldwin Messtechnik (HBM). Mounting instructions t22. <https://www.hbm.com/fileadmin/mediapool/hbmdoc/technical/a2302.pdf>, 2016. [Online; accessed 10-June-2016].
- [41] Wikipedia. Motocross world championship. https://en.wikipedia.org/w/index.php?title=Motocross_World_Championship&oldid=714736842, 2016. [Online; accessed 6-May-2016].
- [42] Honda Powersports homepage. Honda crf250r specifications. <http://powersports.honda.com/2015/crf250r/specifications.aspx>, 2016. [Online; accessed 06-May-2016].
- [43] Mx Real Racing. Mx real racing parts. <http://www.mxrealracing.com/default.aspx>, 2016. [Online; accessed 9-May-2016].
- [44] Herapath, C., Barrans, S., Weston, W. A comparison of design methodologies for journal bearings under pulsatile loads. In *International Conference on Renewable Energies and Power Quality, Las Palmas de Gran Canaria, Spain, April 13–15, 2011*.

- [45] Kinnear, D., Mishra, R., Weston, W., Padgett, C. A design methodology for the prediction of squeeze film stiffness and damping characteristics in hybrid journal bearings under pulsatile load conditions. In *International Conference on Renewable Energies and Power Quality, Granada, Spain, March 23–25*, 2010.
- [46] Flores, P., Ambrosio, J., Claro, J. and Lankarani, H. *Kinematics and Dynamics of Multibody Systems with Imperfect Joints: Models and Case Studies*, pages 129–130. Springer, Berlin, Germany, 2008.
- [47] Bell, A. *Four-stroke Performance Tuning*, pages 415–420. Haynes North America, Inc., California, USA, 4th edition, 2012.
- [48] Inc. Falicon Crankshaft Components. Big bore / stroker kits. <http://www.faliconcranks.com/bbk.html>, 2011. [Online; accessed 30-May-2016].
- [49] Téllez, H. and Rovira, N. Computer aided innovation of crankshafts using genetic algorithms. *IFIP International Federation for Information Processing*, 207:471–476, 2006.
- [50] Mathworks. What is the genetic algorithm? http://se.mathworks.com/help/gads/what-is-the-genetic-algorithm.html?s_tid=gn_loc_drop, 2016. [Online; accessed 16-May-2016].
- [51] Albers, A., Rovira, N., Maier, T. and Aguayo, H. Comparison of strategies for the optimization/innovations of crankshaft balance. *IFIP International Federation for Information Processing*, 250:201–210, 2007.
- [52] Albers, A., Rovira, N., Aguayo, H. and Maier, T. Optimization with genetic algorithms and splines as a way for computer aided innovation. *IFIP International Federation for Information Processing*, 277:7–18, 2008.

Appendix

Appendix A

Journal bearings (often called plain bearings) are often used for crankshafts. The following section present a friction model for journal bearings including oil viscosity and eccentricity between bearing and journal.

Friction in journal bearings

Journal bearings can carry high loads without substantial energy loss under normal operating speed due to the pressurised oil film between the journal and the bearing [29]. A pulsating crankshaft load due to the reciprocating forces and the variable inertia, however, may change this oil film pressure, as well as creating a fluctuating eccentricity between the journal centre axis and the bearing centre axis [44], as seen in Figure 7.1.

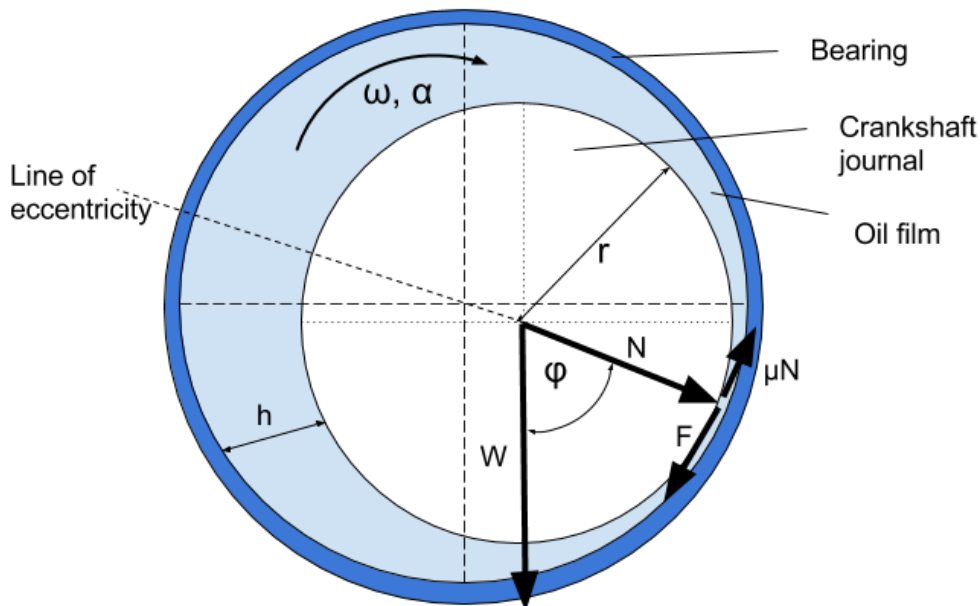


Figure 7.1: The friction force, F , acts in the opposite direction from the journal rotation, ω , reducing its rotational speed.

Journal bearings may operate with hydrostatic effects, hydrodynamic effects, or the two combined as in hybrid bearings [45]. The hydrostatic effect, i.e. when the bearing is subjected to the crankshaft load resulting in a pressurised oil film which creates a gap between the journal and the bearing, is most suitable for low-speed applications. The hydrodynamic effect is a result of the crankshaft's journals rotating inside the bearings and

is speed-dependant. The hydrodynamic effect is, however, insufficient at engine start-up speed, as the viscosity is high at low speeds. The combination of hydrostatic and hydrodynamic effects is therefore desirable to ensure proper lubrication and minimal friction during the whole speed range of the engine [45].

As seen in Figure 7.1 the oil film thickness, h , changes as the journal rotates around an axis that does not coincide with the bearing centre line. The friction in the bearings creates a moment that rotates in the opposite direction of the crankshaft torque, i.e. working against the engine torque:

$$T_{loss,friction} = T_{applied} - T_{friction} \quad (7.1)$$

Heywood [29] presents an equation to calculate the friction torque based on the bearing area, mean velocity gradient in the oil film, the oil viscosity and a correction for the offset of the journal relative to the bearing centre:

$$T_{friction} = F_f \cdot r_j = \left[\frac{\pi^2 \cdot \mu \cdot D_b^2 \cdot L_b \cdot \omega}{(1 - \varepsilon^2)^{1/2} \cdot \bar{h}} + \frac{\bar{h} \cdot \varepsilon \cdot W}{D_b} \cdot \sin\phi \right] \cdot r_j \quad (7.2)$$

where, $D_b = bearing\ diameter$

$L_b = bearing\ length$

$\omega = shaft\ rotational\ speed$

$\mu = oil\ viscosity$

$r_j = crank\ journal\ radius$

$\bar{h} = mean\ radial\ clearance$

$\varepsilon = eccentricity\ ratio = \frac{\bar{h} - h_m}{\bar{h}}$, where $h_m = minimum\ clearance$

$\phi = attitude\ angle$

$W = bearing\ load$

The factor $\frac{1}{(1-\varepsilon^2)^{1/2}}$ and the second term in the equation of the friction force, $\frac{\bar{h} \cdot \varepsilon \cdot W}{D_b} \cdot \sin\phi$, correct for the eccentricity, e , between the journal centre and the bearing centre.

The coefficient of friction is given by:

$$f = \frac{F}{W} \quad (7.3)$$

Damping in journal bearings

The oil film pressure has a damping effect on the journal movement called the *squeeze film damping*. According to Weston *et al.* [45, 44] this squeeze film effect enables conventional journal bearings to operate successfully under pulsating loads, such as the ones the crankshaft bearings are subjected to. The bearing stiffness k and the bearing damping C_D are defined as:

$$k = \frac{3 \cdot A_E}{H} \cdot P_{SQ} = \frac{3 \cdot W}{H} \quad (7.4)$$

$$C_D = \frac{3 \cdot \eta \cdot A_E^2}{H^3 \cdot \left(\frac{Z}{L} + \frac{L}{Z}\right)} \quad (7.5)$$

where W = the shaft load, H = the bearing/journal gap, η = the oil viscosity, A_E = the squeeze area, L = bearing length, and Z = bearing width, as shown in Figure 7.2.

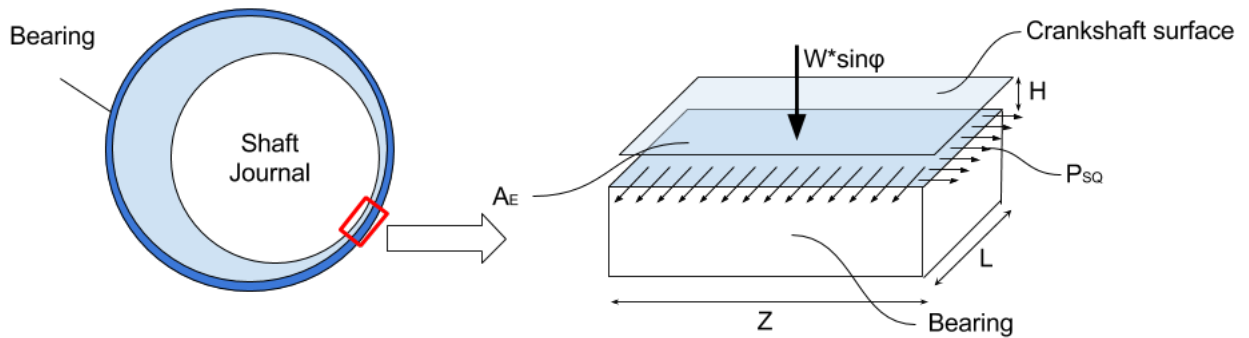


Figure 7.2: Dimensions and loading on the journal bearing from the crankshaft due to eccentricity.

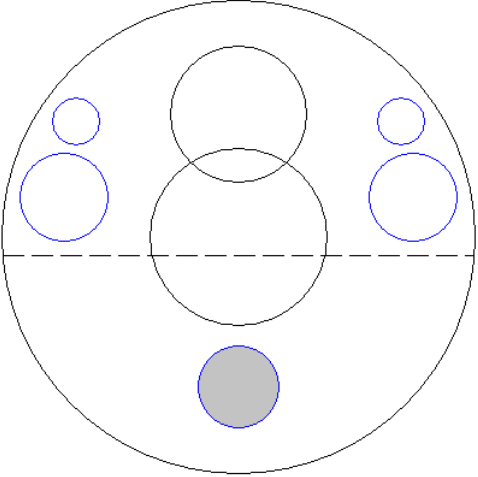
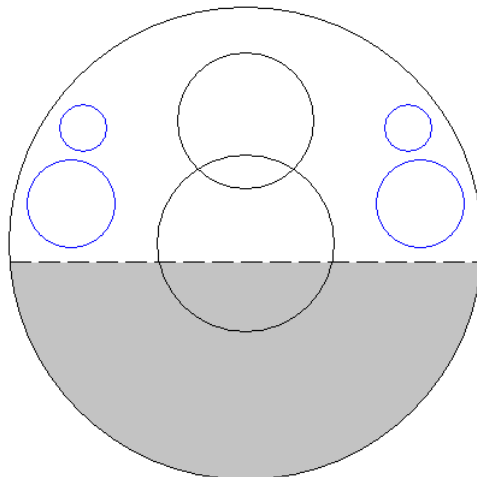
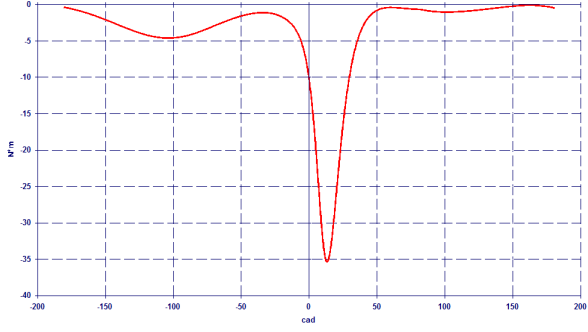
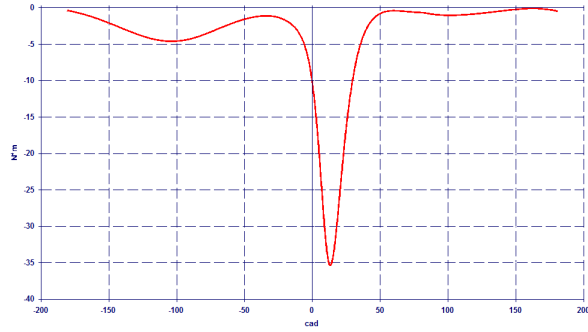
The clearance H between the crankshaft journal and the bearing affects the performance of the journal bearing. According to Flores *et al.* [46], a smaller clearance results in higher hydrodynamic forces, greater system rigidity and therefore also higher reaction forces on the system. It also increases the damping, C_d as can be seen from Equation (7.5), thus lowering the vibrations and any instability problems. However, a smaller clearance also increases the risk of metal-to-metal contact, increasing the possibility of friction and wear massively [29].

Appendix B

Different methods of obtaining balance

Two tests were conducted to achieve a balance factor of 28% for components having similar mass as MXRR parts. The crankshaft used in the test is the same as in Chapter 5.1.

Table 7.1: The two test cases.

Test 1	Test 2
Hole drilled into the crankshaft counterweight	Material is grinded off of the counterweight shoulder surface
	
	

The graphs in Table 7.1 indicate that the correction method has little effect on main bearing friction torque. Future work should investigate how the correction method and balance factor affect the build-up of the gas pressure in the cylinder.

Appendix C

Crankshaft stroking and balance

In the case where material is to be removed from the upper half of the crankshaft (crankweb and crankpin), balancing through *crankshaft stroking* can be an alternative. This method will influence both engine balance and performance; although it is not the balancing itself that results in a performance gain, but the increased displacement of the piston.

Crankshaft stroking is a tuning method where the crankpin diameter is reduced. This reduction will increase bearing loads and reduce the crankpin strength, but will slightly increase the stroke and reduce the crankpin frictional losses due to reduced crankpin diameter. Bell [47] describes cases of 15mm increased stroke by the use of this tuning method. Falicon Crankshaft Components, Inc. offer a big bore/stroker crank-set to Honda CRF250R, increasing the displacement to 297cc [48]. Crankshaft stroking will require additional modifications to the engine, which are not discussed here. Reducing the crankpin diameter results in a lighter top half of the crankshaft, reducing the rotating mass. A lighter top half of the crankshaft allows for more mass to be removed from the counterweight when balancing an engine such as the ones in Chapter 6. Figure 7.3 shows a crankshaft with a reduced crankpin diameter. Some of the crankpin mass is grinded off so that the crankpin centre is moved further away from the main journal, increasing the stroke even more.

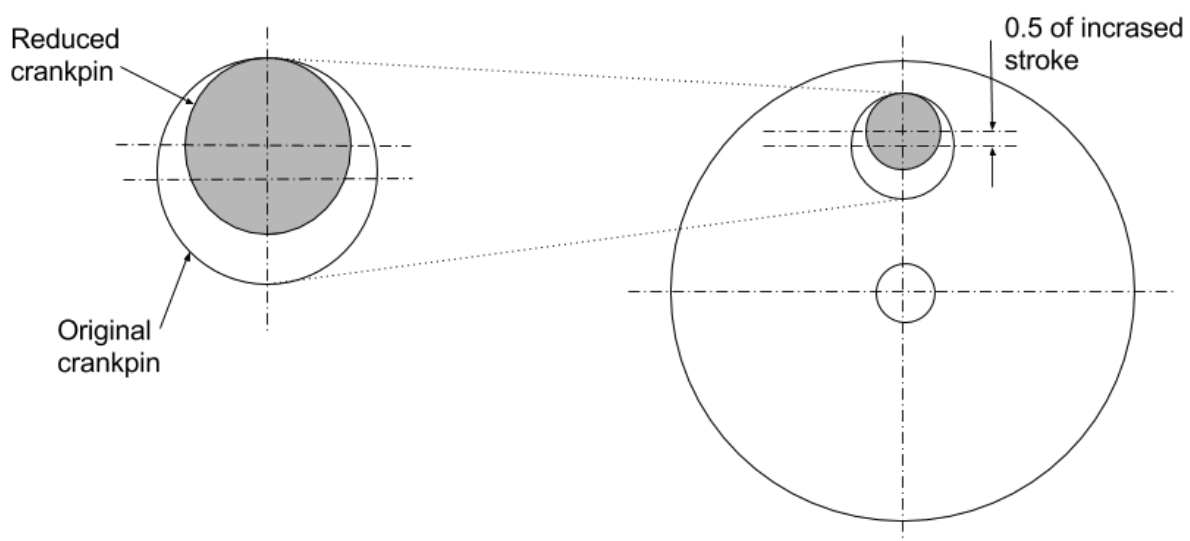


Figure 7.3: Reducing the crankpin diameter increases the stroke.

Appendix D

Approaches for automatic balancing

Balancing of the crankshaft can be both time-consuming and costly, especially if there is a need to involve external companies in performing the balancing. A CAD-based solution for automatic balancing of the crankshaft geometry could prove beneficial. Such a solution could tell the user how to modify the geometry of existing crankshafts, or even optimise the geometry of new improved crankshaft designs for specific applications. The following sections describe techniques for optimising the crankshaft design and approaches for automatic optimisation/balancing of the crankshaft.

Automatic balancing in NX

Restrictions on a modification are some of the challenges when considering automatic balancing. As an automatic balancing software should support a various range of input crankshaft designs, it is difficult to apply a global set of restrictions. One issue is determining which parts of the counterweight should be available for modifications. It seems that some user interaction is inevitable in order to parametrise the sections of the crankshaft that are suitable for modifications.

Automatic crankshaft balancing application

An approach for a simple crankshaft balancing application is developed. The program should be able to balance any crankshaft by adjusting the thickness of the counterweight shoulder. Alternative balancing methods, such as drilling holes into the counterweight, can be implemented at low cost when the application is finished.

The application will comprise of three parts:

- 1 User interface.¹
- 2 Excel spreadsheet for calculations.
- 3 CAD model in NX for geometrical measurements and modifications.

¹Product Template Studio (PTS) is considered as a GUI, but a product template is associated to a specific part-file, which could complicate the loading of different crankshafts for balancing. PTS may be better suited for creating new crankshaft designs based on user input. For re-balancing of different crankshafts, one should consider programming a GUI from scratch.

Excel is highly compatible with NX, and geometrical parameters in NX can be controlled via spreadsheets through *Expressions*.² Even though the application is said to be automatic, some user interaction is required in order to specify the mass of the reciprocating and rotating parts, as well as the desired balance factor and level of imbalance tolerance. The user will also highlight the surface to be modified in order to achieve the desired balance.

As mentioned, balance is achieved by modifying the thickness of the crankshaft shoulders. The number of millimetres to be removed, calculated by the program, is defined as *correction depth* in Figure 7.5. Figure 7.4 shows a crankshaft counterweight being modified utilising the Synchronous Modelling tool *Offset Face* in NX, with a correction depth of 3mm.

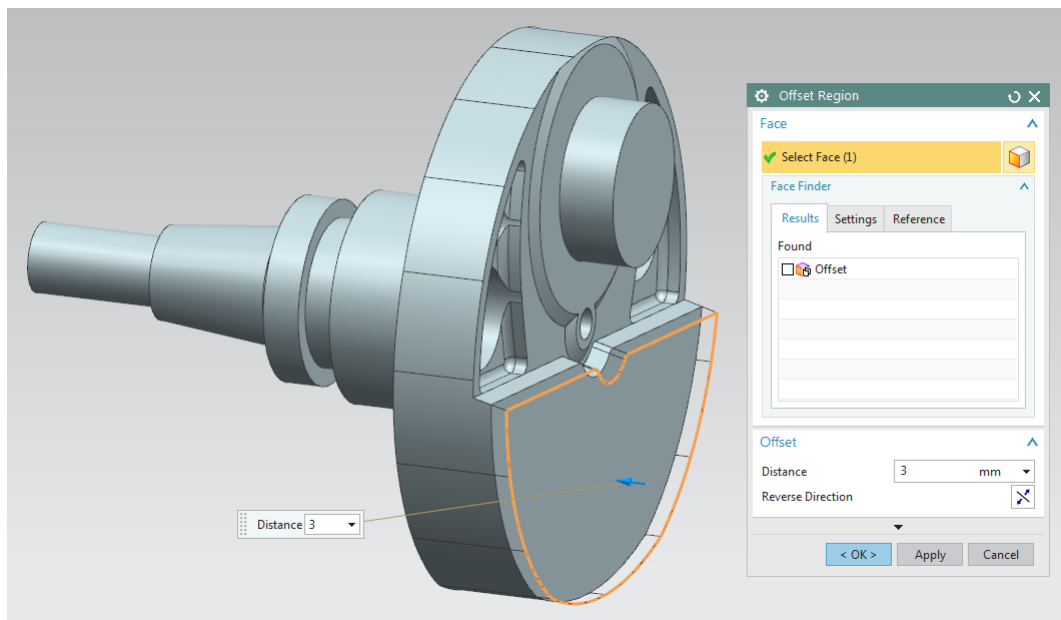


Figure 7.4: A counterweight shoulder being modified with the *Offset Face* command. The correction depth is 3 mm.

Figure 7.5 shows a flowchart describing the flow of the application and the interaction between the involved programs.

²*Expressions* is a tool in NX which allows the geometry to be parametrised and controlled by equations e.g. from a spreadsheet.

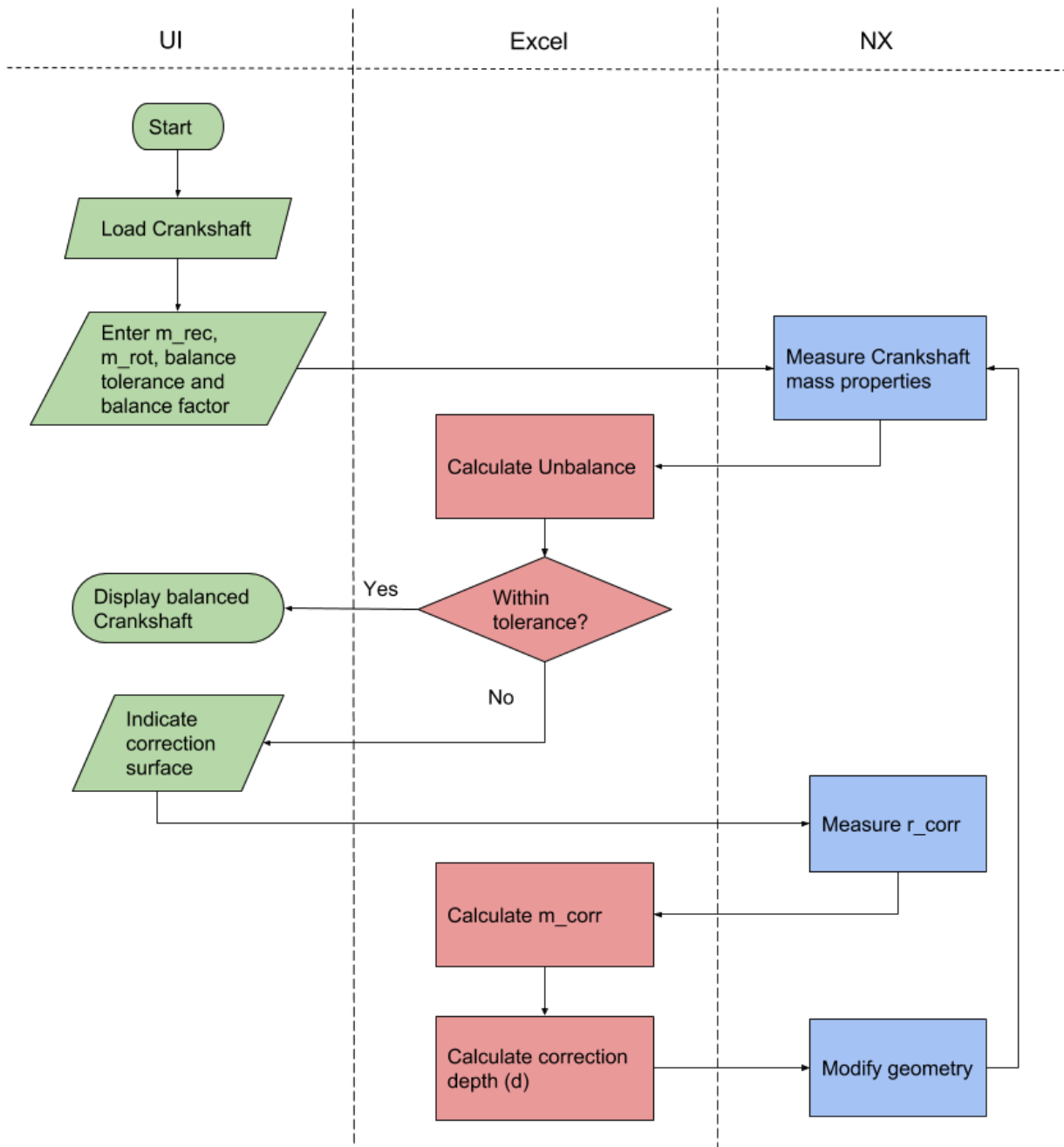


Figure 7.5: Suggested flow of automatic crankshaft balancing program.

Genetic Algorithms

Genetic algorithms (GAs) are a field within artificial intelligence that utilise concepts from evolutionary theory and are based on natural selection. A genetic algorithm is used as a global optimisation technique, and is an iterative procedure that maintains a constant population (P) of candidate solutions (individuals). For each iteration, each candidate in the population is evaluated against a *fitness function*, and a new population is formed. Each iteration is called a *generation* where random individuals are selected to act as parents for the individuals of the next generation. After several iterations/generations, the population evolves towards an optimal solution [49].

GAs use three main rules at each iteration to create the next generation [50]:

1. *Selection rules*: Select parents to contribute to the next generation.
2. *Crossover rules*: Combine two parents to form children.
3. *Mutation rules*: Random changes to parents to form the children.

Computer Aided Innovation of Crankshaft balance and geometry optimisation using Genetic Algorithms

Rovira *et al.* [49][51][52] utilise Genetic Algorithms as a tool in order to explore different crankshaft designs and to optimise the geometry for a specific required balance. The crankshaft to be balanced is modelled in a CAD-software where its mass properties are obtained, and the crankshaft profile is substituted by *splines* (see Figure 7.6). The mass properties are used to calculate the imbalance of the crankshaft, and the fitness function is defined as the difference between the target imbalance and the current imbalance. The initial population consists of the control points of the splines, and a new population of crankshafts is created by changing their position. Each crankshaft in the population is evaluated against the fitness function, and the individuals that are the closest to the target imbalance will form the new population i.e. *survival of the fittest*. Multiple restrictions may be added to the genetic algorithm to ensure structural stability of the crankshaft, such as acceptable stresses and Eigen-frequencies.

The location of the spline's control points need to be transported from the CAD model into the Genetic Algorithm through an interface, as the x and y coordinates of the control points are parametrically manipulated by the GA. This can be performed by e.g. Excel or by programming a script. Figure 7.6 shows a crankshaft with a *splined* counterweight and its control points. The splines are applied to the model in NX using the *Studio Spline* tool with *Through Points* as spline type.

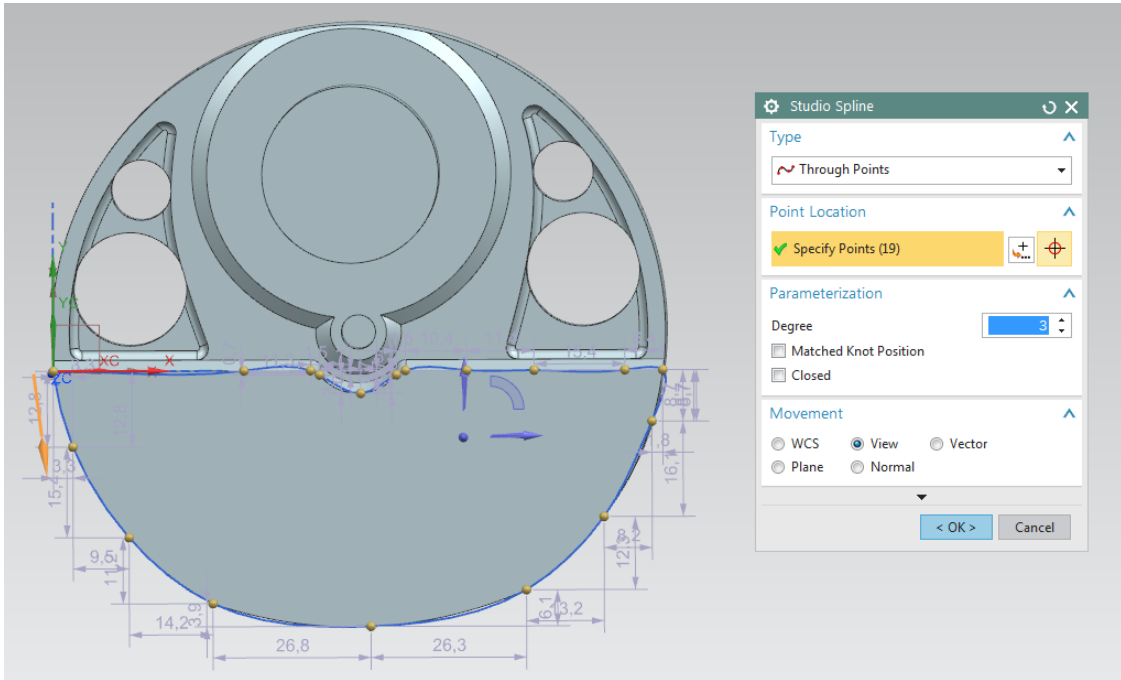


Figure 7.6: A splined crankshaft counterweight with highlighted control points

The benefit of using GAs to search for the optimal crankshaft design is the vast number of evaluated individuals. The population is of constant size in each generation, thus giving a large number of optimal crankshaft designs when the optimal design is reached. The fitness function can be altered such that it describes the optimum performance characteristics, not just the optimal imbalance tolerance as was used by Rovira *et al.* The designer can then choose the most suitable design to implement [52].

Appendix E

Preservation of the mass moment of inertia

The simplified crankshaft used in the test in Chapter 5 is different from the Honda CRF250R crankshaft in terms of geometry, but maintains the original mass moment of inertia (MMOI).

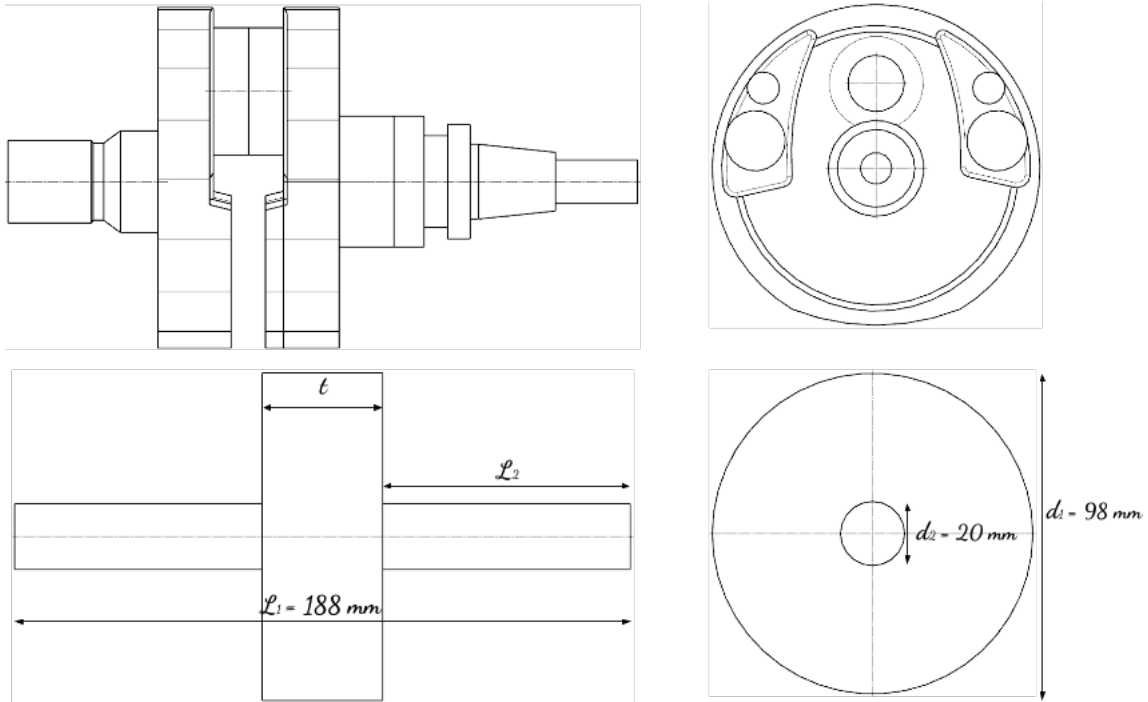


Figure 7.7: The complex Honda CRF250R crankshaft is simplified to a basic rotor.

The formula for the MMOI of a solid cylinder or disk about its axis of symmetry is:

$$I = \frac{m \cdot r^2}{2} = \frac{\rho \cdot V \cdot r^2}{2} \quad (7.6)$$

Based on Equation (7.6) and the dimensions given in Figure 7.7, I_{disc} and I_{shaft} are calculated as:

$$I_{disc} = \frac{\rho \cdot \left(\pi \cdot \left(\frac{d_1}{2} \right)^2 \cdot t \right) \cdot \left(\frac{d_1}{2} \right)^2}{2} = \frac{\rho \cdot \pi \cdot d_1^4 \cdot t}{32}$$

$$I_{shaft} = 2 \cdot \left[\frac{\rho \cdot \left(\pi \cdot \left(\frac{d_2}{2} \right)^2 \cdot \frac{L_1 - t}{2} \right) \cdot \left(\frac{d_2}{2} \right)^2}{2} \right] = \frac{\rho \cdot \pi \cdot d_2^4 \cdot (L_1 - t)}{32}$$

Where $\rho = 7850 \text{ kg/m}^3$.

The total moment of inertia is then calculated as:

$$I_{tot} = I_{shaft} + I_{disc} = \frac{\rho \cdot \pi}{32} \cdot \left(d_1^4 \cdot t + d_2^4 \cdot (L_1 - t) \right) \quad (7.7)$$

The MMOI of the original crankshaft is measured to 2847,335 $kg \cdot mm^2$ in NX. If the simplified crankshaft and the original crankshaft is to have the same moment of inertia, the thickness t of the disc needs to be calculated. As the original moment of inertia is given in units $kg \cdot mm^2$ the factor 10^9 is added and Equation (7.7) is rearranged to:

$$t = \left(\frac{10^9 \cdot 32 \cdot I_{original}}{\rho \cdot \pi} - d_2^4 \cdot l \right) \cdot \frac{1}{d_1^4 - d_2^4} \quad , \quad [mm] \quad (7.8)$$

Now, the values of different variables can be inserted directly without any unit conversions.

Once the thickness of the disc is calculated, the length of the crankshaft journal ends can be calculated as:

$$L_2 = \frac{L_1 - t}{2} \quad (7.9)$$

The simplified crankshaft is created based on the data in Table 7.2.

Table 7.2: Dimensions of the simplified crankshaft and the moment of inertia of the original Honda CRF250R crankshaft.

d_1	98 mm
d_2	20 mm
L_1	188 mm
ρ	7850 kg/m^3
$I_{original}$	2847.335 $kg \cdot mm^2$
t	36.704 mm
L_2	75.648 mm

Appendix F

Required torque curves from FEDEM simulations

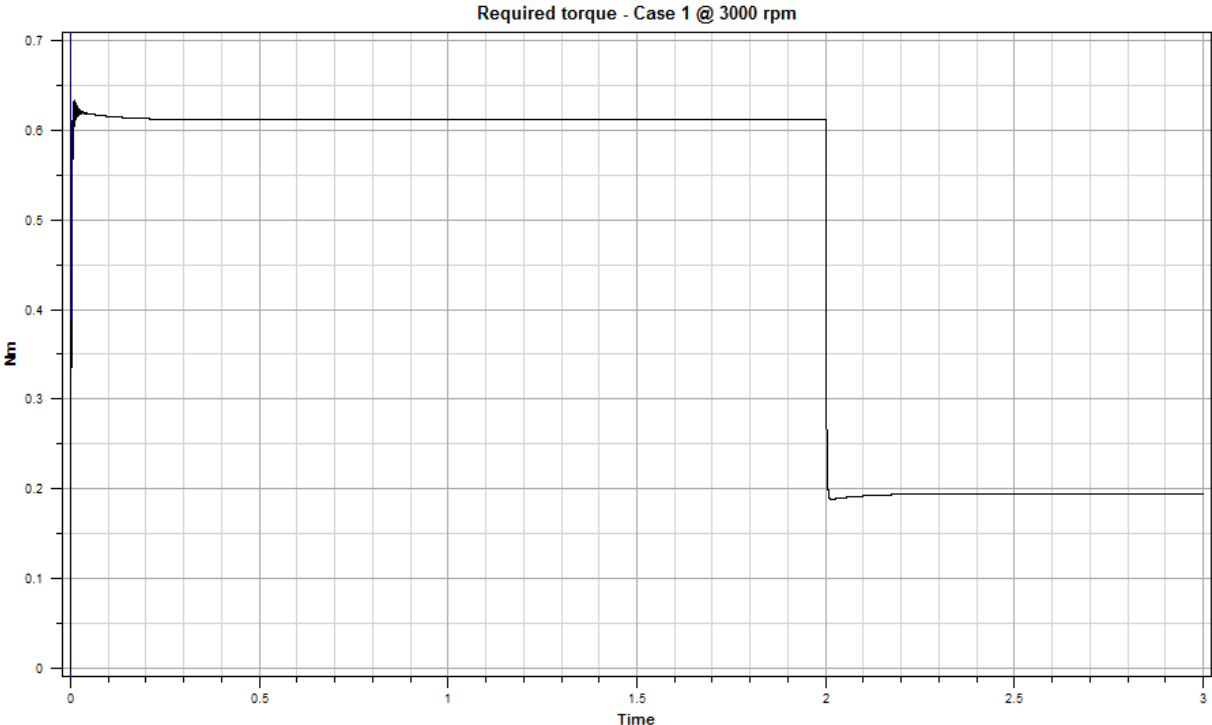


Figure 7.8: Required torque to keep the rotor in Case 1 at 3000 RPM is 0.1949 Nm.

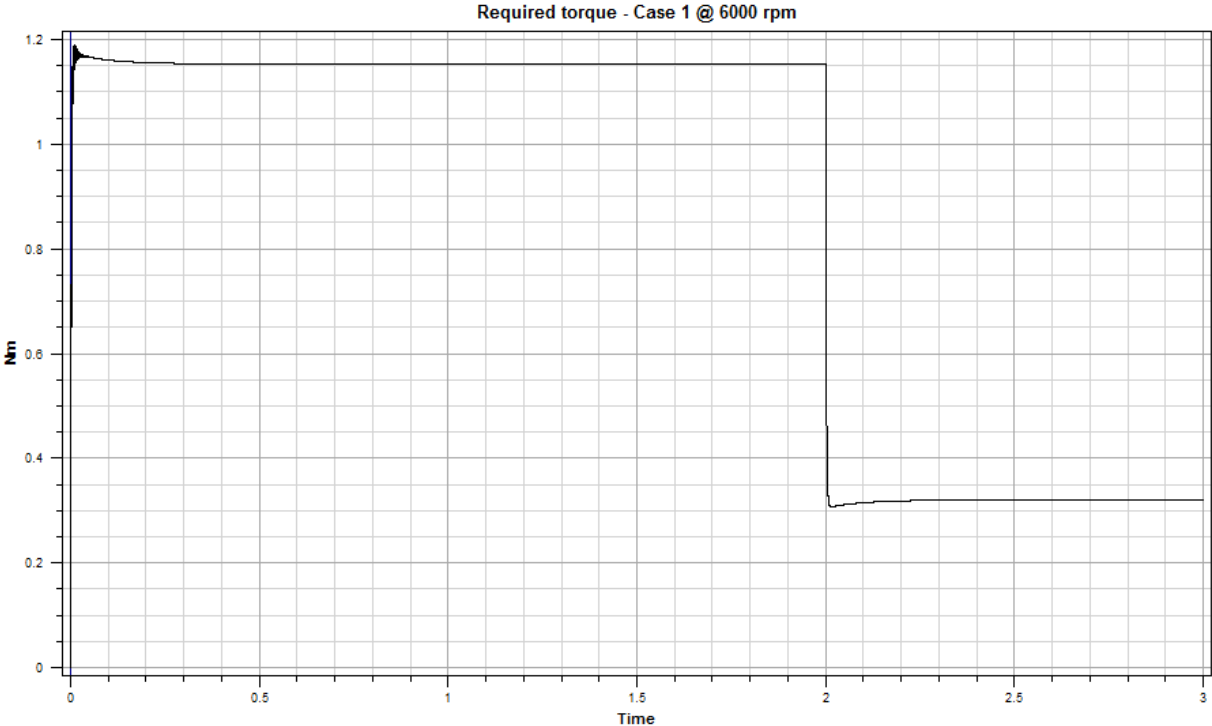


Figure 7.9: Required torque to keep the rotor in Case 1 at 6000 RPM is 0.3204 Nm.

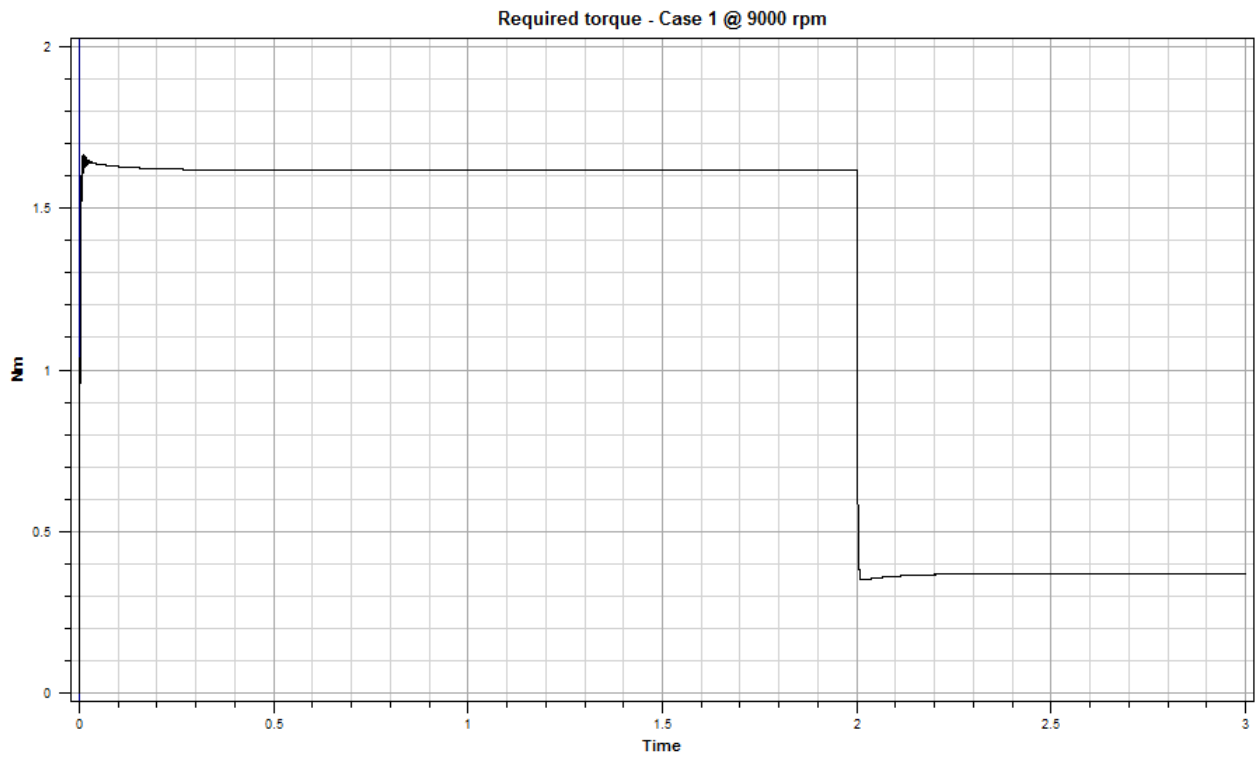


Figure 7.10: Required torque to keep the rotor in Case 1 at 9000 RPM is 0.3696 Nm.

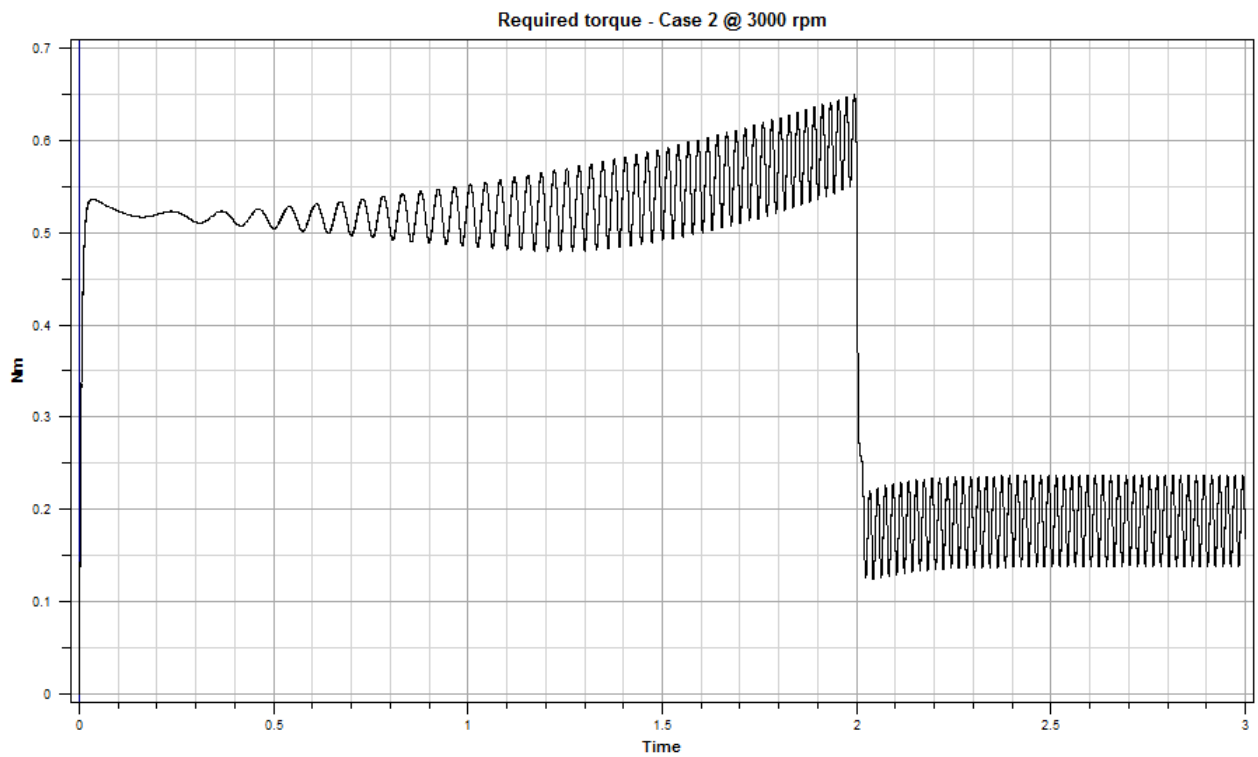


Figure 7.11: Required torque to keep the rotor in Case 2 at 3000 RPM is 0.1897 Nm.

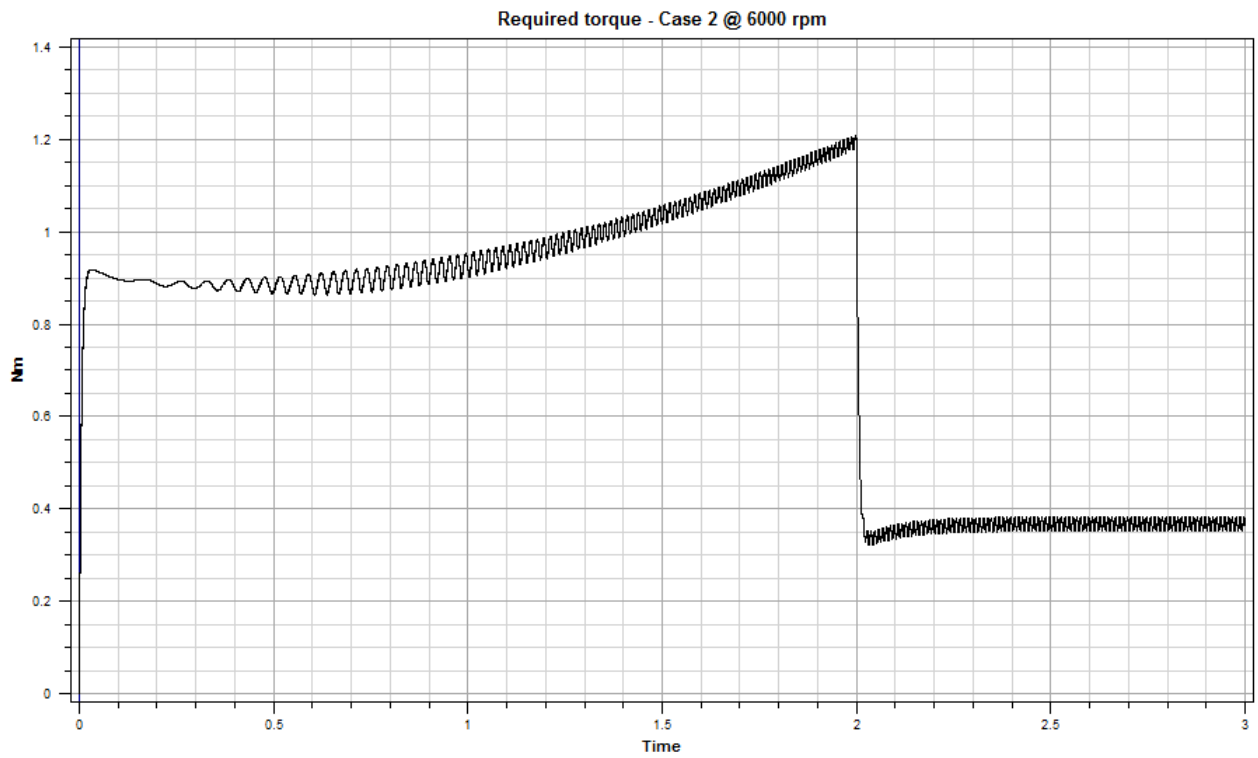


Figure 7.12: Required torque to keep the rotor in Case 2 at 6000 RPM is 0.3670 Nm.

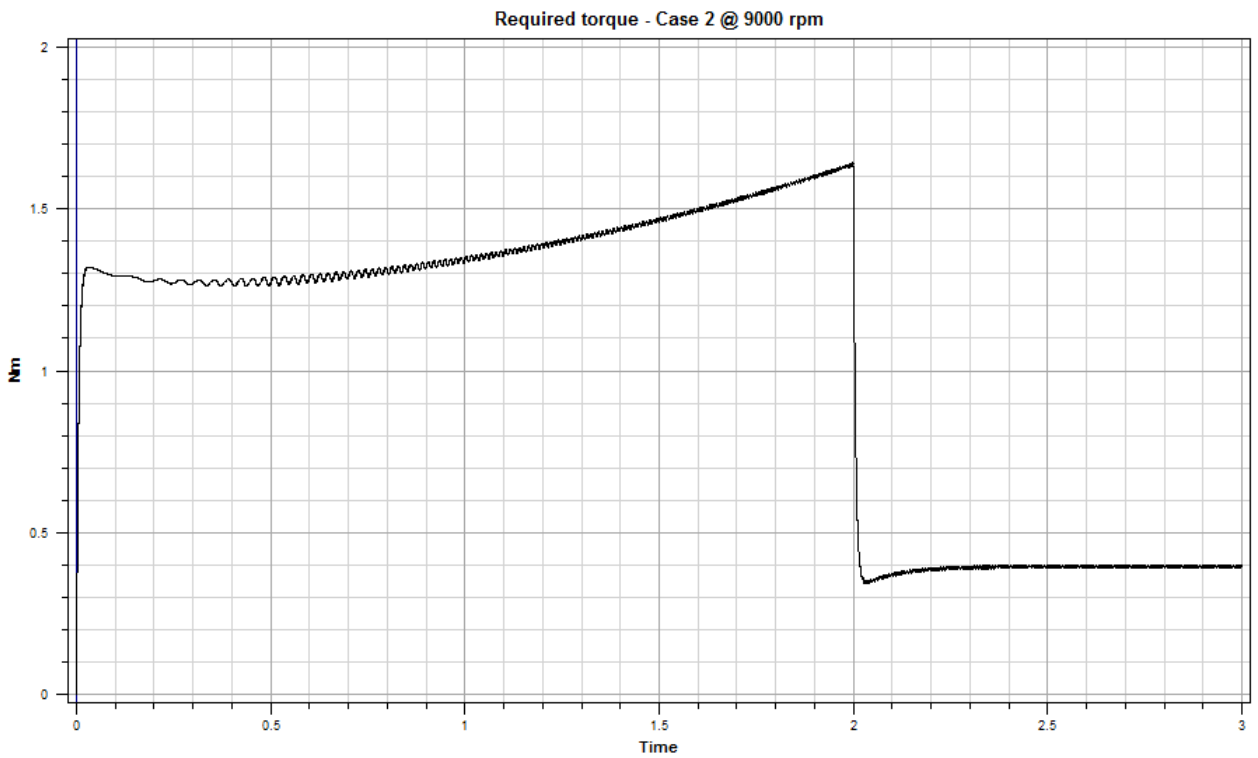


Figure 7.13: Required torque to keep the rotor in Case 2 at 9000 RPM is 0.3948 Nm.

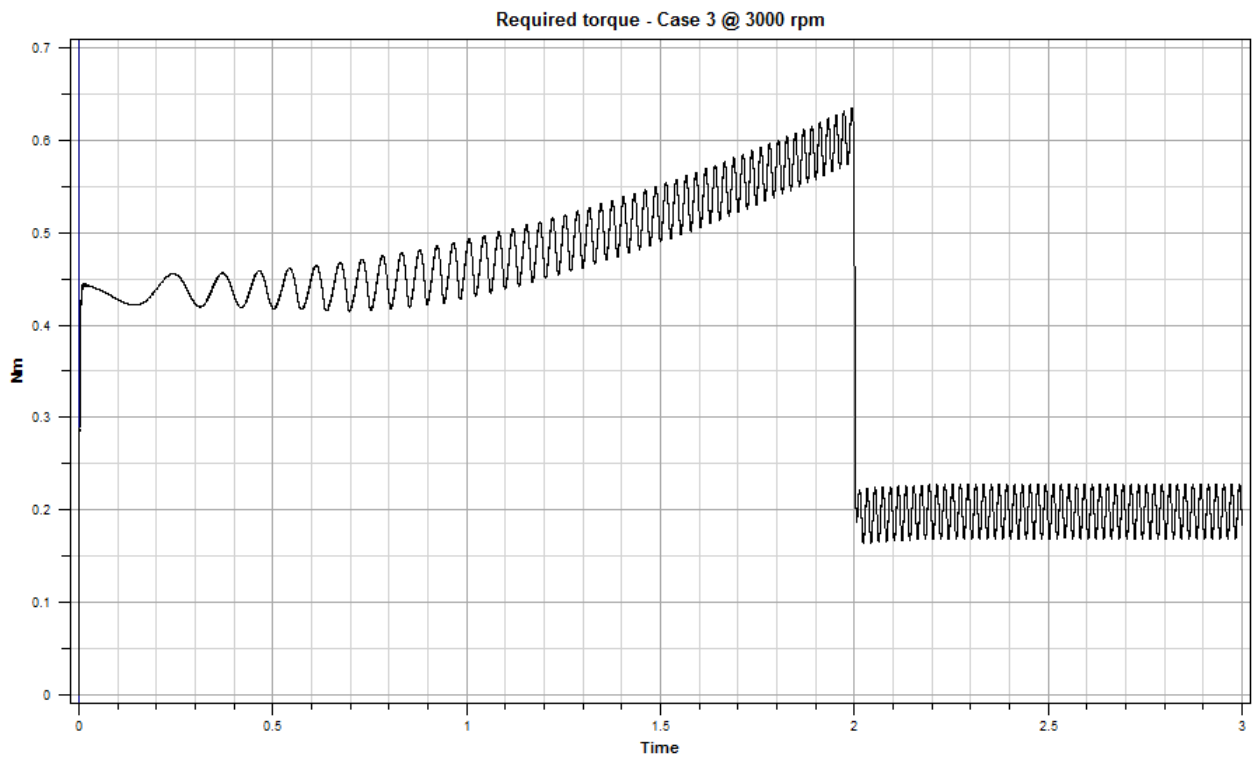


Figure 7.14: Required torque to keep the rotor in Case 3 at 3000 RPM is 0.1988Nm.

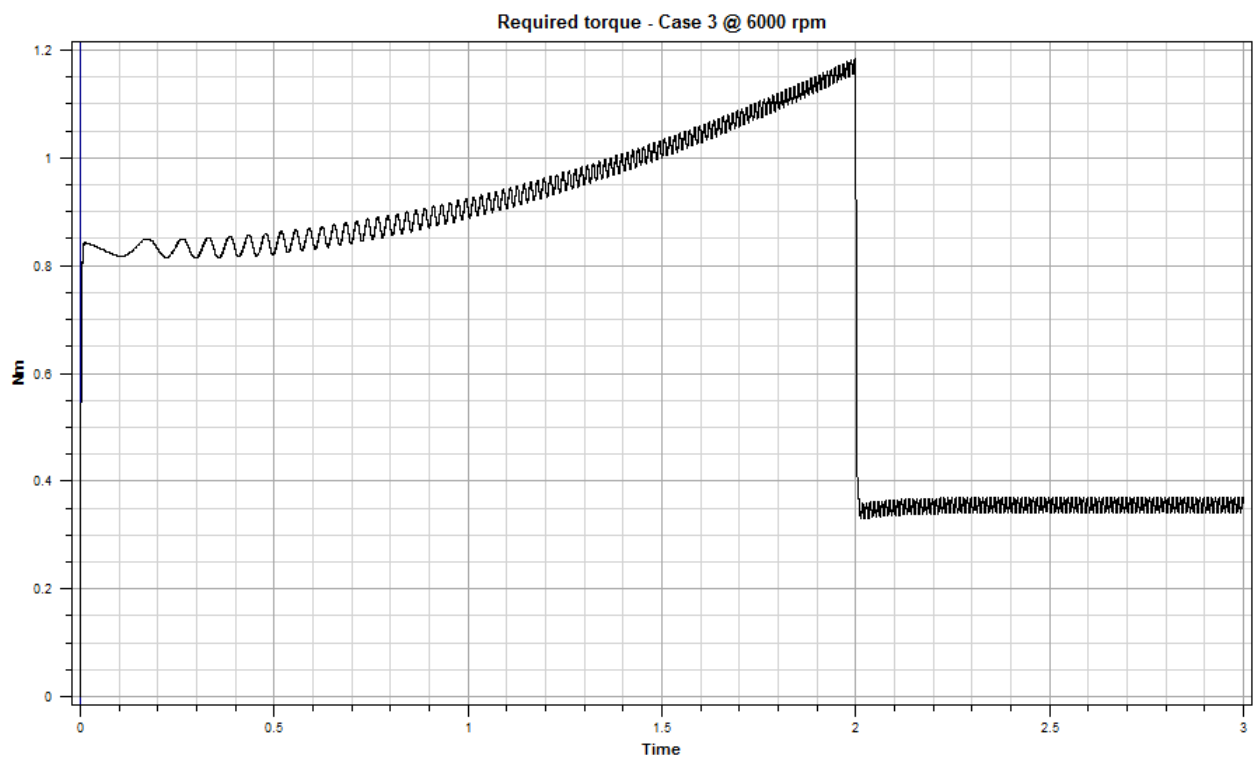


Figure 7.15: Required torque to keep the rotor in Case 3 at 6000 RPM is 0.3555 Nm.

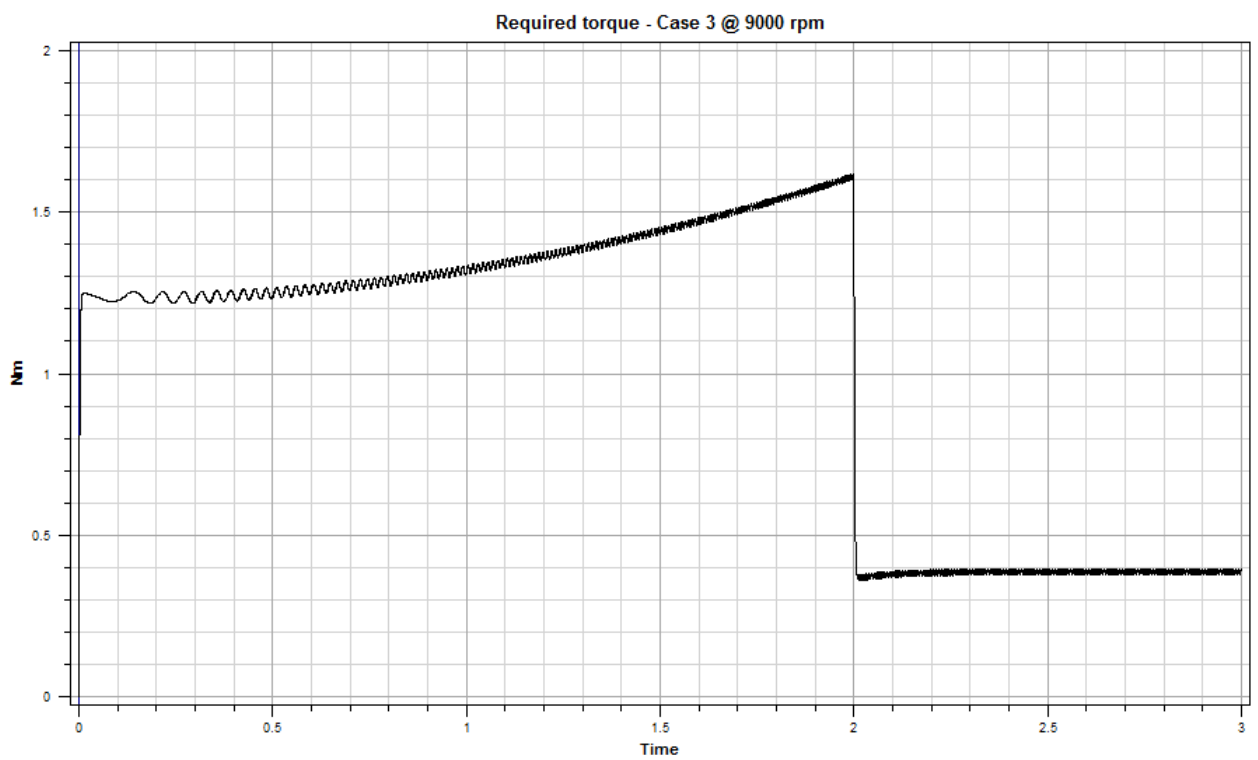


Figure 7.16: Required torque to keep the rotor in Case 3 at 9000 RPM is 0.3861 Nm.

Appendix G

Master thesis

THE NORWEGIAN UNIVERSITY
OF SCIENCE AND TECHNOLOGY
DEPARTMENT OF ENGINEERING DESIGN
AND MATERIALS

MASTER THESIS AUTUMN 2015 FOR STUD. TECHN. ODA ENGER HOEM

ENGINE BALANCING FOR MAXIMUM PERFORMANCE

Balansering av motorer for maksimal ytelse

Piston engine balancing is a complicated subject that covers many areas in the design, production, tuning and operation. The engine considered to be well balanced in a particular usage may produce unacceptable level of vibration in another usage for the difference in driven mass and mounting method, and slight variations in resonant frequencies of the environment and engine parts could be big factors in throwing a smooth operation off balance. An engine should be in both static and dynamic balance.

Static balance refers to the balancing of weight and the location of CG on moving parts.

1. Reciprocating mass - e.g. Piston and conrod weight and CG uniformity.
2. Rotating mass - e.g. Crank web weight uniformity and flywheel concentricity

Dynamic balance refers to the balancing of inertia and friction forces. All accelerations of a mass can be divided into two components opposing in the direction. For example, in order for a piston in a single cylinder engine to be accelerated upward, something must receive (support) the downward force, and it is usually the mass of the entire engine that moves downward a bit as there is no counter-moving piston. This means one cause of engine vibration usually appears in two opposing directions. Often the movement or deflection in one direction appears on a moving mass, and the other direction appears on the entire engine, but sometimes both sides appear on moving parts, e.g. a torsional vibration killing a crankshaft, or a push-pull resonance breaking a chain.

This project will focus on methods to identify and eliminate unbalances in crankshafts due to the (reciprocating) crankshaft, connecting rod, piston and pin masses. The candidate must study the theory in order to understand the effect of unbalanced crankshafts on the engine performance and ride comfort (project). Then he/she must find and implement methods for automatic balancing of single cylinder crankshafts in FEDEM (master). Have a look at <http://www.quora.com/How-is-the-balancing-of-rotating-and-reciprocating-masses-done>

Piston engine balancing is a complicated subject that covers many areas in the design, production, tuning and operation. The engine considered to be well balanced in a particular usage may produce unacceptable level of vibration in another usage for the difference in driven mass and mounting method, and slight variations in resonant frequencies of the environment and engine parts could be big factors in throwing a smooth operation off balance. An engine should be in both static and dynamic balance.

Static balance refers to the balancing of weight and the location of CG on moving parts.

1. Reciprocating mass - e.g. Piston and conrod weight and CG uniformity.
2. Rotating mass - e.g. Crank web weight uniformity and flywheel concentricity

Dynamic balance refers to the balancing of inertia and friction forces. All accelerations of a mass can be divided into two components opposing in the direction. For example, in order for a piston in a single cylinder engine to be accelerated upward, something must receive (support) the downward force, and it is usually the mass of the entire engine that moves downward a bit as there is no counter-moving piston. This means one cause of engine vibration usually appears in two opposing directions. Often the movement or deflection in one direction appears on a moving mass, and the other direction appears on the entire engine, but sometimes both sides appear on moving parts, e.g. a torsional vibration killing a crankshaft, or a push-pull resonance breaking a chain.

This master will focus on methods to identify and eliminate unbalances in crankshafts due to the (reciprocating) crankshaft, connecting rod, piston and pin masses. The candidate must study the theory in order to understand the effect of unbalanced crankshafts on the engine performance and ride comfort (project). Then he/she must find and implement methods for automatic balancing of single cylinder crankshafts in FEDEM (master). Have a look at <http://www.quora.com/How-is-the-balancing-of-rotating-and-reciprocating-masses-done>

The master will include the following tasks:

1. Study state of art in engine balancing for maximum performance. Review both theory and tools
2. Evaluate possible approaches for automatic balancing of engines (CAD based).
3. Perform sensitivity studies on how engine balancing influence the performance (throttle response, maximum power and torque)
4. Model and optimize the performance of a Suzuki or Honda racing engine based on the results from task 1-3
5. Prepare a paper on engine balancing and performance (the thesis can be formatted as scientific paper)

Formal requirements:

Three weeks after start of the thesis work, an A3 sheet illustrating the work is to be handed in. A template for this presentation is available on the IPM's web site under the menu "Masteroppgave" (<http://www.ntnu.no/ipm/masteroppgave>). This sheet should be updated one week before the master's thesis is submitted.

Risk assessment of experimental activities shall always be performed. Experimental work defined in the problem description shall be planned and risk assessed up-front and within 3 weeks after receiving the problem text. Any specific experimental activities which are not properly covered by the general risk assessment shall be particularly assessed before performing the experimental work. Risk assessments should be signed by the supervisor and copies shall be included in the appendix of the thesis.

The thesis should include the signed problem text, and be written as a research report with summary both in English and Norwegian, conclusion, literature references, table of contents, etc. During preparation of the text, the candidate should make efforts to create a well arranged and well written report. To ease the evaluation of the thesis, it is important to cross-reference text, tables and figures. For evaluation of the work a thorough discussion of results is appreciated.

The thesis shall be submitted electronically via DAIM, NTNU's system for Digital Archiving and Submission of Master's theses.

The contact person is Matteo Bella from MXRR and Glenn from Falcon Crankshaft.



Torgeir Welo
Head of Division



Terje Rølvåg
Professor/Supervisor



THE NORWEGIAN UNIVERSITY
OF SCIENCE AND TECHNOLOGY
DEPARTMENT OF ENGINEERING DESIGN
AND MATERIALS

**MASTER THESIS AUTUMN 2015
FOR
STUD. TECHN. VEGARD RØSHOLM**

ENGINE BALANCING FOR MAXIMUM PERFORMANCE

Balansering av motorer for maksimal ytelse

Piston engine balancing is a complicated subject that covers many areas in the design, production, tuning and operation. The engine considered to be well balanced in a particular usage may produce unacceptable level of vibration in another usage for the difference in driven mass and mounting method, and slight variations in resonant frequencies of the environment and engine parts could be big factors in throwing a smooth operation off balance. An engine should be in both static and dynamic balance.

Static balance refers to the balancing of weight and the location of CG on moving parts.

1. Reciprocating mass - e.g. Piston and conrod weight and CG uniformity.
2. Rotating mass - e.g. Crank web weight uniformity and flywheel concentricity

Dynamic balance refers to the balancing of inertia and friction forces. All accelerations of a mass can be divided into two components opposing in the direction. For example, in order for a piston in a single cylinder engine to be accelerated upward, something must receive (support) the downward force, and it is usually the mass of the entire engine that moves downward a bit as there is no counter-moving piston. This means one cause of engine vibration usually appears in two opposing directions. Often the movement or deflection in one direction appears on a moving mass, and the other direction appears on the entire engine, but sometimes both sides appear on moving parts, e.g. a torsional vibration killing a crankshaft, or a push-pull resonance breaking a chain.

This project will focus on methods to identify and eliminate unbalances in crankshafts due to the (reciprocating) crankshaft, connecting rod, piston and pin masses. The candidate must study the theory in order to understand the effect of unbalanced crankshafts on the engine performance and ride comfort (project). Then he/she must find and implement methods for automatic balancing of single cylinder crankshafts in FEDEM (master). Have a look at <http://www.quora.com/How-is-the-balancing-of-rotating-and-reciprocating-masses-done>

Piston engine balancing is a complicated subject that covers many areas in the design, production, tuning and operation. The engine considered to be well balanced in a particular usage may produce unacceptable level of vibration in another usage for the difference in driven mass and mounting method, and slight variations in resonant frequencies of the environment and engine parts could be big factors in throwing a smooth operation off balance. An engine should be in both static and dynamic balance.

Static balance refers to the balancing of weight and the location of CG on moving parts.

1. Reciprocating mass - e.g. Piston and conrod weight and CG uniformity.
2. Rotating mass - e.g. Crank web weight uniformity and flywheel concentricity

Dynamic balance refers to the balancing of inertia and friction forces. All accelerations of a mass can be divided into two components opposing in the direction. For example, in order for a piston in a single cylinder engine to be accelerated upward, something must receive (support) the downward force, and it is usually the mass of the entire engine that moves downward a bit as there is no counter-moving piston. This means one cause of engine vibration usually appears in two opposing directions. Often the movement or deflection in one direction appears on a moving mass, and the other direction appears on the entire engine, but sometimes both sides appear on moving parts, e.g. a torsional vibration killing a crankshaft, or a push-pull resonance breaking a chain.

This master will focus on methods to identify and eliminate unbalances in crankshafts due to the (reciprocating) crankshaft, connecting rod, piston and pin masses. The candidate must study the theory in order to understand the effect of unbalanced crankshafts on the engine performance and ride comfort (project). Then he/she must find and implement methods for automatic balancing of single cylinder crankshafts in FEDEM (master). Have a look at <http://www.quora.com/How-is-the-balancing-of-rotating-and-reciprocating-masses-done>

The master will include the following tasks:

1. Study state of art in engine balancing for maximum performance. Review both theory and tools
2. Evaluate possible approaches for automatic balancing of engines (CAD based).
3. Perform sensitivity studies on how engine balancing influence the performance (throttle response, maximum power and torque)
4. Model and optimize the performance of a Suzuki or Honda racing engine based on the results from task 1-3
5. Prepare a paper on engine balancing and performance (the thesis can be formatted as scientific paper)

Formal requirements:

Three weeks after start of the thesis work, an A3 sheet illustrating the work is to be handed in. A template for this presentation is available on the IPM's web site under the menu "Masteroppgave" (<http://www.ntnu.no/ipm/masteroppgave>). This sheet should be updated one week before the master's thesis is submitted.

Risk assessment of experimental activities shall always be performed. Experimental work defined in the problem description shall be planned and risk assessed up-front and within 3 weeks after receiving the problem text. Any specific experimental activities which are not properly covered by the general risk assessment shall be particularly assessed before performing the experimental work. Risk assessments should be signed by the supervisor and copies shall be included in the appendix of the thesis.

The thesis should include the signed problem text, and be written as a research report with summary both in English and Norwegian, conclusion, literature references, table of contents, etc. During preparation of the text, the candidate should make efforts to create a well arranged and well written report. To ease the evaluation of the thesis, it is important to cross-reference text, tables and figures. For evaluation of the work a thorough discussion of results is appreciated.

The thesis shall be submitted electronically via DAIM, NTNU's system for Digital Archiving and Submission of Master's theses.

The contact person is Matteo Bella from MXRR and Glenn from Falcon Crankshaft.



Torgeir Welo
Head of Division



Terje Rølvåg
Professor/Supervisor



Risk analysis

NTNU	Kartlegging av risikofylt aktivitet				Utlåst av	Nummer	Dato
HMS					HMS-ansl.	HMSRV2601	22.03.2011
		Godkjent av		Erstatter			
		Rektor		01.12.2006			

Enhet: **Dato:**

Linjeleder:

Deltakere ved kartleggingen (m/ funksjon): **VEHARD RØSHOLM (STUDENT) ODA E. HOEM (STUDENT) TERJE RØLVÅG (A. UFFLEIDER)**

Kort beskrivelse av hovedaktivitet/hovedprosess: **Prosjekt oppgave-student xx- Tittel på oppgaven. ENLIGNERMANUE FOR MAX PERFE- «JA» betyr at veileder innestår for at oppgaven ikke inneholder noen aktiviteter som krever risikovurdering. Dersom «JA»: Beskriv kort aktiviteten i kartleggingskjemaet under. Risikovurdering trenger ikke å fylles ut. MANUE**

Er oppgaven rent teoretisk? (JA/NEI): **NEI**

Signaturer: Ansvarlig veileder: *[Signature]* Student: *Vegard Røsholm, Oda Hoem, Terje Rølvåg*

ID nr.	Aktivitet/prosess	Ansvarlig	Eksisterende dokumentasjon	Eksisterende sikringstiltak	LoV, forskrift b.l.	Kommentar
1	Fysisk testing av funksjon i <i>veivaksel.</i>	<i>VR</i> <i>DEH</i>				

NTNU	Risikovurdering			Dato	
HMS				Utarbeidet av	Nnummer
		HMS-avd.	HMSRV2601	Emittent	
		Godkjent av		01.12.2008	
		Rektor			

Enhet: **Dato: 9/5/16**

Linjeleder:

Deltakere ved kartleggingen (m/ funksjon): **V. RUSTHOLM (student), D.E. HOEM (student), T. ROLVÅG (4. vilerder).**
 (Ansv. Veileder, student, evt. medveiledere, evt. andre m. kompetanse)

Risikovurderingen gjelder hovedaktivitet: **Mastroppgave student-xx-Tittel på oppgaven. ENKINE BALANCE FOR MAX PERFORMACE (MASTEROPPGAVE)**

Signaturer: **Ansvarlig veileder: (Lene Kjøig 9/5-16) Student: (Vegard Rolden, Ada Enger Horn)**

ID nr	Aktivitet fra kartleggings-skjemaet	Mulig uønsket hendelse/ belastning	Vurdering av sannsynlighet (1-5)	Vurdering av konsekvens:				Risiko-Verdi (menneske)	Kommentarer/status Forslag til tiltak
				Menneske (A-E)	Ytre miljø (A-E)	ØK/ materiell (A-E)	Om-domme (A-E)		
1	Fysisk test av frisjipen	Feil i testring	1	C	A	B	B		

NTNU	Risikovurdering				Utarbeidet av	Nummer	Dato
HMS					HMS-ans. Godkjent av	HMSRV/2601	22.03.2011
		Rektor		Erstatler			01.12.2006



Sannsynlighet vurderes etter følgende kriterier:

Svært liten 1	Liten 2	Middels 3	Stor 4	Svært stor 5
1 gang pr 50 år eller sjeldnere	1 gang pr 10 år eller sjeldnere	1 gang pr år eller sjeldnere	1 gang pr måned eller sjeldnere	Stjer ukentlig

Konsekvens vurderes etter følgende kriterier:

Gradering	Menneske	Ytre miljø Vann, jord og luft	Øk/materiell	Omdømme
E Svært Alvorlig	Død	Svært langvarig og ikke reversibel skade	Drifts- eller aktivitetsstans > 1 år.	Troverdighet og respekt betydelig og varig svekket
D Alvorlig	Alvorlig personskade. Mulig uførelse.	Langvarig skade. Lang restitusjonstid	Driftstans > ½ år Aktivitetsstans i opp til 1 år	Troverdighet og respekt betydelig svekket
C Moderat	Alvorlig personskade.	Mindre skade og lang restitusjonstid	Drifts- eller aktivitetsstans < 1 mnd	Troverdighet og respekt svekket
B Liten	Skade som krever medisinsk behandling	Mindre skade og kort restitusjonstid	Drifts- eller aktivitetsstans < 1 uke	Negativ påvirkning på troverdighet og respekt
A Svært liten	Skade som krever førstehjelp	Ubetydelig skade og kort restitusjonstid	Drifts- eller aktivitetsstans < 1 dag	Liten påvirkning på troverdighet og respekt

Risikoverdi = Sannsynlighet x Konsekvens

Beregn risikoverdi for Menneske. Enheten vurderer selv om de i tillegg vil beregne risikoverdi for Ytre miljø, Økonomi/materiell og Omdømme. I så fall beregnes disse hver for seg.

Til kolonnen "Kommentarer/status, forslag til forebyggende og korrigerende tiltak":

Tiltak kan påvirke både sannsynlighet og konsekvens. Prioriter tiltak som kan forhindre at hendelsen inntreffer, dvs. sannsynlighetsreducerende tiltak foran skjerpet beredskap, dvs. konsekvensreducerende tiltak.

NTNU		Risikomatrix			
		Utarbeidet av HMS-avd. godkjent av Rektor		Nummer HMSRV2604	
				Dato 08.03.2010 Erstatet 09.02.2010	

MATRISSE FOR RISIKOVURDERINGER ved NTNU

		KONSEKVENNS									
Svært alvorlig	E1	E2	E3	E4	E5						
Alvorlig	D1	D2	D3	D4	D5						
Moderat	C1	C2	C3	C4	C5						
Liten	B1	B2	B3	B4	B5						
Svært liten	A1	A2	A3	A4	A5						
	Svært liten	Liten	Middels	Stor	Svært stor	SANNSYNLIGHET					

Prinsipp over akseptkriterium. Forklaring av fargene som er brukt i risikomatriksen.

Farge	Beskrivelse
Rød	Uakseptabel risiko. Tiltak skal gjennomføres for å redusere risikoen.
Gul	Vurderingsområde. Tiltak skal vurderes.
Grønn	Akseptabel risiko. Tiltak kan vurderes ut fra andre hensyn.